RECONSTRUCTING PHYSICAL AND HYDROLOGIC PROCESSES BENEATH THE MERCER ICE STREAM, ANTARCTICA USING SUBGLACIAL SEDIMENTS

by

Timothy David Campbell

A dissertation submitted in partial fulfillment
of the requirements for the degree

of

Doctor of Philosophy

in

Earth Sciences

MONTANA STATE UNIVERSITY
Bozeman, Montana

December 2023

DEDICATION

To my family,

who continue to love and support me even though I still play with mud.

ACKNOWLEDGEMENTS

I consider myself an incredibly very lucky person and, in many ways, this dissertation and degree reflect this good fortune. Most notably, I have a remarkable community of individuals who have supported me, not only in this journey but outside of academics as well. Without this collective support system, I would not have made it far. Here is to these exceptional people.

First and foremost, I would like to express my deepest appreciation to Dr. Mark Skidmore, my advisor. Thank you for offering me the opportunity to work on this project, welcoming me to Antarctic research, and giving me the freedom and support to explore my ideas in my research. You have read and edited countless manuscript drafts of mine and were always encouraging and positive. Thank you for your commitment to my success and the foundation to grow as a scientist.

I am grateful to my committee members, Dr. Devon Orme, Dr. David Mogk, and Dr. John Priscu for their guidance and input that greatly improved the quality of my research and dissertation. Special thanks to John Priscu. Your passion for polar research is contagious. Thank you for your time, edits, and mentorship. I am grateful to Dr. David Bowen, Dr. Dave Lageson, Dr. Rob Payn, and Dr. Madison Myers for support in furthering my education and research.

This work would not have been possible without the contributions and collaboration of the SALSA science team. I extend my sincere appreciation to Christina Davis, Molly Patterson, David Harwood, Amy Leventer, John Dore, Alex Michaud, Tristy Vick-Majors, Brad Rosenheim, Ryan Venturelli, Martyn Tranter, Wei Li, Brent Christner, Joel Barker, Chris Gardner, Alan Gagnon, and Matthew Siegfried.

To my lab mates, Annie and Gus, I thank you for your camaraderie, encouragement, and patience in teaching and guiding me.

To my family, you have supported me on this long and often challenging road. Mom, Dad, and Allie, thank you for your unwavering love and belief in me, especially when I had doubts.

Stella, you have been my support and foundation in more ways than words can convey. I could not have accomplished this without you there by my side.

To my friends near and far (Ben, Jeff, Nick, Hannah, Scott, Bates friends, Big Sky crew, and AMC folks) who helped carry me through this, you were vital to my success. Your friendships mean the world to me.

Finally, to all my former teachers, professors, and mentors, I send a heartfelt thank you to all of you. Your efforts to guide me over the years were instrumental in shaping my career and are deeply appreciated.

TABLE OF CONTENTS

TABLE OF CONTENTS CONTINUED

LIST OF TABLES

Table Page

CHAPTER ONE

CHAPTER TWO

CHAPTER THREE

LIST OF FIGURES

Figure Page

CHAPTER ONE

LIST OF FIGURES CONTINUED

LIST OF FIGURES CONTINUED

LIST OF FIGURES CONTINUED

LIST OF FIGURES CONTINUED

CHAPTER THREE

ABSTRACT

The West Antarctic Ice Sheet's (WAIS) response to warming ocean and atmospheric temperatures is of scientific interest because of its potential contributions to global sea level rise. Beneath the ice sheet is a dynamic hydrologic network of channels, lakes, and groundwater reservoirs that in part lubricate the base, supporting fast ice flow, and have a profound effect on ice sheet dynamics. Expanding our records of the temporal and spatial variability of subglacial hydrology and basal conditions will improve our understanding to the future behavior of the ice sheet. I employed a suite of sedimentological, geochemical, and image processing analyses to reconstruct past basal conditions and meltwater activity at Mercer Subglacial Lake (SLM), West Antarctica. A composite 2.06 m sediment record comprised massive-to-stratified diamicts, massive muds, and laminated muds with drop stones. I interpret the lithostratigraphic variability to reflect the emplacement of glacial tills interbedded with meltwater drainage deposits and capped by rhythmically laminated subglacial lake sediments. The meltwater sediments were deposited by suspension settling in a slowly flowing or ponded setting. The rhymically laminated lake sediments were produced by changes in the sedimentation rate and sorting of suspended sediment transported into the lake and fallout of material from melting basal ice. Borehole camera imagery revealed a ~5 m thick accreted basal ice sequence directly above the ice-lake water interface. Image analysis of the borehole wall imagery demonstrated that the basal ice layer was composed of two main ice sequences and were differentiated by sediment debris content. The lower sequence contained up to 25 times more sediment than the upper unit. The observed stratigraphic variability in basal ice sequence represents contrasting periods of meltwater availability that range from meltwater abundant to restrictive. Meltwater availability also determines the style and volume of sediment incorporation into basal ice, forming two ice types. Collectively, the two geologic records presented here provide a complex archive of subglacial hydrologic conditions and thermal histories that are linked to past ice stream variability within the late Holocene.

CHAPTER ONE

INTRODUCTION

Antarctica and Sea Level Rise

Increased concentrations of greenhouse gases in the atmosphere have led to rapid atmosphere, land, cryosphere, and ocean warming (Guluv et al., 2021). Global surface temperatures between 2011 – 2020 were 1.1°C warmer than temperatures from 1850 – 1900 (Lee, 2023). Future global warming is predicted to cause widespread and rapid changes across the Earth system, which will include intensification of heavy precipitation events and more frequent heat waves (Seneviratne et al., 2021). Sea-level rise is driven by the alteration of the density of water and by transferring water stored on land and in the cryosphere to the ocean. Between 1993 and 2010, the transfer of terrestrially stored water to the ocean contributed 1.84 ± 0.41 mm yr^{-1} to eustatic sea-level rise, while an additional 1.1 ± 0.3 mm yr^{-1} was from thermal expansion (Church et al., 2013). The average rate of global mean sea level rise has further increased to 3.7 (3.2 to 4.2) mm yr^{-1} between 2006 and 2018 (Lee et al., 2023), raising global sea level by almost 4 cm in the last decade.

Satellite observations and geophysical surveys have shown that the rate Antarctica is losing mass from its ice sheets and ice shelves is increasing and is associated with warming atmospheric and oceanic temperatures (Rignot et al., 2019). The total ice mass loss from the Antarctic Ice Sheet (AIS) increased from 40 ± 9 Gt yr^{-1} in 1979–1990 to 252 ± 26 Gt yr^{-1} in 2009–2017 (Rignot et al., 2019). Recent projections show that Antarctica may contribute between 0.11 ± 0.11 m and 1.05 ± 0.30 m to global sea level rise within this century (DeConto

and Pollard, 2016). Edwards et al. (2021) reported that under risk-averse conditions (pessimistic assumptions) Antarctic ice loss could be five times greater than conservative estimates, and sea-level equivalent could exceed half a meter by 2100. Such scenarios will impact millions of people living in coastal cities within 1 m of local sea level worldwide (Mercer, 1978; Neumann et al., 2015). Constraining projections of future Antarctic ice loss and contributions to sea level rise are of critical societal importance.

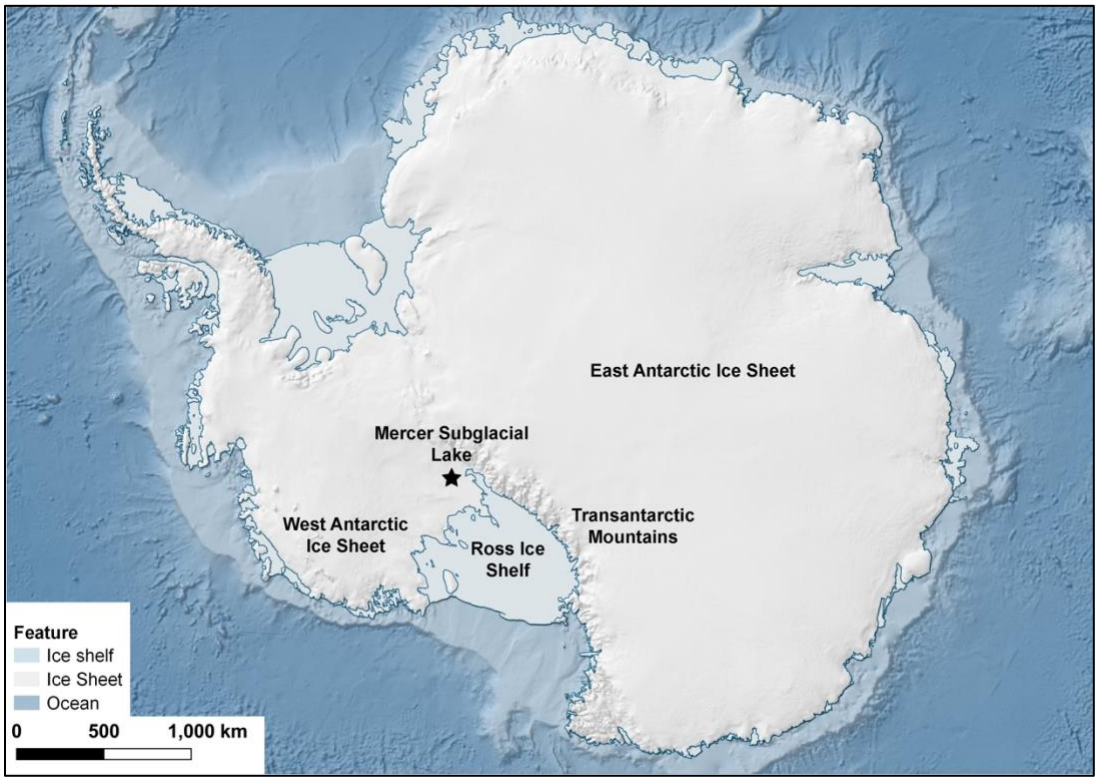

Figure 1.1 Overview map of the Antarctic Ice Sheet. Includes the East Antarctic Ice Sheet and West Antarctic Ice Sheet which are separated by the Transantarctic Mountains. Transitions from a grounded ice sheet (shaded white) to a floating ice shelf (shaded light blue) is called the grounding line (blue line). The focus of this dissertation, Mercer Subglacial Lake (SLM), is highlighted by a star and is located inland from the Ross Ice Shelf. The overlying hillshade is from the ETOP01 data set (NOAA National Geophysical Data Center, 2009).

The Antarctic Ice Sheet (AIS), which is divided by the Transantarctic Mountains into the West Antarctic Ice Sheet (WAIS) and East Antarctic Ice Sheet (EAIS), contains nearly 27 million km^3 of ice (Figure 1.1). If fully melted, this ice volume would raise the global sea level by over 57 m and is the planet's single largest freshwater repository (Fretwell et al., 2013). While the complete collapse of the entire Antarctic ice sheet in the next century is unlikely due to its elevated bed elevation, constraining how much and how fast the WAIS, which is vulnerable to rapid deglaciation due to its underlying topography being largely below sea level (Figure 1.2), will change are the most urgent priorities to be addressed by polar science research (Scambos et al., 2017). Obtaining observations of modern ice sheet behavior as well as records of past ice sheet dynamics and conditions contribute to this endeavor. The primary objective of this dissertation is to improve our understanding and extend the observational record of ice stream behavior of the Mercer Ice Stream (MIS), specifically, subglacial hydrology and ice stream basal boundary conditions using the subglacial sediment archive (Chapter 2) and accreted basal ice sequence (Chapter 3) from Mercer Subglacial Lake (SLM), West Antarctica (Figure 1.1).

Dynamic Ice Behavior

Projected contributions from WAIS to twenty-first century sea-level rise are uncertain for two main reasons: 1) ~45% of its bed rests on bedrock and sediments hundreds to thousands of meters below modern-day sea level and 2) the dynamic behavior of its ice streams that flow up to 100s of m yr^{-1} and oscillate between active ($>10^2$ m yr^{-1}) and stagnant ($<10^1$ m yr^{-1}) phases (Figures 1.2 and 1.3) (Catania et al., 2012; Morlighem et al., 2020). Large ice shelves like the Ross Ice Shelf, buttress the flow of ice seaward and help stabilize the position of marine grounding lines (Figure 1.1). However, warming ocean waters are thinning the underside of ice

shelves, reducing back stress, which enhances both seaward ice flow and grounding line retreat onto a retrograde bed (Figure 1.2). The development of a positive feedback loop has the potential to trigger a runaway Marine Ice Sheet Instability (MISI) and WAIS collapse (Hughes, 1973; Weertman, 1974; Mercer, 1978; Schoof, 2007; 2011; Favier et al., 2014; Joughin and Alley, 2014; DeConto and Pollard, 2016). The presence of Quaternary-aged marine diatoms and elevated ^{10}Be concentrations in subglacial tills recovered from beneath the grounded WAIS are evidence of past ice sheet collapse events in the Pleistocene (Scherer et al., 1998); while recent reports of organic-bearing sediments that have been dated by radiocarbon methods provide new constrains on the timing of a marine incursion as recently as 6.3 ± ka (Venturelli et al., 2023). Collectively, the geologic evidence demonstrates the marine-based WAIS susceptibility to rapid retreat.

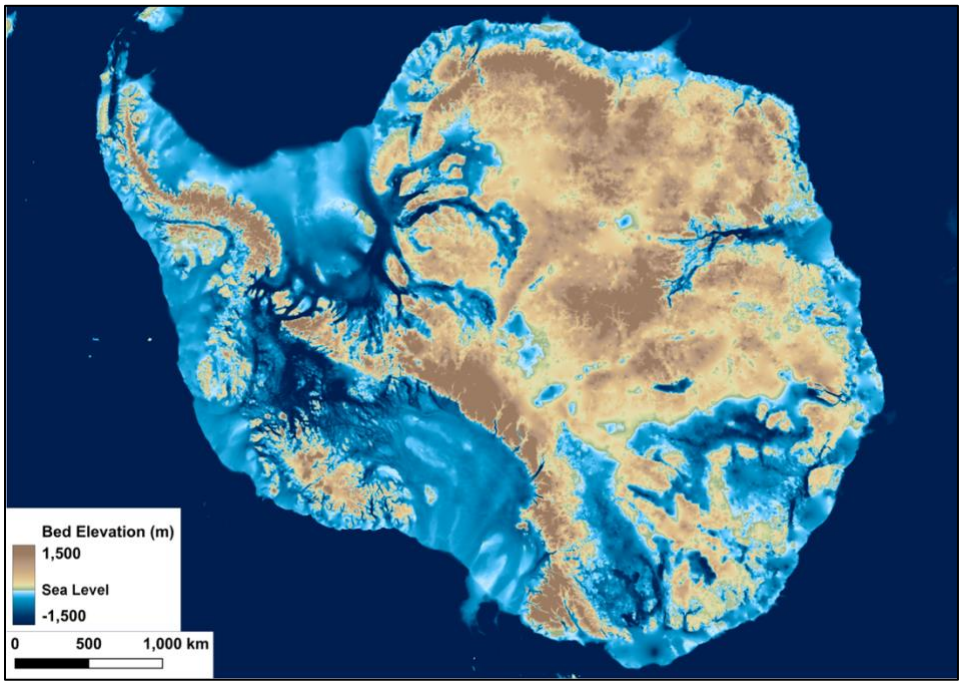

Figure 1.2 Subglacial bed elevations of the Antarctic Ice Sheet, truncated at -1,500 and 1,500 m (Morlighem et al., 2020). Portions of the bed with elevations below modern-day sea level are

shown in blue, while elevations above sea level are shown in tan to brown. Note that almost half of the WAIS is resting on ground that is below sea level which was once a shallow sea and often exceeds -1,000 m. Portions of the EAIS are below sea level, for example, Wilkes Subglacial Basin, along the Sabrina Coast, and inland of the Amery Ice Shelf.

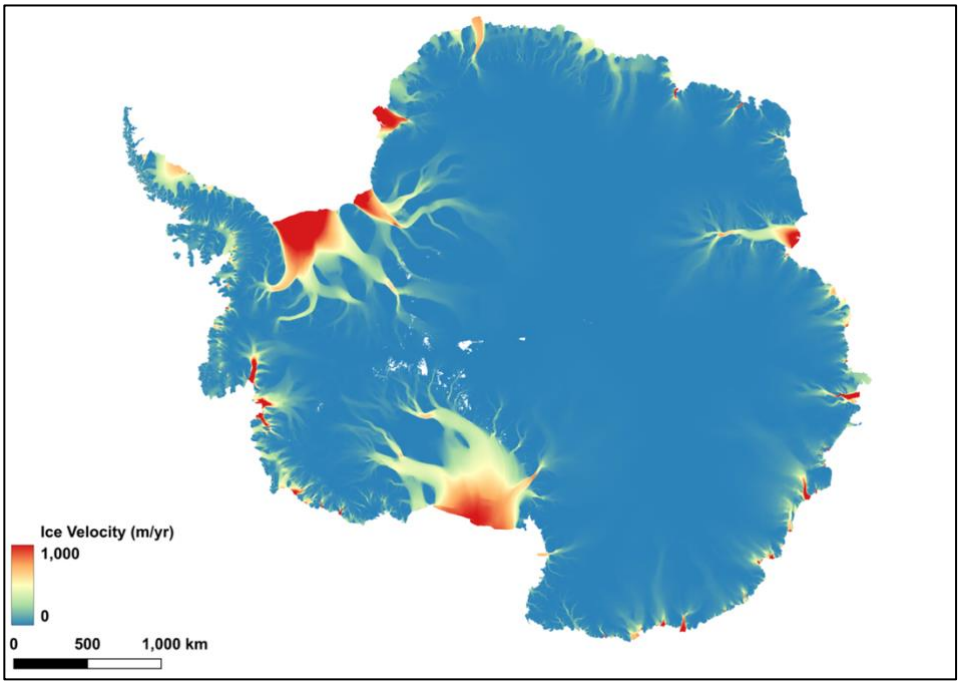

Figure 1.3 Surface ice flow velocity of the Antarctic Ice Sheet in m yr^{-1} (Mouginot et al., 2019). High ice velocities are concentrated to narrow ice streams. Ice flow velocities are orders of magnitude greater than the adjacent ice and are the primary tributaries to the ice shelves. Elevated flow velocity is concentrated primarily in West Antarctica, but isolated East Antarctic ice streams and outlet glaciers also exhibit high velocities as well.

Ice streams supply 90% of ice drained to the ice shelves and are the primary arteries of the ice sheet (Bamber et al., 2000; Kamb, 2001; Bennett, 2003; Rignot et al., 2011; Mouginot et al., 2019; Rignot et al., 2019). High flow rates despite low driving stresses are achieved due to the easily deformable, water-saturated sediments that underlie many of the ice streams and the distribution of abundant subglacial meltwater (Alley et al., 1986; Blankenship et al., 1986; Tulaczyk et al., 1998; Kamb, 2001; Hodson et al., 2016). Quasi-cyclical ice stream variability has been observed on relatively short timescales (decadal to centennial) with these changes

ranging from variability in flow rate to stagnation and reactivation events (Catania et al., 2012; Beem et al., 2014). Since ice streams are the primary supply of ice to the ice shelves, understanding the controls on ice stream flow and their temporal variations is critical to predicting future WAIS stability and mass balance (e.g. Rignot et al., 2019).

The Ross Sea sector is the focus of my dissertation research and drains 25% of Antarctic ice from the continental interior via several fast-flowing ice streams into the Ross Ice Shelf (Bennet et al., 2003; Halberstadt et al., 2016). From north to south these are: MacAyeal Ice Stream (MacIS), Bindschadler Ice Stream (BIS), Kamb Ice Stream (KIS), Whillans Ice Stream (WIS) and the Mercer Ice Stream (MIS), formerly known as Ice Streams A-E, respectively (Figure 1.4). Currently, this sector has a positive mass balance, which is attributed to the stagnation of the Kamb Ice Stream ~170 years ago (Catania et al., 2006; 2012) and the deceleration of the adjacent Whillans Ice Stream (Beem et al., 2014), partially offsetting the net negative balance from other WAIS drainages (Rignot et al., 2019). Switches in ice stream flow between active streaming and stagnation is hypothesized to be controlled by changes in subglacial water routing, ice thickness, and basal thermal regime (Alley et al., 1994). Reactivation of KIS has been hypothesized, which could reverse the observed positive mass balance of this sector (Vogel et al., 2005). Much of our understanding of the routing of subglacial meltwater comes from satellite radar and laser altimetry since 2003 (Siegfried and Fricker, 2023). Currently, there is a lack of observations and records of Antarctica's subglacial environment that extend beyond the modern satellite missions covering the last 20 years and are critical for making accurate projections.

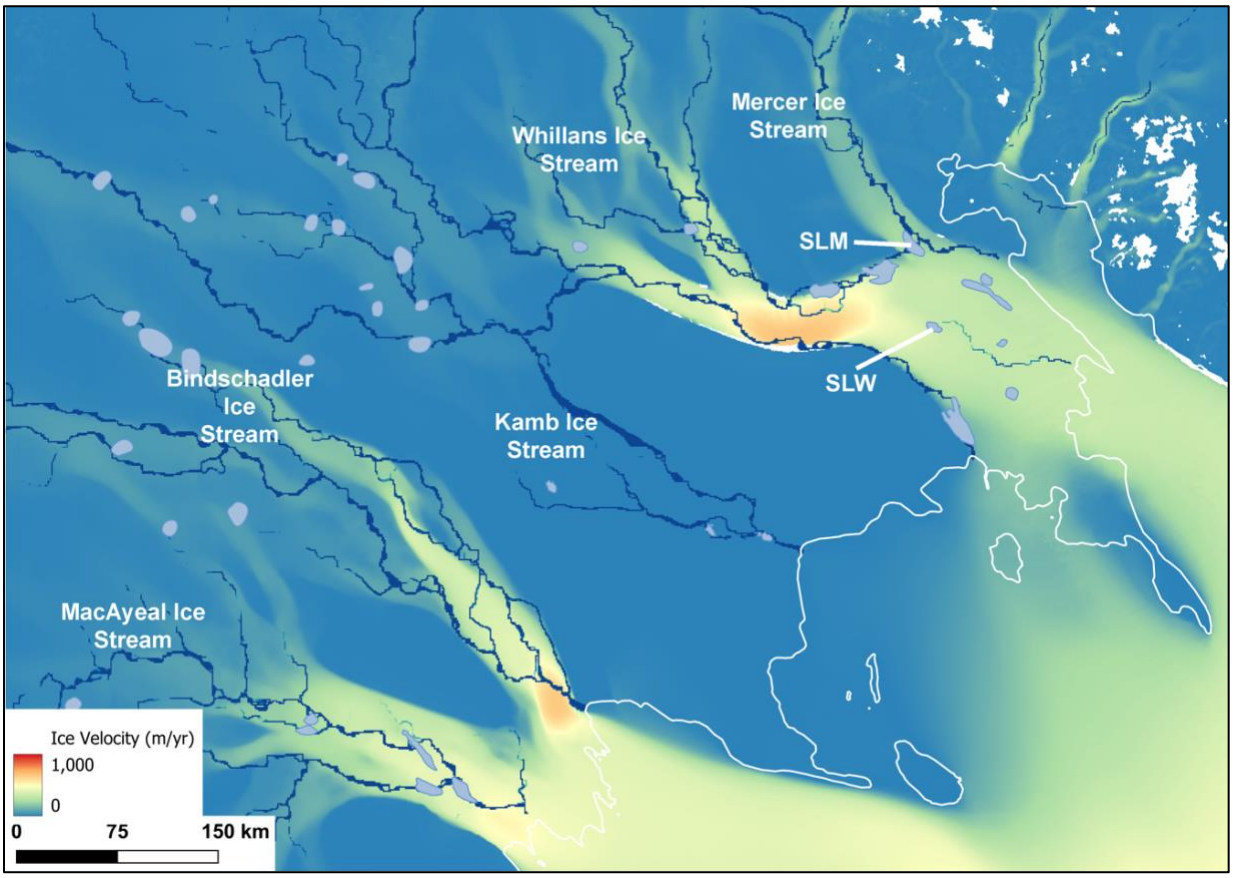

Figure 1.4 Surface ice flow velocity of the Ross Sea ice streams, West Antarctica (Mouginot et al., 2019). The marine grounding line is drawn in white (Depoorter et al., 2013). Each of the five ice streams are labeled. Note that the Kamb Ice Stream (formerly named Ice Stream C) is currently inactive. Locations of known subglacial lakes are outlined and shaded blue (Siegfried and Fricker, 2021). Modeled subglacial hydrologic channels are shown (Le Brocq et al., 2013). SLM = Mercer Subglacial Lake. SLW = Whillans Subglacial Lake.

Subglacial Hydrology and Effects on Ice Dynamics

The availability and distribution of subglacial meltwater have a profound influence on the behavior of Antarctica's fast-flowing ice streams by lubricating the ice-bed interface and enabling fast ice flow by reducing the friction between the ice and the underlying substrate (e.g. Kamb, 1987; 2001; Zwally et al., 2002; Bell, 2008; Siegfried et al., 2016). Constraining the configuration of Antarctica’s subglacial hydrologic system and understanding its temporal

variability beyond the instrumental record is needed to predict future ice sheet evolution. Under glaciers and ice sheets, the production of meltwater is controlled by the energy balance at the base of the ice sheet:

$$iLm=Qg+Qf-Qb$$

Where i is the ice density, L is the specific latent heat, m is the basal melt rate, Qg is geothermal heat, Qf is frictional heat, and Qb is the heat carried away by conduction (Cuffey and Paterson, 2010). Antarctica experiences almost no surface melt due to low mean annual temperatures and the primary sources of mass loss are frictional, geothermal, and calving of ice shelves. West Antarctica exhibits geothermal heat fluxes that exceed 100 mW m^{-2} in certain regions, which is associated with recent extension while much of the East Antarctic craton has a lower reported geothermal heat flux of 50 – 80 mW m^{-2} (see review by Artemieva, 2022). The pressure melting temperature of ice decreases under increasing pressure due to the weight of the overlying ice sheet. Large portions of WAIS are 1 - 2 km thick, while the thicker EAIS can exceed 3 km in thickness (Figure 1.5). The insulation, high pressures, geothermal heating, and frictional heating at the bottom of the ice sheet lead to basal ice melt. If there is sufficient heat energy, basal melting will occur and will produce meltwater. Currently, modelling estimates indicate that basal melting conditions exist at ~50% of the bed in Antarctica (Pattyn, 2010).

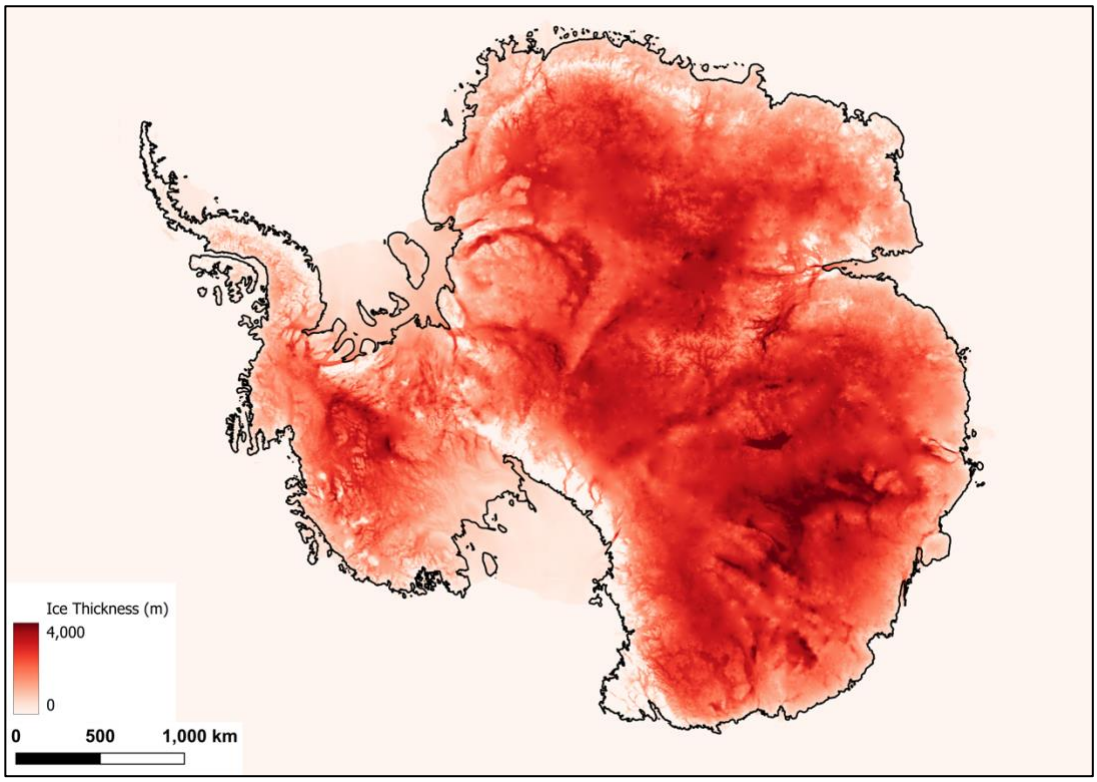

Figure 1.5 Antarctic ice thicknesses (Morlighem et al., 2020). Thicker ice is in East Antarctica, while West Antarctica is thinner. Generally, the ice sheets are thicker in the interior and thin towards the margins, which drives the hydraulic potential of subglacial water flow in this direction. The groundline line is shown in black (Depoorter et al., 2013).

The flow and storage of meltwater beneath ice sheets is determined by the gradient in hydraulic potential (θ), flowing from areas of high hydraulic potential to areas with lower hydraulic potential, and is a function of the elevation head and water pressure (Shreve, 1972):

$$\theta = \rho_w g h + p_w$$

where ρ_w is the density of water, g is gravitational acceleration, h is the bed elevation, and p_w is the water pressure. Following this equation, the ice-surface elevation gradient is ~10x more important than the bedrock elevation profile in controlling the hydraulic potential; thus, the flow direction may be opposite to the bed slope (Clarke, 2005).

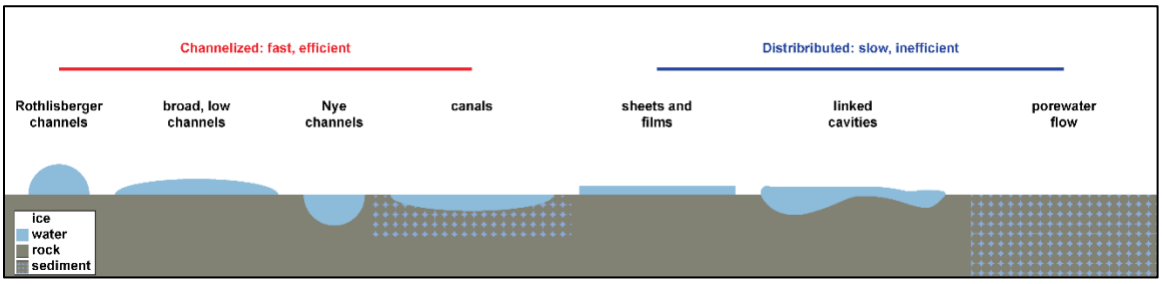

Figure 1. 6 Conceptual diagram showing the idealized components of the subglacial drainage system (modified after Flowers (2015). Components are grouped into channelized systems (left, red) and distributed systems (right, blue) based on transport efficiency.

Numerous components of subglacial drainage systems have been proposed over the past ~60 years (e.g., Weertman, 1957; Röthlisberger, 1972; Nye, 1976; Walder, 1986) and have helped to improve our understanding of the basal boundary conditions beneath glaciers and ice sheets. Broadly, subglacial hydrologic systems can be divided into two main groups: channelized and distributed systems (summarized in Flowers, 2015) (Figure 1.6). In channelized drainages, meltwater is transported through efficient and often fast narrow conduits that incise into the overlying ice (R channels, e.g., Röthlisberger, 1972) and erode into the underlying substrate (Nye channels, e.g., Nye, 1976). Distributed systems are broad networks that cover larger portions of the bed through configurations that include thin distributed sheets or films (e.g. Weertman, 1957; Creyts and Schoof, 2009), linked cavities separating the ice and bed (e.g., Walder, 1986; Kamb, 1987), or as porewater flow (Clarke, 1987). Meltwater that flows through distributed systems tends to be slower and inefficient. Broad canals should form distributed systems (Walder and Fowler, 1994), but can develop channelized geometries as well (Ng, 2000).

Meltwater beneath the AIS is produced from the insulation and pressure of the overlying ice sheet, geothermal heating, and frictional heating. Once created, the meltwater is transported and stored in subglacial lakes, channels/canals, and deep groundwater aquifers, creating a

dynamic subglacial hydrologic system (Figure 1.4) (Fricker et al., 2007; Dow et al., 2022; Gustafson et al., 2022). To date, 675 subglacial lakes have been identified beneath the Antarctic ice sheet, of which 140 are "active" lakes that fill and drain on sub-decadal timescales (Livingstone et al., 2022). Subglacial lakes will form in areas where there is relatively low hydraulic potential. Lake drainage events occur when the hydropotential seal breaks or when water leakage from the lake basin is sufficient to siphon water to erode a channel into the underlying soft sediments or to cause the ice to lift from its bed (decouple) (Dow et al., 2016; Carter et al., 2017).

Ice stream dynamics are controlled by changes in the volume of subglacial meltwater lubricating the ice-bed interface and the filling and draining of subglacial lakes. The size of the effect on ice dynamics is determined based on whether lake drainage exceeds the hydrologic capacity of the drainage system. For example, if the discharge volume is large and enters an inefficient, distributed drainage system, the overall ice velocity response will be high (Zwally et al., 2002). Subglacial lake fill-drain events have been shown to increase ice velocity by up to 10% (Siegfried et al., 2016).

Using NASA's Ice, Cloud, and land Elevation Satellite (ICESat) laser altimetry (2003 – 2009), Fricker et al. (2007) detected localized ice-sheet surface deformation occurring on monthly to annual timescales and interpreted the high anomalies to be the result of subglacial lakes filling and draining. Despite the recognized importance of subglacial hydrology on broader ice sheet dynamics and evolution, the observational record of hydrologic change beneath the ice is relatively short and limited to modern satellite missions since 2003 (Siegfried and Fricker, 2021). Subglacial sediments and accreted basal ice layers contain valuable archives of ice sheet

history and subglacial conditions (hydrological and thermal histories) that can be used to extend the record of subglacial lake and meltwater activity (e.g. Siegfried et al., 2023).

Mercer Subglacial Lake (SLM) is located at the confluence of the Mercer and Whillans Ice Streams (MIS and WIS, respectively) (Figure 1.4). Based on multi-mission satellite altimetry and continuous GPS data, SLM completes a fill-drain cycle every 4 – 6 years (Siegfried and Fricker, 2021) and is strongly connected to hydrologic activity in upstream Conway Subglacial Lake (SLC). Subglacial hydrologic modeling estimates that ~80% of SLM lake water was derived from basal melting of the WAIS and the remaining ~20% was produced from basal melting of the EAIS (Venturelli et al., 2023).

Antarctic Sedimentary Archive

Seismic studies have inferred that the Ross Sea Ice Streams flow over a several meters thick water-saturated till layer, that overlies up to 600 m thick bedded sedimentary succession that accumulated in the broad West Antarctic Rift System (Blankenship et al., 1986, 1987; Rooney et al., 1987). Previous direct observations and interpretations of West Antarctica's modern subglacial sedimentology has been limited to sediment cores retrieved from the Whillans (WIS), Kamb (KIS), and Bindschadler (BIS) ice streams. Sediment cores (0.25 to 3.1 m long) were composed entirely of dark gray, wet, very sticky, clay-rich diamicts without any grading, bedding, or structure (Tulaczyk et al., 1998; Kamb, 2001) (Table 1.1). Sediment cores from Whillans Subglacial Lake (SLW), the first sediment recovered from an active subglacial lake, was composed of glacial till that was deposited during intermittent grounding of the ice stream following lake drainage events (Hodson et al., 2016) (Table 1.1). Despite a history of filling and draining, the sediment record for SLW showed no evidence of erosion or deposition by flowing

water. Active subglacial lake sedimentation was not reported until cores were recovered from SLM, which is the primary focus of this dissertation.

Table 1.1 Summary of subglacial sediment locations, sediment descriptions, and depositional environments from the Ross Sea region. UpB = Whillans Ice Stream. UpC = Kamb Ice Stream. UpD Bindschadler Ice Stream. SLW = Whillans Subglacial Lake.

Location	**Sediment description(s)**	**Depositional Environment(s)**	**References**
UpB	Poorly sorted, structureless diamict including marine microfossils	Subglacial, grounded ice sheet	Tulaczyk et al., 1998
UpC	Dark gray, wet, clay-rich diamict, lacking grading or structures	Subglacial, grounded ice sheet	Kamb, 2001
UpD	Diamict, water content 8% higher than UpB and UpC	Subglacial, grounded ice sheet	Kamb, 2001
SLW	Dark gray muddy diamict	Subglacial, grounded ice sheet	Hodson et al., 2016
Ross Sea	Massive, mud-rich diamicts; Stratified sandy, muddy gravel; Sorted, fine-grained sand; Siliceous mud and ooze; **Dark gray silt (10 μm peak)*	Subglacial setting, Thin water film between the basal debris and sea floor, Sub-ice shelf, Open marine, **Meltwater deposit*	Domack et al., 1999; Licht et al., 1999 McKay et al., 2016; Robinson et al., 2021; **Prothro et al., 2018*

Since the discovery of active subglacial lakes within the Ross Sea region of the WAIS hydrologic system (Fricker et al., 2007), there have been increased efforts to constrain the evolution of Antarctic subglacial hydrology and persistence of meltwater activity through the pre-satellite era. Sediment cores collected from the deglaciated continental shelf have been used to reconstruct meltwater drainage events (e.g., Witus et al., 2014; Simkins et al., 2017; Prothro et al., 2018; 2020; Lepp et al., 2022). Subglacial meltwater deposits are characterized by silt-rich sediments with high water content and low biogenic and ice-rafted debris (IRD), low shear strength, and low magnetic susceptibility. These characteristics allow for the differentiation of subglacial meltwater deposits from subglacial, ice-proximal, and open-marine sediment facies (Prothro et al., 2018) (Table 1.1).

Direct access to modern Antarctic subglacial environments is limited, but several hundred sediment cores have been collected from the Ross Sea and contain units deposited under past subglacial conditions which have been used to characterize subglacial sedimentary sequences (e.g. Domack et al., 1999; Licht et al., 1999; Licht and Andrews, 2002; Mosola and Anderson; 2006; Halberstadt et al., 2018). The results from these studies demonstrated that till and proximal glaciomarine sediments are widespread in the Ross Sea and indicate that grounded ice previously extended across most of the continental shelf (Anderson et al., 2014). The typical stratigraphic succession recorded in western Ross Sea sediment cores is described as an upward progression from till to proximal glaciomarine to distal glaciomarine sediments that generally display increasing abundances of diatoms upwards (Domack et al., 1999; Licht et al., 1999; McKay et al., 2016; Robinson et al., 2021) (Table 1.1). Domack et al. (1999) described the subglacial till unit as massive, mud-rich diamicts with low water contents, minimal textural variation, and low but uniform total organic carbon values. This sequence reflects a progressive landward migration of the retreating grounding line across the continental shelf and the subsequent onset of an open-marine environment as a product of deglaciation (Anderson et al., 2014). Much of our current knowledge of past and present ice sheet dynamics comes from sediment core reconstructions using physical data (e.g., McKay et al., 2016; Prothro et al., 2018). Despite the importance of subglacial sediments in the paleoenvironmental reconstructions, these data from Antarctica's contemporary subglacial environment remains scarce.

Accreted Basal Ice Sequences

Knowledge of the boundary conditions beneath the West Antarctic ice streams over a range of spatial and temporal scales is critical to developing accurate ice sheet mass balance

projections. At the bottom of most glaciers and ice sheets is a thin ice layer that is formed by processes operating at the bed as subglacial water is frozen onto the sole of the ice mass in areas with basal temperatures below the pressure melting point of ice. This basal ice layer (BIL) is physically and chemically distinct from the overlying ice and often contains incorporated subglacial sediments (e.g., Hubbard and Sharp, 1989; Alley et al., 1997; Knight, 1997; Hubbard et al., 2009; Goossens et al., 2016). Debris-bearing BIL can form by several different processes driven by the abundance of meltwater and the persistence of basal freezing conditions, of which the most important are regelation, glaciohydraulic supercooling, and net adfreezing (Weertman, 1961; 1964; Alley et al., 1998; Lawson et al.., 1998). BILs are important because they provide evidence of subglacial hydrologic activity, transport entrained sediment, and redistribute heat and mass within an ice mass. This is important for the Antarctic Ice Sheet (e.g. Bell et al., 2011; Tulaczyk and Hossainzadeh, 2011). Thus, subglacially accreted layers are important archives of spatial and temporal dynamics of subglacial hydrology and thermal history operating at the base of an ice mass. The properties of basal ice layers from SLM can be used to better understand the dynamics and histories of fast flowing ice streams, such as the Mercer and Whillans ice streams.

When ice masses flow over bed obstacles, restive stresses on the up-glacier side of the obstacle cause locally high pressures to develop (Hallet, 1979). The increase in effective pressure lowers the melting point of ice and can generate basal melting. Meltwater can be refrozen on the down-glacier side of the obstacle if there is a drop in pressure and subsequent increase in the pressure melting temperature. This process of ice melting and freezing under changing pressures is known as regelation (Weertman, 1964).

Glaciohydraulic supercooling is similar to regelation, except it occurs on larger spatial scales (e.g., Alley et al., 1998; Cook et al., 2007; 2009; 2012; Lawson et al., 1998; Roberts et al., 2002). BILs can form from the freezing of supercooled basal meltwater that undergoes a pressure drop, which raises the pressure melting point. The meltwater will freeze unless it can be warmed to the new pressure melting point by heat supplied. Freezing of supercooled meltwater is likely to occur in areas where water flows out of overdeepenings and/or is driven up a reverse slope that exceeds 1.2 times the magnitude of the surface slope (Röthlisberger, 1972).

Net basal adfreezing requires the migration of a freezing front into water saturated sediments (Weertman, 1961) or through water trapped above bedrock (Hubbard, 1991). Since the ice pressure at the ice base is equal to the overlying ice sheet's gravitational load, freezing at the base will be associated with a decrease of the pore water pressure. Lowering the pore water pressure develops a hydraulic gradient that causes water to flow towards the freezing ice base. In the early stages of this process, sediment will largely be rejected and as such, a lens of clean segregation ice will form (Christoffersen et al., 2006). Over time a new thermodynamically more favorable location for ice crystal grown will form, which causes the freezing front to advance down into the underlying sediment, thereby entraining debris into the ice (Christoffersen et al., 2006).

Previous WAIS Basal Ice Research

Some of the first reports of basal ice layers came from observations of ice cores. Basal ice was observed by in the bottom 4.8 m of the Byrd Station ice core, Antarctica (Gow et al., 1979). The transition from air-rich glacial ice to bubble-free ice coincided with the first appearance of sediment debris (Gow et al., 1979). The absence of air bubbles and presence of

debris indicated that this zone of ice was formed by freezing on to the base of the ice sheet and not from surface firnification. Other Antarctic studies have also investigated sequences of basal ice. For example, the Vostok ice contained ~210 m of accreted basal ice containing carbon and sediment that formed due to freezing onto the bottom of the ice sheet due to the supercooling of water over Subglacial Lake Vostok (Priscu et al., 1999; Jouzel et al., 2000; Souchez et al., 2000).

The basal ice of Kamb Ice Stream is divided into an upper section composed of clear, dispersed, and stratified dispersed facies and a lower unit consisting of alternating layers of clear, dispersed, and stratified solid facies. Christoffersen et al. (2010) argued that the upper clear ice formed by the growth of accreted ice from the interior of the ice sheet where subglacial meltwater was abundant. The properties of the debris-rich bottom unit (~1.25 m) suggest that this unit accreted under high freezing rates (>3 mm per year) and highly restricted water conditions (<30%), which were likely the conditions that caused ice stream stoppage to occur (Christoffersen et al., 2010). Vogel et al. (2005) used estimates of basal freeze on rates (~4 mm yr^{-1}) to show that stagnation of Kamb Ice Stream occurred ~170 years ago (time required to grow 0.6 m of basal ice) but may reactivate as the hydrologic system restarted ~75 years ago as inferred by the presence of a 0.27 m thick clear ice layer at the ice stream base (Vogel et al., 2005).

Objectives of Dissertation

This dissertation research is part of the Subglacial Antarctic Lakes Scientific Access (SALSA) project, which is an integrated research program studying the geologic, biogeochemical, and geomicrobiological processes in the water column and sediment from one of West Antarctica's active subglacial lakes, Mercer Subglacial Lake (SLM). The overarching

hypothesis of the SALSA project is: *contemporary biodiversity and carbon cycling in hydrologically active subglacial environments associated with the Mercer and Whillans ice streams are regulated by the mineralization and cycling of relict marine organic matter and through interactions among ice, rock, water, and sediments.* My component of this larger research endeavor focuses on 1) the characterization of the lake sediments to understand the lifespan of the subglacial lake, the temporal variability of meltwater discharge, and more broadly, the basal hydrologic conditions of the Mercer Ice Stream (MIS) (Chapter 2) and 2) describing the stratigraphy of the basal ice sequence overlying the subglacial lake to constrain past hydrologic conditions and basal thermal history of the MIS (Chapter 3).

There is a paucity of direct observations and data from Antarctica's subglacial environment on basal conditions and subglacial hydrology on a range of temporal and spatial scales. Subglacial sediment records processes of erosion, transportation, and deposition, and therefore can be used as proxies for reconstructing paleoenvironmental conditions beneath the Antarctic ice sheet. The overarching goal of the dissertation is to extend the observational record of subglacial meltwater activity, basal thermal conditions, and physical processes beneath the Mercer Ice Stream. This will be accomplished through the following objectives:

1. Characterize the properties of sediments collected from SLM and those observed in the basal ice layer above the lake.
2. Develop an understanding of the processes and conditions responsible for the stratigraphic variability observed in the SLM sediment core record and basal ice sequence.

3. Reconstruct the paleoenvironment of MIS, with specific attention to the hydrologic and basal thermal histories, thereby extending the observational record of these processes.

Dissertation Outline

This dissertation is divided into four chapters. The next two chapters are written as stand-alone manuscripts that are being prepared for submission to peer-reviewed journals. This dissertation is structured around the following chapters:

Chapter 2: **Dynamic subglacial hydrologic conditions archived in Antarctic subglacial lake sediments** includes work that is currently in preparation for peer-review. In this chapter, I employed a suite of sedimentological and geochemical analyses to reconstruct basal conditions and meltwater activity from sediment cores collected from Mercer Subglacial Lake, West Antarctica. This work was motivated by the following research questions:

- What are the physical, compositional, and structural properties of sediment cores from SLM?
- What depositional processes and environments are archived by SLM sediments? What evidence do we have for meltwater discharge? How common is subglacial meltwater beneath the MIS?
- How has the MIS subglacial environment at SLM evolved during the late Holocene?

Chapter 3: Implications for sub-ice stream accretionary processes and conditions from the Basal Ice Layer of the Mercer Ice Stream, West Antarctica includes work that is currently in preparation for peer-review. In this chapter, I developed a new method for determining the concentration of sediment entrained in basal ice sequences using image analyses. I apply this

method to evaluate the stratigraphic changes in the SLM basal ice sequence and to answer the following research questions:

- What are the physical characteristics of the basal ice sequence of the Mercer Ice Stream observed above Mercer Subglacial Lake, West Antarctica?
- How do these properties, primarily the sediment load, inform our understanding of sub-ice stream (accretionary) processes, basal thermal history, and the subglacial hydrologic system?

I use these results to improve our understanding of the availability of subglacial meltwater, basal thermal regime, and the mechanisms of basal freeze-on beneath the MIS.

Chapter 4: provides a summary and synthesis of Chapters 2 and 3, some concluding remarks, and discusses potential for future research.

Additional Research

In addition to the work described in this Ph.D. dissertation, I have conducted field and analytical research that is not included here. I was a member of the field science team that successfully recovered 12 sediment cores from Mercer Subglacial Lake. My work has resulted in the publication of three separate papers that I coauthored, which are listed below.

Rosenheim, B. E., Michaud, A. B., Broda, J., Gagnon, A., Venturelli, R. A., **Campbell, T. D.**, Leventer, A, Patterson, M., Siegfried, M. R., Christner, B. C., Duling, D., Harwood, D., Dore, J. E., Tranter, M., Skidmore, M. L., Priscu, J. C. & SALSA Science Team. (2023). A method for successful collection of multicores and gravity cores from Antarctic subglacial lakes. *Limnology and Oceanography: Methods*.

In Rosenheim et al. (2023) I served as a team member contributing to modifications and decisions regarding sediment coring in the field and provided edits to the manuscript prior to submission. In addition, I created one key figure (Figure 8) for this manuscript.

Siegfried, M. R., Venturelli, R. A., Patterson, M. O., Arnuk, W., **Campbell, T. D.**, Gustafson, C. D., ... & SALSA Science Team. (2023). The life and death of a subglacial lake in West Antarctica. *Geology*, *51*(5), 434-438.

In Siegfried et al. (2023) I contributed to the research investigation, generated sedimentological data used in the interpretation, and provided edits to the manuscript.

Priscu, J. C., Kalin, J., Winans, J., **Campbell, T.D.**, Siegfried, M. R., Skidmore, M., Dore, J. E., Leventer, A., Harwood, D. M., Duling, D., Zook, R., Burnett, J., Gibson, D., Krula, E., Mironov, A., McManis, J., Roberts, G., ... & SALSA Science Team. (2021). Scientific access into Mercer Subglacial Lake: scientific objectives, drilling operations and initial observations. *Annals of Glaciology*, *62*(85-86), 340-352.

In Priscu et al. (2021) I wrote the section titled: Evaluating potential impact of sediment fallout to surface lake sediments, created Figure 10 (assisted with Figures 7 and 8), and provided edits to the manuscript.

References Cited

Alley, R., Anandakrishnan, S., Bentley, C., and Lord, N., 1994, A water-piracy hypothesis for the stagnation of Ice Stream C, Antarctica: Annals of Glaciology, v. 20, p. 187–194.

Alley, R.B., Blankenship, D.D., Bentley, C.R., and Rooney, S., 1986, Deformation of till beneath ice stream B, West Antarctica: Nature, v. 322, p. 57–59.

Alley, R.B., Cuffey, K., Evenson, E., Strasser, J., Lawson, D., and Larson, G., 1997, How glaciers entrain and transport basal sediment: physical constraints: Quaternary Science Reviews, v. 16, p. 1017–1038.

Alley, R.B., Lawson, D.E., Evenson, E.B., Strasser, J.C., and Larson, G.J., 1998, Glaciohydraulic supercooling: a freeze-on mechanism to create stratified, debris-rich basal ice: II. Theory: Journal of Glaciology, v. 44, p. 563–569.

Amante, C., and Eakins, B.W., 2009, ETOPO1 arc-minute global relief model: procedures, data sources and analysis:

Anderson, J.B., Conway, H., Bart, P.J., Witus, A.E., Greenwood, S.L., McKay, R.M., Hall, B.L., Ackert, R.P., Licht, K., and Jakobsson, M., 2014, Ross Sea paleo-ice sheet drainage and deglacial history during and since the LGM: Quaternary Science Reviews, v. 100, p. 31–54.

Artemieva, I.M., 2022, Antarctica ice sheet basal melting enhanced by high mantle heat: Earth-science reviews, v. 226, p. 103954.

Beem, L.H., Tulaczyk, S.M., King, M.A., Bougamont, M., Fricker, H.A., and Christoffersen, P., 2014, Variable deceleration of Whillans Ice Stream, West Antarctica: Journal of Geophysical Research: Earth Surface, v. 119, p. 212–224, doi:https://doi.org/10.1002/2013JF002958.

Bell, R.E., 2008, The role of subglacial water in ice-sheet mass balance: Nature Geoscience, v. 1, p. 297–304, doi:10.1038/ngeo186.

Bell, R.E., Ferraccioli, F., Creyts, T.T., Braaten, D., Corr, H., Das, I., Damaske, D., Frearson, N., Jordan, T., and Rose, K., 2011, Widespread persistent thickening of the East Antarctic Ice Sheet by freezing from the base: Science, v. 331, p. 1592–1595.

Bennett, M.R., 2003, Ice streams as the arteries of an ice sheet: their mechanics, stability and significance: Earth-Science Reviews, v. 61, p. 309–339.

Blankenship, D.D., Bentley, C.R., Rooney, S., and Alley, R.B., 1986, Seismic measurements reveal a saturated porous layer beneath an active Antarctic ice stream: Nature, v. 322, p. 54–57.

Blankenship, D.D., Bentley, C.R., Rooney, S.T., and Alley, R.B., 1987, Till beneath ice stream B: 1. Properties derived from seismic travel times: Journal of Geophysical Research: Solid Earth, v. 92, p. 8903–8911, doi:10.1029/JB092iB09p08903.

Carter, S.P., Fricker, H.A., and Siegfried, M.R., 2017, Antarctic subglacial lakes drain through sediment-floored canals: theory and model testing on real and idealized domains: The Cryosphere, v. 11, p. 381–405, doi:10.5194/tc-11-381-2017.

Catania, G., Hulbe, C., Conway, H., Scambos, T.A., and Raymond, C.F., 2012, Variability in the mass flux of the Ross ice streams, West Antarctica, over the last millennium: Journal of Glaciology, v. 58, p. 741–752, doi:10.3189/2012JoG11J219.

Catania, G.A., Scambos, T.A., Conway, H., and Raymond, C.F., 2006, Sequential stagnation of Kamb Ice Stream, West Antarctica: Geophysical Research Letters, v. 33, doi:10.1029/2006GL026430.

Center, N., 2009, ETOPO1 1 arc-minute global relief model: NOAA National Centers for Environmental Information.(date accessed: 2021-1-05) doi, v. 10, p. V5C8276M.

Christoffersen, P., Tulaczyk, S., and Behar, A., 2010, Basal ice sequences in Antarctic ice stream: Exposure of past hydrologic conditions and a principal mode of sediment transfer: Journal of Geophysical Research: Earth Surface, v. 115, doi:https://doi.org/10.1029/2009JF001430.

Christoffersen, P., Tulaczyk, S., Carsey, F.D., and Behar, A.E., 2006, A quantitative framework for interpretation of basal ice facies formed by ice accretion over subglacial sediment: Journal of Geophysical Research: Earth Surface, v. 111, doi:10.1029/2005JF000363.

Church, J.A., Clark, P.U., Cazenave, A., Gregory, J.M., Jevrejeva, S., Levermann, A., Merrifield, M.A., Milne, G.A., Nerem, R.S., and Nunn, P.D., 2013, Sea level change: PM Cambridge University Press.

Clarke, G.K., 2005, Subglacial processes: Annu. Rev. Earth Planet. Sci., v. 33, p. 247–276.

Clarke, G.K.C., 1987, Subglacial till: A physical framework for its properties and processes: Journal of Geophysical Research: Solid Earth, v. 92, p. 9023–9036, doi:https://doi.org/10.1029/JB092iB09p09023.

Cook, S.J., and Knight, P.G., 2009, Glaciohydraulic supercooling: Progress in Physical Geography: Earth and Environment, v. 33, p. 705–710, doi:10.1177/0309133309342653.

Cook, S.J., Knight, P.G., Waller, R.I., Robinson, Z.P., and Adam, W.G., 2007, The geography of basal ice and its relationship to glaciohydraulic supercooling: Svínafellsjökull, southeast Iceland: Quaternary Science Reviews, v. 26, p. 2309–2315, doi:10.1016/j.quascirev.2007.07.010.

Creyts, T.T., and Schoof, C.G., 2009, Drainage through subglacial water sheets: Journal of Geophysical Research: Earth Surface, v. 114, doi:10.1029/2008JF001215.

Cuffey, K.M., and Paterson, W.S.B., 2010, The physics of glaciers: Academic Press.

DeConto, R.M., and Pollard, D., 2016, Contribution of Antarctica to past and future sea-level rise: Nature, v. 531, p. 591–597, doi:10.1038/nature17145.

Depoorter, M.A., Bamber, J.L., Griggs, J.A., Lenaerts, J.T.M., Ligtenberg, S.R.M., van den Broeke, M.R., and Moholdt, G., 2013, Calving fluxes and basal melt rates of Antarctic ice shelves: Nature, v. 502, p. 89–92, doi:10.1038/nature12567.

Domack, E.W., Jacobson, E.A., Shipp, S., and Anderson, J.B., 1999, Late Pleistocene–Holocene retreat of the West Antarctic Ice-Sheet system in the Ross Sea: Part 2—Sedimentologic and stratigraphic signature: GSA Bulletin, v. 111, p. 1517–1536, doi:10.1130/0016-7606(1999)111<1517:LPHROT>2.3.CO;2.

Dow, C.F., Ross, N., Jeofry, H., Siu, K., and Siegert, M.J., 2022, Antarctic basal environment shaped by high-pressure flow through a subglacial river system: Nature Geoscience, v. 15, p. 892–898, doi:10.1038/s41561-022-01059-1.

Dow, C.F., Werder, M.A., Nowicki, S., and Walker, R.T., 2016, Modeling Antarctic subglacial lake filling and drainage cycles: The Cryosphere, v. 10, p. 1381–1393, doi:10.5194/tc-10-1381-2016.

Edwards, T.L., Nowicki, S., Marzeion, B., Hock, R., Goelzer, H., Seroussi, H., Jourdain, N.C., Slater, D.A., Turner, F.E., and Smith, C.J., 2021, Projected land ice contributions to twenty-first-century sea level rise: Nature, v. 593, p. 74–82.

Favier, L., Durand, G., Cornford, S.L., Gudmundsson, G.H., Gagliardini, O., Gillet-Chaulet, F., Zwinger, T., Payne, A., and Le Brocq, A.M., 2014, Retreat of Pine Island Glacier controlled by marine ice-sheet instability: Nature Climate Change, v. 4, p. 117–121.

Flowers, G.E., 2015, Modelling water flow under glaciers and ice sheets: Proceedings of the Royal Society A: Mathematical, Physical and Engineering Sciences, v. 471, p. 20140907, doi:10.1098/rspa.2014.0907.

Fretwell, P. et al., 2013, Bedmap2: improved ice bed, surface and thickness datasets for Antarctica: The Cryosphere, v. 7, p. 375–393, doi:10.5194/tc-7-375-2013.

Fricker, H.A., Scambos, T., Bindschadler, R., and Padman, L., 2007, An Active Subglacial Water System in West Antarctica Mapped from Space: Science, v. 315, p. 1544–1548, doi:10.1126/science.1136897.

Goossens, T., Sapart, C.J., Dahl-Jensen, D., Popp, T., El Amri, S., and Tison, J.-L., 2016, A comprehensive interpretation of the NEEM basal ice build-up using a multi-parametric approach: The Cryosphere, v. 10, p. 553–567, doi:10.5194/tc-10-553-2016.

Gow, A.J., Epstein, S., and Sheehy, W., 1979, On the Origin of Stratified Debris in Ice Cores from the Bottom of the Antarctic Ice Sheet: Journal of Glaciology, v. 23, p. 185–192, doi:10.3189/S0022143000029828.

Gulev, S.K., Thorne, P.W., Ahn, J., Dentener, F.J., Domingues, C.M., Gerland, S., Gong, D., Kaufman, D.S., Nnamchi, H.C., and Quaas, J., 2021, Changing state of the climate system:

Gustafson, C.D., Key, K., Siegfried, M.R., Winberry, J.P., Fricker, H.A., Venturelli, R.A., and Michaud, A.B., 2022, A dynamic saline groundwater system mapped beneath an Antarctic ice stream: Science, v. 376, p. 640–644, doi:10.1126/science.abm3301.

Halberstadt, A.R.W., Simkins, L.M., Anderson, J.B., Prothro, L.O., and Bart, P.J., 2018, Characteristics of the deforming bed: till properties on the deglaciated Antarctic continental shelf: Journal of Glaciology, v. 64, p. 1014–1027, doi:10.1017/jog.2018.92.

Halberstadt, A.R.W., Simkins, L.M., Greenwood, S.L., and Anderson, J.B., 2016, Past ice-sheet behaviour: retreat scenarios and changing controls in the Ross Sea, Antarctica: The Cryosphere, v. 10, p. 1003–1020, doi:10.5194/tc-10-1003-2016.

Hallet, B., 1979, Subglacial Regelation Water Film: Journal of Glaciology, v. 23, p. 321–334, doi:10.3189/S0022143000029932.

Hodson, T.O., Powell, R.D., Brachfeld, S.A., Tulaczyk, S., and Scherer, R.P., 2016, Physical processes in Subglacial Lake Whillans, West Antarctica: Inferences from sediment cores: Earth and Planetary Science Letters, v. 444, p. 56–63, doi:10.1016/j.epsl.2016.03.036.

Hubbard, B., 1991, Freezing-rate effects on the physical characteristics of basal ice formed by net adfreezing: Journal of Glaciology, v. 37, p. 339–347, doi:10.3189/S0022143000005773.

Hubbard, B., Cook, S., and Coulson, H., 2009, Basal ice facies: a review and unifying approach: Quaternary Science Reviews, v. 28, p. 1956–1969, doi:10.1016/j.quascirev.2009.03.005.

Hubbard, B., and Sharp, M., 1989, Basal ice formation and deformation: a review: Progress in Physical Geography: Earth and Environment, v. 13, p. 529–558, doi:10.1177/030913338901300403.

Hughes, T., 1973, Is the west Antarctic Ice Sheet disintegrating? Journal of Geophysical Research (1896-1977), v. 78, p. 7884–7910, doi:10.1029/JC078i033p07884.

Joughin, I., and Alley, R.B., 2011, Stability of the West Antarctic ice sheet in a warming world: Nature Geoscience, v. 4, p. 506–513, doi:10.1038/ngeo1194.

Jouzel, J., Petit, J.R., Souchez, R., Barkov, N.I., Lipenkov, V.Ya., Raynaud, D., Stievenard, M., Vassiliev, N.I., Verbeke, V., and Vimeux, F., 1999, More Than 200 Meters of Lake Ice Above Subglacial Lake Vostok, Antarctica: Science, v. 286, p. 2138–2141, doi:10.1126/science.286.5447.2138.

Kamb, B., 2001, Basal Zone of the West Antarctic Ice Streams and its Role in Lubrication of Their Rapid Motion, *in* The West Antarctic Ice Sheet: Behavior and Environment, Antarctic Research Series, p. 157–199, doi:10.1029/AR077p0157.

Kamb, B., 1987, Glacier surge mechanism based on linked cavity configuration of the basal water conduit system: Journal of Geophysical Research: Solid Earth, v. 92, p. 9083–9100, doi:10.1029/JB092iB09p09083.

Kingslake, J., Scherer, R.P., Albrecht, T., Coenen, J., Powell, R.D., Reese, R., Stansell, N.D., Tulaczyk, S., Wearing, M.G., and Whitehouse, P.L., 2018, Extensive retreat and re-advance of the West Antarctic Ice Sheet during the Holocene: Nature, v. 558, p. 430–434, doi:10.1038/s41586-018-0208-x.

Knight, P.G., 1997, The basal ice layer of glaciers and ice sheets: Quaternary Science Reviews, v. 16, p. 975–993, doi:10.1016/S0277-3791(97)00033-4.

Lawson, D.E., Strasser, J.C., Evenson, E.B., Alley, R.B., Larson, G.J., and Arcone, S.A., 1998, Glaciohydraulic supercooling: a freeze-on mechanism to create stratified, debris-rich basal ice: I. Field evidence: Journal of Glaciology, v. 44, p. 547–562, doi:10.3189/S0022143000002069.

Lee, H., Calvin, K., Dasgupta, D., Krinner, G., Mukherji, A., Thorne, P., Trisos, C., Romero, J., Aldunce, P., and Barrett, K., 2023, Climate change 2023: synthesis report. Contribution of working groups I, II and III to the sixth assessment report of the intergovernmental panel on climate change:, doi:doi: 10.59327/IPCC/AR6-9789291691647.001.

Lepp, A.P. et al., 2022, Sedimentary Signatures of Persistent Subglacial Meltwater Drainage From Thwaites Glacier, Antarctica: Frontiers in Earth Science, v. 10, https://www.frontiersin.org/articles/10.3389/feart.2022.863200.

Licht, K.J., and Andrews, J.T., 2002, The 14C Record of Late Pleistocene Ice Advance and Retreat in the Central Ross Sea, Antarctica: Arctic, Antarctic, and Alpine Research, v. 34, p. 324–333, doi:10.1080/15230430.2002.12003501.

Licht, K.J., Dunbar, N.W., Andrews, J.T., and Jennings, A.E., 1999, Distinguishing subglacial till and glacial marine diamictons in the western Ross Sea, Antarctica: Implications for a last glacial maximum grounding line: GSA Bulletin, v. 111, p. 91–103, doi:10.1130/0016-7606(1999)111<0091:DSTAGM>2.3.CO;2.

Livingstone, S.J. et al., 2022, Subglacial lakes and their changing role in a warming climate: Nature Reviews Earth & Environment, v. 3, p. 106–124, doi:10.1038/s43017-021-00246-9.

McKay, R., Golledge, N.R., Maas, S., Naish, T., Levy, R., Dunbar, G., and Kuhn, G., 2016, Antarctic marine ice-sheet retreat in the Ross Sea during the early Holocene: Geology, v. 44, p. 7–10, doi:10.1130/G37315.1.

Mercer, J.H., 1978, West Antarctic ice sheet and CO2 greenhouse effect: a threat of disaster: Nature, v. 271, p. 321–325, doi:10.1038/271321a0.

Morlighem, M. et al., 2020, Deep glacial troughs and stabilizing ridges unveiled beneath the margins of the Antarctic ice sheet: Nature Geoscience, v. 13, p. 132–137, doi:10.1038/s41561-019-0510-8.

Mosola, A.B., and Anderson, J.B., 2006, Expansion and rapid retreat of the West Antarctic Ice Sheet in eastern Ross Sea: possible consequence of over-extended ice streams? Quaternary Science Reviews, v. 25, p. 2177–2196, doi:10.1016/j.quascirev.2005.12.013.

Mouginot, J., Rignot, E., and Scheuchl, B., 2019, Continent-Wide, Interferometric SAR Phase, Mapping of Antarctic Ice Velocity: Geophysical Research Letters, v. 46, p. 9710–9718, doi:10.1029/2019GL083826.

Neumann, B., Vafeidis, A.T., Zimmermann, J., and Nicholls, R.J., 2015, Future Coastal Population Growth and Exposure to Sea-Level Rise and Coastal Flooding - A Global Assessment: PLOS ONE, v. 10, p. e0118571, doi:10.1371/journal.pone.0118571.

Ng, F.S.L., 2000, Canals under sediment-based ice sheets: Annals of Glaciology, v. 30, p. 146–152, doi:10.3189/172756400781820633.

Nicholls, R.J., Lincke, D., Hinkel, J., Brown, S., Vafeidis, A.T., Meyssignac, B., Hanson, S.E., Merkens, J.-L., and Fang, J., 2021, A global analysis of subsidence, relative sea-level change and coastal flood exposure: Nature Climate Change, v. 11, p. 338–342, doi:10.1038/s41558-021-00993-z.

Nye, J.F., 1976, Water Flow in Glaciers: Jökulhlaups, Tunnels and Veins: Journal of Glaciology, v. 17, p. 181–207, doi:10.3189/S002214300001354X.

Priscu, J.C. et al., 1999, Geomicrobiology of Subglacial Ice Above Lake Vostok, Antarctica: Science, v. 286, p. 2141–2144, doi:10.1126/science.286.5447.2141.

Priscu, J.C. et al., 2021, Scientific access into Mercer Subglacial Lake: scientific objectives, drilling operations and initial observations: Annals of Glaciology, v. 62, p. 340–352, doi:10.1017/aog.2021.10.

Prothro, L.O., Majewski, W., Yokoyama, Y., Simkins, L.M., Anderson, J.B., Yamane, M., Miyairi, Y., and Ohkouchi, N., 2020, Timing and pathways of East Antarctic Ice Sheet retreat: Quaternary Science Reviews, v. 230, p. 106166, doi:10.1016/j.quascirev.2020.106166.

Prothro, L.O., Simkins, L.M., Majewski, W., and Anderson, J.B., 2018, Glacial retreat patterns and processes determined from integrated sedimentology and geomorphology records: Marine Geology, v. 395, p. 104–119, doi:10.1016/j.margeo.2017.09.012.

Rignot, E., Mouginot, J., Scheuchl, B., van den Broeke, M., van Wessem, M.J., and Morlighem, M., 2019, Four decades of Antarctic Ice Sheet mass balance from 1979–2017: Proceedings of the National Academy of Sciences, v. 116, p. 1095–1103, doi:10.1073/pnas.1812883116.

Roberts, M.J., Tweed, F.S., Russell, A.J., Knudsen, Ó., Lawson, D.E., Larson, G.J., Evenson, E.B., and Björnsson, H., 2002, Glaciohydraulic supercooling in Iceland: Geology, v. 30, p. 439–442, doi:10.1130/0091-7613(2002)030<0439:GSII>2.0.CO;2.

Robinson, D.E., Menzies, J., Wellner, J.S., and Clark, R.W., 2021, Subglacial sediment deformation in the Ross Sea, Antarctica: Quaternary Science Advances, v. 4, p. 100029, doi:10.1016/j.qsa.2021.100029.

Rooney, S.T., Blankenship, D.D., Alley, R.B., and Bentley, C.R., 1987, Till beneath ice stream B: 2. Structure and continuity: Journal of Geophysical Research: Solid Earth, v. 92, p. 8913–8920, doi:10.1029/JB092iB09p08913.

Rosenheim, B.E. et al., 2023, A method for successful collection of multicores and gravity cores from Antarctic subglacial lakes: Limnology and Oceanography: Methods, v. 21, p. 279–294, doi:10.1002/lom3.10545.

Röthlisberger, H., 1972, Water Pressure in Intra- and Subglacial Channels: Journal of Glaciology, v. 11, p. 177–203, doi:10.3189/S0022143000022188.

Scambos, T.A. et al., 2017, How much, how fast?: A science review and outlook for research on the instability of Antarctica's Thwaites Glacier in the 21st century: Global and Planetary Change, v. 153, p. 16–34, doi:10.1016/j.gloplacha.2017.04.008.

Scherer, R.P., Aldahan, A., Tulaczyk, S., Possnert, G., Engelhardt, H., and Kamb, B., 1998, Pleistocene collapse of the West Antarctic ice sheet: Science, v. 281, p. 82–85.

Schoof, C., 2007, Ice sheet grounding line dynamics: Steady states, stability, and hysteresis: Journal of Geophysical Research: Earth Surface, v. 112, doi:10.1029/2006JF000664.

Schoof, C., 2011, Marine ice sheet dynamics. Part 2. A Stokes flow contact problem: Journal of Fluid Mechanics, v. 679, p. 122–155.

Seneviratne, S.I., Wartenburger, R., Guillod, B.P., Hirsch, A.L., Vogel, M.M., Brovkin, V., van Vuuren, D.P., Schaller, N., Boysen, L., and Calvin, K.V., 2018, Climate extremes, land–climate feedbacks and land-use forcing at 1.5 C: Philosophical Transactions of the Royal Society A: Mathematical, Physical and Engineering Sciences, v. 376, p. 20160450.

Shreve, R.L., 1972, Movement of Water in Glaciers: Journal of Glaciology, v. 11, p. 205–214, doi:10.3189/S002214300002219X.

Siegfried, M.R. et al., 2023, The life and death of a subglacial lake in West Antarctica: Geology, v. 51, p. 434–438, doi:10.1130/G50995.1.

Siegfried, M.R., and Fricker, H.A., 2021, Illuminating Active Subglacial Lake Processes With ICESat-2 Laser Altimetry: Geophysical Research Letters, v. 48, p. e2020GL091089, doi:10.1029/2020GL091089.

Siegfried, M.R., Fricker, H.A., Carter, S.P., and Tulaczyk, S., 2016, Episodic ice velocity fluctuations triggered by a subglacial flood in West Antarctica: Geophysical Research Letters, v. 43, p. 2640–2648, doi:10.1002/2016GL067758.

Simkins, L.M., Anderson, J.B., Greenwood, S.L., Gonnermann, H.M., Prothro, L.O., Halberstadt, A.R.W., Stearns, L.A., Pollard, D., and DeConto, R.M., 2017, Anatomy of a meltwater drainage system beneath the ancestral East Antarctic ice sheet: Nature Geoscience, v. 10, p. 691–697, doi:10.1038/ngeo3012.

Souchez, R., Petit, J.R., Tison, J.-L., Jouzel, J., and Verbeke, V., 2000, Ice formation in subglacial Lake Vostok, Central Antarctica: Earth and Planetary Science Letters, v. 181, p. 529–538, doi:10.1016/S0012-821X(00)00228-4.

Sweet, W.V., Hamlington, B.D., Kopp, R.E., Weaver, C.P., Barnard, P.L., Bekaert, D., Brooks, W., Craghan, M., Dusek, G., and Frederikse, T., 2022, Global and regional sea level rise scenarios for the United States: Updated mean projections and extreme water level probabilities along US coastlines: National Oceanic and Atmospheric Administration.

Tulaczyk, S., and Hossainzadeh, S., 2011, Antarctica's Deep Frozen "Lakes": Science, v. 331, p. 1524–1525, doi:10.1126/science.1202888.

Tulaczyk, S., Kamb, B., Scherer, R.P., and Engelhardt, H.F., 1998, Sedimentary processes at the base of a West Antarctic ice stream; constraints from textural and compositional properties of subglacial debris: Journal of Sedimentary Research, v. 68, p. 487–496, doi:10.2110/jsr.68.487.

Venturelli, R.A. et al., 2023, Constraints on the Timing and Extent of Deglacial Grounding Line Retreat in West Antarctica: AGU Advances, v. 4, p. e2022AV000846, doi:10.1029/2022AV000846.

Vogel, S.W., Tulaczyk, S., Kamb, B., Engelhardt, H., Carsey, F.D., Behar, A.E., Lane, A.L., and Joughin, I., 2005, Subglacial conditions during and after stoppage of an Antarctic Ice Stream: Is reactivation imminent? Geophysical Research Letters, v. 32, doi:10.1029/2005GL022563.

Walder, J.S., 1986, Hydraulics of Subglacial Cavities: Journal of Glaciology, v. 32, p. 439–445, doi:10.3189/S0022143000012156.

Walder, J.S., and Fowler, A., 1994, Channelized subglacial drainage over a deformable bed: Journal of Glaciology, v. 40, p. 3–15, doi:10.3189/S0022143000003750.

Weertman, J., 1961, Mechanism for the Formation of Inner Moraines Found Near the Edge of Cold Ice Caps and Ice sheets: Journal of Glaciology, v. 3, p. 965–978, doi:10.3189/S0022143000017378.

Weertman, J., 1957, On the Sliding of Glaciers: Journal of Glaciology, v. 3, p. 33–38, doi:10.3189/S0022143000024709.

Weertman, J., 1974, Stability of the junction of an ice sheet and an ice shelf: Journal of Glaciology, v. 13, p. 3–11.

Weertman, J., 1964, The Theory of Glacier Sliding: Journal of Glaciology, v. 5, p. 287–303, doi:10.3189/S0022143000029038.

Witus, A.E., Branecky, C.M., Anderson, J.B., Szczuciński, W., Schroeder, D.M., Blankenship, D.D., and Jakobsson, M., 2014, Meltwater intensive glacial retreat in polar environments and investigation of associated sediments: example from Pine Island Bay, West Antarctica: Quaternary Science Reviews, v. 85, p. 99–118, doi:10.1016/j.quascirev.2013.11.021.

Zwally, H.J., Abdalati, W., Herring, T., Larson, K., Saba, J., and Steffen, K., 2002, Surface Melt-Induced Acceleration of Greenland Ice-Sheet Flow: Science, v. 297, p. 218–222, doi:10.1126/science.1072708.

CHAPTER TWO

DYNAMIC SUBGLACIAL HYDROLOGIC CONDITIONS ARCHIVED IN ANTARCTIC SUBGLACIAL LAKE SEDIMENTS

Contribution of Authors and Co-Authors

Manuscript in Chapter 2

Author: Timothy D. Campbell

Contributions: Project conception, sample preparation, data collection and analysis, manuscript preparation

Co-Author: Mark L. Skidmore

Contributions: Project conception and contributed to the manuscript.

Co-Author: Molly O. Patterson

Contributions: Field team member, project conception, assisted in lithological descriptions, advised on lithological interpretations, and contributed to the manuscript.

Co-Author: John E. Dore

Contributions: Field team member, provided porewater conductivity measurements, and contributed to the manuscript.

Co-Author: David M. Harwood

Contributions: Field team member, assisted in lithological descriptions, advised on lithological interpretations, and contributed to the manuscript.

Co-Author: Amy Leventer

Contributions: Field team member, assisted in lithological descriptions, advised on lithological interpretations, and contributed to the manuscript.

Co-Author: Alexander Michaud

Contributions: Field team member and contributed to the manuscript.

Contributions: Brad E. Rosenheim

Contributions: Field team member, assisted in lithological descriptions, advised on lithological interpretations, and contributed to the manuscript.

Co-Author: Matthew R. Siegfried

Contributions: Contributed to the manuscript.

Co-Author: August Steigmeyer

Contributions: Conducted chloride analysis of sediment porewater, and contributed to the manuscript.

Co-Author: Martyn Tranter

Contributions: Field team member and contributed to the manuscript.

Co-Author: Ryan A. Venturelli

Contributions: Field team member, developed composite depth scale, and contributed to the manuscript.

Co-Author: John C. Priscu

Contributions: Chief Scientist, project conception, and contributed to the manuscript.

Manuscript Information

Status of Manuscript:
X Prepared for submission to a peer-reviewed journal
☐ Officially submitted to a peer-reviewed journal
☐ Accepted by a peer-reviewed journal
☐ Published in a peer-reviewed journal

Abstract

There is a paucity of direct records that demonstrate the stratigraphic variability associated with the dynamic hydrologic network beneath West Antarctica's ice streams. We employed a suite of sedimentological and geochemical methods to assess the stratigraphic distribution of lithofacies and associated mechanisms from sediment cores collected from Mercer Subglacial Lake, located beneath the Mercer Ice Stream on West Antarctica. The composite 2.06 m sediment record consists of stratigraphic changes in massive-to-stratified diamict, muds, and laminated muds. Chloride concentrations throughout the entire record indicate sediment porewater is primarily derived from glacial melt with deposition under freshwater conditions. While diamicts are associated with basal ice contact conditions, sorted fine-grained mud beds below 1.4 m of the record lack coarse-grained material (>2 mm), and thus indicate deposition from suspension settling in slowly flowing (<20 cm s^{-1}) water or a ponded meltwater system. Whereas the rhythmically laminated lacustrine sediments, reflecting modern subglacial lake conditions, in the upper 0.12 m are influenced by a continuum of processes associated with the fall-out from basal ice melt, upstream meltwater input into the lake, and water column thickness changes associated with fill-drain cycles. Thus, the sedimentary facies characterize a complex subglacial hydrologic system showing that basal conditions alternated from grounded ice to water filled cavities fed and drained by subglacial fluvial networks. Our results provide new information on subglacial sediments beneath the Mercer Ice Stream that can be used to refine models of subglacial hydrology and its coupling with ice dynamics.

Introduction

West Antarctic Ice Sheet (WAIS) is drained by several fast-flowing ice streams that feed the southern Ross Ice Shelf along the Siple Coast (Figure 2.1). Water and soft, deformable saturated sediments underly these ice streams and lubricate the bed to facilitate ice flow despite low driving stresses (Alley et al., 1986; 1987; Engelhardt and Kamb, 1997; Tulaczyk et al., 1998; Kamb, 2001; Bell, 2008).

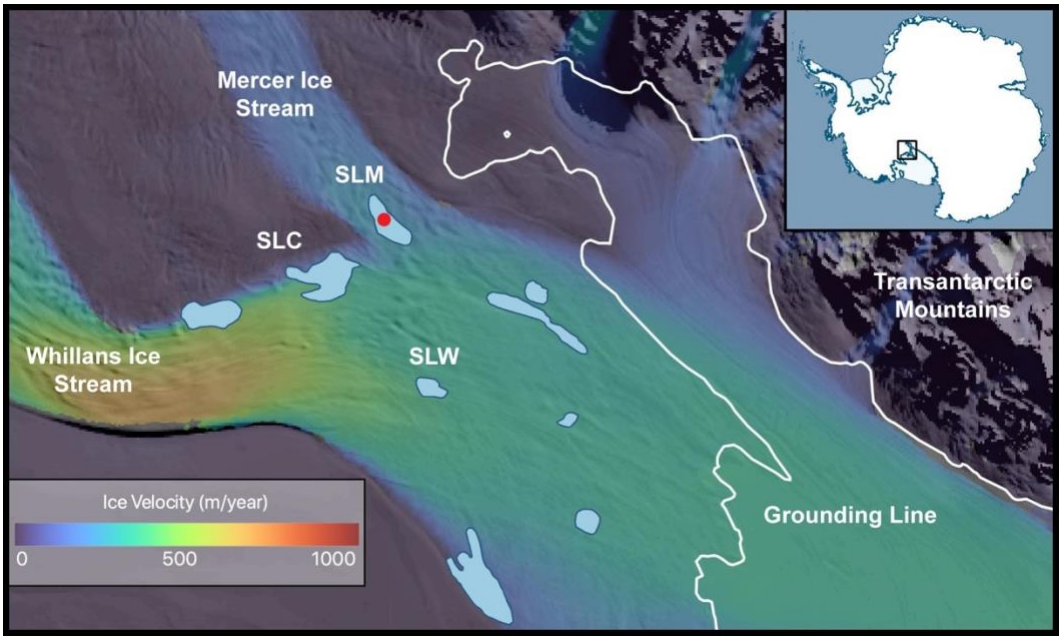

Figure 2.1 Map showing Mercer Subglacial Lake (SLM) and its location at the confluence of the Mercer and Whillans Ice Streams, West Antarctica. Drill site at SLM is shown by a red dot. Surface ice velocity (Mouginot et al., 2019), subglacial lake outlines (Siegfried and Fricker, 2021), and modern grounding line position (Depoorter et al., 2013) are shown superimposed on a satellite image mosaic (Scambos et al., 2007).

Over decadal to millennial time scales these ice streams are highly variable and exhibit large velocity changes (Beem et al., 2014; Hulbe et al., 2016; Siegfried et al., 2016), switches in flow direction (Conway et al., 2002; Catania et al., 2012; Hulbe and Fahnestock, 2007), and

stagnation-reactivation cycles (Catania et al., 2006; Retzlaff and Bentley, 1993), which can have a profound influence over ice sheet mass balance. Almost half of the net ice loss from WAIS is offset by the positive mass balance along the Siple Coast (Pritchard et al., 2009; Rignot et al., 2019), which is partially attributed to the stagnation of Kamb Ice Stream (KIS) ~170 years ago and the deceleration of Whillans Ice Stream (WIS) (Joughin and Tulaczyk, 2002; Beem et al., 2014). Because ice flow variability is largely modulated by the generation and routing of subglacial meltwater (Alley et al., 1989; Anandakrishnan and Alley, 1997; Carter et al., 2013; Christofferson et al., 2010; Elsworth and Suckale, 2016; Siegfried et al., 2016), it is plausible that changes in the distribution of basal meltwater could trigger future ice stream reorganization and reduce the positive mass balance of Siple Coast sector within the near future (10s – 100s of years) (Bougamont et al., 2015; Siegfried et al., 2023).

Direct observations and geologic records from beneath the Siple Coast ice streams are spatially limited but are critical to understanding the development of subglacial hydrologic systems and their influence on ice stream dynamics. At least 675 subglacial lakes have been identified beneath the Antarctic ice sheet (Livingstone et al., 2022), many of which are “active”, filling and draining on sub-decadal timescales and transporting large volumes of water through a connected hydrologic system (Fricker et al., 2007; Siegfried & Fricker, 2018, Siegfried & Fricker, 2021). Sediments recovered from beneath fast flowing ice streams with active subglacial lake systems can potentially archive environmental change, providing insight into subglacial processes beyond the modern instrumental record as well as environmental conditions before lake formation (Bentley et al., 2011; Yan et al., 2022; Siegfried et al 2023). Sediments from Whillans Subglacial Lake (SLW), the only other WAIS subglacial lake sampled directly prior to

this study, were comprised of massive diamict and interpreted as subglacial till deposited by grounded ice from the Whillans Ice Stream (Hodson et al., 2016). No record of *in situ* subglacial lake sedimentation or erosional surfaces were found in the SLW sediments (Hodson et al., 2016). However, evidence for paleo-subglacial lake and relict meltwater deposits have been observed from the deglaciated continental shelf (Prothro et al., 2018; Simkins et al., 2017) as well as offshore from Pine Island Glacier (Kuhn et al., 2017; Lepp et al., 2022; Witus et al., 2014), and the laminated sediments from Mercer Subglacial Lake (SLM) (Siegfried et al. 2023). Here we describe the stratigraphy distribution of lithofacies (hereinafter referred to as facies) of the 2.06 m sediment sequence from SLM, located beneath Mercer Ice Stream, West Antarctica, (Figure 2.1) to reconstruct the evolution of basal and subglacial hydrologic conditions throughout the geologic history.

Methods

During the 2018-2019 field season, SLM was cleanly accessed using a hot water drill to melt a 1087 m deep borehole into the 15 m deep lake water cavity (Priscu et al., 2013; Michaud et al., 2020; Priscu et al., 2021). Sediment cores collected included a series of 0.06 m diameter multicores that preserved the sediment-water interface and recovered up to 0.49 m of sediment, as well as longer 0.10 m diameter gravity cores that extended to 1.72 m (Supplementary Table 1.1) (Rosenheim, Michaud et al., 2023). A composite 2.06 m record was obtained by correlating all cores collected within ~ 5 m of each other using multiple physical parameters and standard splicing methods (Hagelberg et al., 1992; Lisiecki et al., 2007). The lateral ~5 m core offset resulted from 0.64 m day^{-1} downstream ice movement and ensured that each core was retrieved from undisturbed sediment (Priscu et al. 2021).

Core Collection

The lake cavity was accessed via a ~0.4 m diameter borehole through the overlying ice (1,087 m) using a hot water drill and following clean access protocols (Priscu et al., 2013; Michaud et al., 2020). Cores recovered adjacent sediments but avoided penetrating the same location due to ice movement. Short sediment cores (0.06 cm diameter) were collected using a three-barrel UWITEC multicoring device (Rosenheim, Michaud et al., 2023). In total, 10 multicores (0.3 – 0.5 m long) were collected over 4 deployments with undisturbed sediment water interfaces. Cores from the first multicorer deployment are described here (01UW-A, 01UW-B, and 01UW-C; Supplementary Table 1.1). Two longer cores (1 and 1.7 m long) were collected using a free-fall gravity corer (Rosenheim, Michaud et al. 2023) and are hereafter referred to as 01FF and 02FF. Cores 01UW-A, 01UW-C, 01FF and 02FF were stored and shipped upright at 4˚C to the Marine and Geology Core Repository at Oregon State University (OSU).

Sediment Cores

Computed tomography (CT) scans were performed on unsplit cores using a Toshiba Aquilon 64 Slide Medical CT Scanner. The resulting high-resolution CT images were processed using SedCT MATLAB to produce a coronal slice through the center of each core at an effective pixel resolution of 0.5 x 0.5 mm and a vertical interval of 0.25 mm (Reilly et al., 2017). The quantitative data were stored in pixels as relative gray scale values or Hounsfield units (HU) (Hounsfield, 1973). HU are defined as the attenuation coefficient of the sediment relative to water. By this definition, the HU value of water is 0 and the HU value of air is −1000. HU values are dependent on sediment density (Hounsfield, 1973; Reilly et al., 2017). CT HU values were

converted to wet bulk density (WBD) following methods of Reilly et al. (2017) for fine-grained glacial sediments using the equation:

$$\text{Wet Bulk Density (g cm}^{-3}) = (8 \times 10^{-4})\text{HU} + 1.$$

The coarse clastic material was quantified for each sediment core using the CT scans and an automated image analysis code that counted the number of clasts greater than 2 mm (but less than 60 mm and 100 mm, the core diameters – hereafter >2 mm) per coronal slice using the algorithm from Reilly et al. (2019). Clast numbers were normalized to 10 cm^3 volumes based on core diameter and coronal slice thickness of 2 cm. For example, a 2 cm thick slice of the 6 cm diameter core would have a volume of 5.66 x 10 cm^3. This provided an automated and objective method but should be considered as a clast index rather than an absolute count of grains >2 mm (Reilly et al., 2019). 3-dimensional surface rendering was performed in open-source software Horos to create images of clast distribution using a specific attenuation value of 2000 to remove the fine-grained, low-density matrix sediment, leaving the high-density coarse-grained material, following Ketcham and Carlson, (2001) and Reilly et al., (2019).

Following CT scanning, cores were split, visually described using classification schemes for poorly sorted terrigenous clastic sediments containing gravel (Moncrieff 1989) and photographed using a GEOTEK Line Scan Camera at OSU. Gamma ray attenuation bulk density (GD) was logged for split cores using a GEOTEK Multi-Sensor Core Logger (MSCL) at 1 cm intervals. GD was calculated using the second order polynomial equation:

$$\ln(GA) = A(GD \times H)^2 + B(GD \times X) + C.$$

where H is core thickness, GA is MSCL-measured gamma attenuation, and A, B, and C are coefficients. Sediment porosity values were calculated using the equation:

$$FP = (MGD - GD) / (MGD - WD).$$

where FP = fractional porosity, MGD = mineral grain density (g cm^{-3}) (used 2.75), GD = gamma density as determined by the gamma density processing panel, WD = fluid phase density (g cm^{-3}; assumed to be 1.00). We have assumed that: 1) the sediment is fully saturated with either water or air 2) mineral grain density is constant 3) fluid density is constant. Absolute porosity values presented here are likely higher than *in situ* conditions due to the production of air-filled voids in the cores created by degassing as the cores equilibrated at the surface upon collection. Thus, changes in MSCL porosity downcore should be treated relatively, assuming degassing was constant throughout the cores.

X-ray fluorescence (XRF) elemental profiles were made on the split core at 0.5 mm intervals using an ITRAX XRF Core Scanner at the OSU Marine and Geology Repository. Sediment shear strength was measured with a handheld Torvane shear tester on split cores at discrete intervals down core.

A continuous sedimentary record was constructed by correlating cores using bulk density, elemental composition (XRF data), and porewater conductivity, with standard splicing methods (Hagelberg et al., 1992; Lisiecki et al., 2007). The core top of 01UW-A from our first deployment of the multicorer represents the sediment water interface with lengths of 5.5 cm, 109 cm, and 30 cm added to the measured core depths of 01UW-C, 01FF, and 02FF, respectively, to generate the composite record. We observed no indication of core stretching or compaction between cores and only use offset lengths to correlate them.

Grain Size Analysis

Particle size distribution of the sediment matrix (<2 mm, i.e., sand-silt-clay fraction) was measured at 10 cm intervals over the entire core. Approximately 1 g of sediment was transferred into 50 ml plastic centrifuge tubes containing 30 ml of 2.5 g L^{-1} sodium hexametaphosphate solution as a dispersant agent modified from Sperazza et al. (2004). Samples were subjected to gyratory shaking at 200 rpm for at least 10 h and then wet-sieved at 2 mm to remove gravel, before analysis on a Malvern Mastersizer 3000 (Sperazza et al., 2004). For each analysis, the Mastersizer 3000 made five measurements that were averaged by the Mastersizer software to produce a single grain size output. Each sample was analyzed three times following this methodology and the average distribution, presented here, was calculated manually.

Bulk Mineralogy

Bulk mineral identification of the <63 μm fraction of the sediments was determined using X-ray powder diffraction (XRD) following Moore and Reynolds (1989). Samples were dried at 95°C for 24 h and crushed using a mortar and pestle to disaggregate and homogenize, sieved <63 μm to remove large nodules, and then loaded on XRD slide holders to ensure full crystallite randomization. XRD analyses were conducted using a Scintag X1 Diffraction System with Cu K alpha X-rays generated with a 40 kV beam voltage and 45 mA beam in the range 2–72° 2Θ, with a step size of 0.02° 2Θ and a measuring time of 2 s per step. All mineral identifications and semi-quantitative estimates were completed using MDI JADE 6 software.

Organic Carbon and Inorganic Carbon

Samples were taken at 10 cm intervals over entire cores (01UW-A, 01FF and 02FF) with additional samples collected at lithological transitions to determine total carbon (TC) and total

organic carbon (TOC) using a Thermo Finnigan Elemental Analyzer. Total inorganic carbon (TIC) was calculated as the difference between the TC (unacidified) and TOC (acidified after fuming concentrated (12N) HCl for 24h) values (Meyers and Teranes, 2002).

Porewater Conductivity and Chloride Concentrations

Samples of sediment pore water were extracted at 2 cm depth intervals through pre-drilled holes from core 01UW-B using syringes attached to MicroRhizon samplers (0.15 μm pore size; Michaud et al., 2016). The filtrate was distributed into acid-washed vials. Sediment samples (25 cm^3 and 35 cm^3, respectively), were collected with cut-off plastic syringes from whole rounds of core 01FF at two depths (154-159 cm and 189-194 cm); pore waters from these samples were similarly extracted using MicroRhizons. Specific conductance was determined in the field using an Oakton cup-style sensor; the two deeper samples were diluted with 18.2MΩ water prior to analysis. Pore water vials for major ions (including chloride) were frozen in the field, thawed in the laboratory, and diluted with 18.2MΩ water before analysis on a Metrohm Peak Ion Chromatograph as described in Hawkings et al. (2020).

Analysis of Variance in Physical Properties

Kruskal-Wallis tests were used to assess the probability of statistically significant differences in the clast counts, bulk density, porosity, magnetic susceptibility, and Ca/Fe ratio between lithostratigraphic units (1- 4), Supplementary Figure 1.1 and Supplementary Table 1.2; McKnight and Najab, 2010). Statistically significant differences provided a quantitative method to support boundaries drawn based on visual appearance between the lithostratigraphic units (LU1- LU4) and to aid in grouping of units into facies associations (facies 1-3).

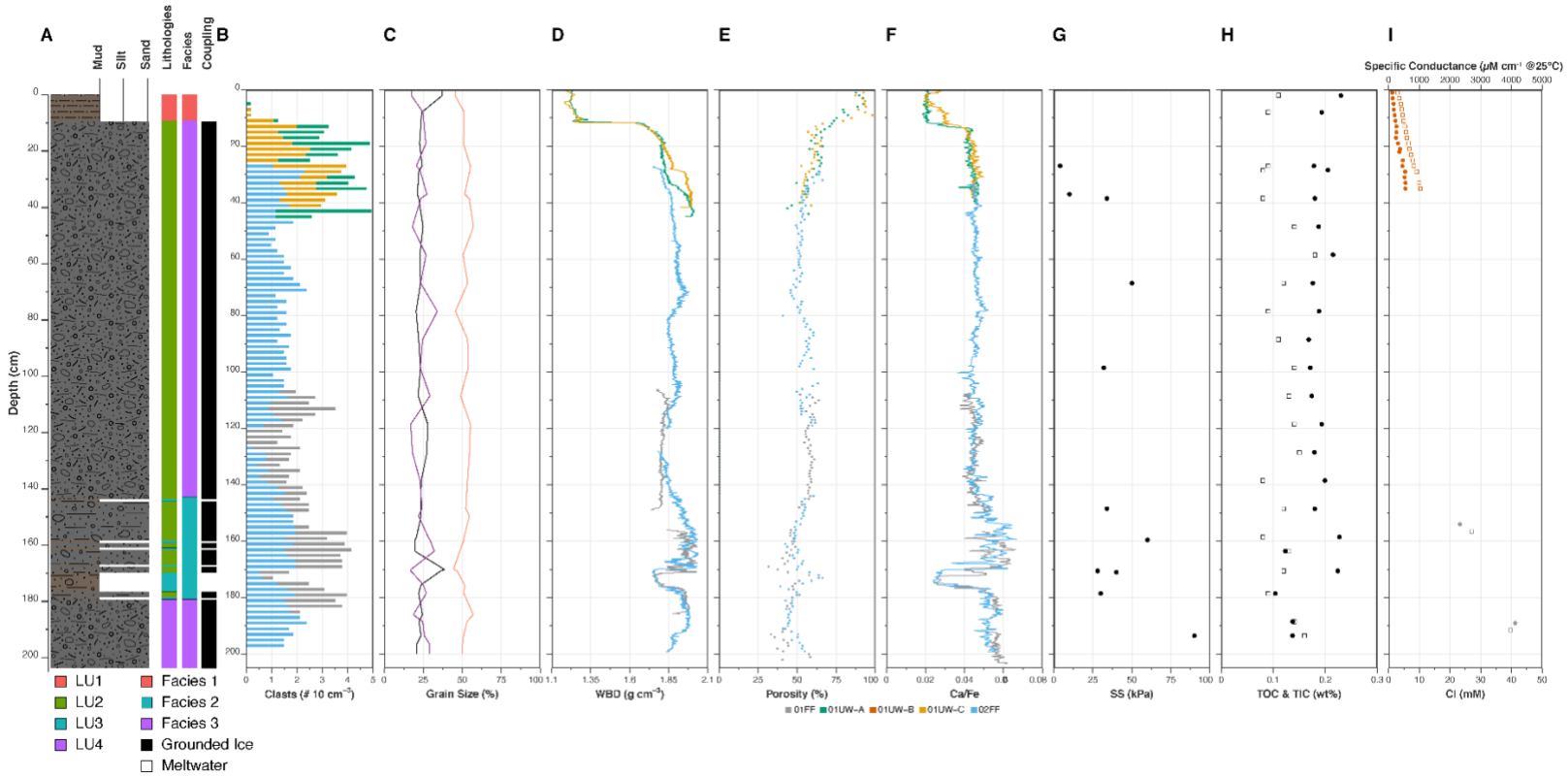

Figure 2.2 Lithostratigraphic units and sedimentological profiles of sediment cores from SLM, West Antarctica. (A) Lithostratigraphic units based on lithological changes that are grouped into facies associations which reflect ice-bed coupling. (B) Clast counts per 10 cm3, based on CT analysis (2 cm interval). (C) Particle size analysis of sediment matrix (10 cm interval), Clay – purple, Silt – orange, Sand – black. (D) Sediment wet bulk density (WBD) (g cm^{-3}) (0.025 cm interval). (E) Sediment porosity (1 cm interval). (F) Ca/Fe from XRF (0.05 cm interval). (G) Shear strength (H) Weight % total organic carbon (TOC) (closed circle), weight % total inorganic carbon (TIC) (open circle) (I) Chloride concentration (open square) and specific conductance of the sediment porewater at 25°C (closed circle) (2 cm intervals for 01UW-B; discrete samples from 01FF). Unit designation LU1 – LU4 and Facies associations 1- 3, see text for full details. Cores for high resolution records, panels B, D, E, & F: Green = 01UW-A, Orange = 01UW-B, Yellow = 01UW-C, Grey = 01FF, Blue = 02FF (See Supplemental Table 1.1 for full details on the cores)

Results

Lithostratigraphic Units

The SLM stratigraphy is composed of four main lithologic units (LUs) that are clearly observed in CT imagery and characterized by differences in physical properties, grain size distributions, clast abundance, and XRF inorganic geochemistry (Figures 2.2 and 2.3). Tables 2.1 and Supplementary Table 1.2 summarize the distinctions between each of the four units and show the distribution of three statistically significant facies associations that are used to interpret the paleoenvironmental history of the Mercer Ice Stream.

Lithostratigraphic Unit 4

The lowermost lithologic unit (LU4) contains a 0.31 m thick (179 – 206 cm below surface) massive matrix-supported muddy diamict (following Moncrieff, 1989) and was recovered only in cores 01FF and 02FF (Figures 2.2 and 2.3). This unit contains abundant granule (2-4 mm) and pebble-sized (4-64 mm) clasts that account for a high mean wet bulk density (1.94 ± 0.04 g cm^{-3}) and volume-specific magnetic susceptibility (dimensionless) (74 ± 13 SI x 10^{-5}) (Figure 2.2 and Supplementary Table 1.2). This clast-rich (5-30 vol. %) diamict is very poorly sorted (defined as SD = 2.7) as defined by Folk and Ward (1957). Grain size distribution is composed of predominantly an 8 μm, silt mode (52 vol.%), with contributions of sand (25 vol.%) and clay (23 vol.%), warranting the mud-rich designation (Figure 2.4). The pebble fraction is composed of sub-rounded to rounded clasts, whereas angular- and subangular-shaped clasts are uncommon and supported by a mud matrix (Figures 2.2C, 2.3D, 2.3E, 4, and 2.7A). This unit is macroscopically structureless and homogenous in composition based on bulk mineralogy, TOC and TIC (Figure 2.2H and 2.8), and MSCL porosity varies from 35 – 55% (Figure 2.2E). The

single shear strength value in the unit was 90 kPa, the highest measured in the entire sedimentary sequence (Figure 2.2G). The mean Ca/Fe and K/Ti are 0.05 ± 0.003 and 1.5 ± 0.07, relatively higher compared to the mud beds and laminae of the overlying LU3 (Figures 2.2F, 2.7D – E, Supplementary Table 1.2). The Ca/Fe ratio is a proxy for textural variations within a sedimentary unit as it corresponds closely with mean grain size, with a lower ratio consistent with a smaller average grain size (Rothwell et al., 2006). The upper boundary is sharp and highlighted in CT imagery (Figures 2.3D – E, 5).

Lithostratigraphic Unit 3

LU3 comprises matrix-supported, stratified diamict with a massive gray mud bed and laminae (<1 cm to 5 cm thick laminae and beds). This unit extends from the top of LU4 to 142 cm below surface. Mud and laminae are best observed in CT images rather than visually on the split core face (n = 6) (Figures 2.3D – E, 2.4). The darker coloring in the CT-scanning images compared to the diamict matrix is due to the enrichment of clay-sized particles (<4 μm; 38.5 vol. %) over sands (17.1 vol. %) in the sediment matrix (lighter coloring = coarser grains = higher bulk density) (Figures 2.3D – E, 2.5). These muds are separated by diamict beds. Although the sediment matrix material in the diamict is classified as very poorly sorted (Folk and Ward, 1957), we describe this unit as relatively well sorted due to the absence of granule and pebble-sized clasts within the muds following Prothro et al (2018) and relative to LU 4. There is an overall decrease in wet bulk density (1.79 ± 0.04 g cm^{-3}) and Ca/Fe, K/Ti, as well as an increase in porosity compared to the underlying LU4 because coarser sediments tend to have a lower porosity and higher bulk density (Figures 2.2D – E, 2.4B – C, S1). Compositional analysis of the

silt and clay fraction (< 63 µm) shows an increase in the abundance of clay minerals, which is likely due to an increase in the particles < 4 µm in diameter (Figures 2.8).

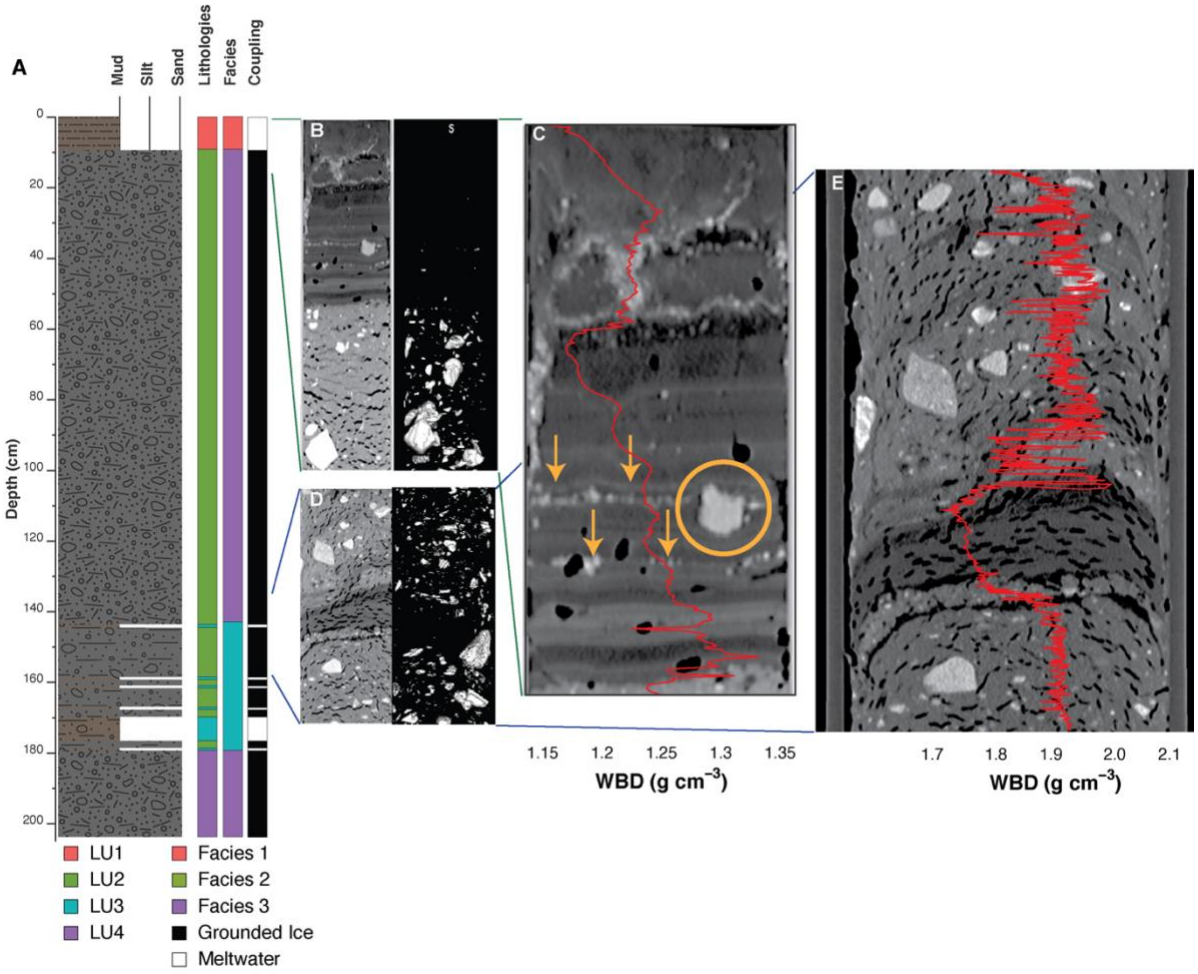

Figure 2.3 Characteristics of facies 1 – 3 from SLM sediment cores highlighted using X-ray computed tomography (CT) images. (A) Lithostratigraphic units based on lithological changes are grouped into facies associations which reflect ice-bed coupling (from Figure 2.2). (B) Complete CT image (left panel) and slices from 3-D surface rendering - sediment matrix has been rendered black (right panel) showing contact between facies 1 and facies 2. (C) CT image slice of top 11.5 cm (facies 1) of 01UW-C and overlain by CT Wet Bulk Density (WBD) in red. Note the dropstone (circled) and the coarse sand beds at ~8 cm and ~9 cm (arrows) See also Figure 2.5. Note, the top 4 cm of the core exhibit signs of disturbance from coring. (D) Complete CT image (left panel) and slices from 3-D surface rendering - sediment matrix has been rendered black (right panel) showing contact between facies 2 and facies 3. Pebbles are absent in the mud bed and laminae of facies 3 (dark sediment) (E) CT image slice and overlain by CT WBD (red) of 01FF (156-186 cm) shows transition from facies 2 (lighter coloring, high density) interbedded

with facies 3 (dark sediment, low density) and highlights massive mud bed (5 cm) and laminae (<1 cm) (facies 3) interbedded with massive clast-rich diamict (facies 2). Dark circles are voids in the core created by degassing.

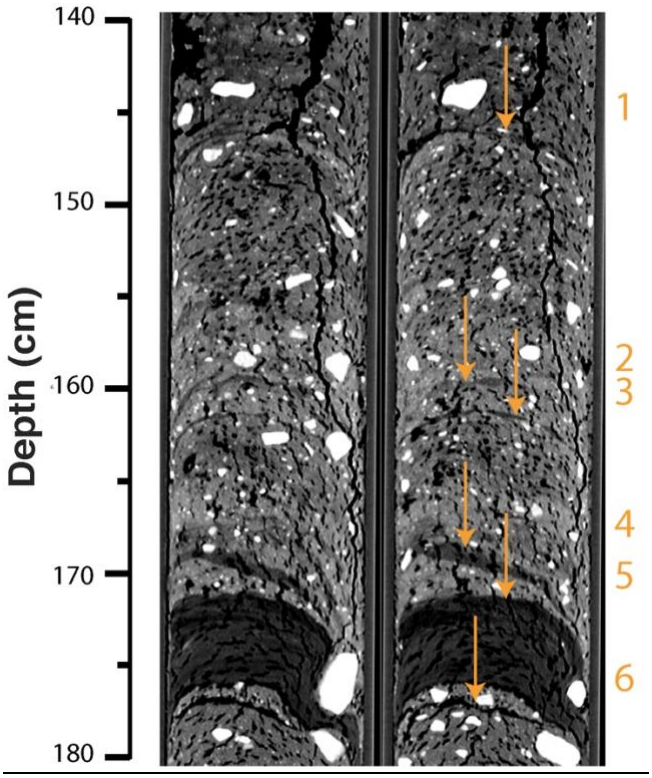

Figure 2.4 Stratified diamict (facies 2), in SLM sediments in X-ray computed tomography images. The stratification results from the interbeds comprised of massive muds (n = 6); orange arrows and numbered sequentially downcore. Images are from core 02FF-2.

Lithostratigraphic Unit 2

LU2 extends from 11.5 – 142 cm, and is a second matrix-supported, massive diamict ~130 cm thick) containing large granule to pebble-sized clasts (5-30%) (Figures 2.2 and 2.3). LU2 is characterized by a mean bulk density of 1.87 ± 0.07 g cm^{-3}, mean Ca/Fe (0.05), and abundant clast content (Figures 2.2 and Supplementary Figure 1.1). LU2 displays textural and compositional similarities to LU4 (Figures 2.2 – 5, S1, Supplementary Table 1.2). The top 15 cm of LU2 has increased porosity relative to the lower part of the unit (Figures 2.2E). This sediment

also shows a lower bulk density (HU #) which reflects an increase in the void ratio (Figure 2.2D). The shear strength of this upper 15 cm is lower than the underlying sediments of the same unit (Figure 2.2G).

Lithostratigraphic Unit 1

LU1 extends from 11.5 cm below the surface to the top of the cored sequence. It consists of planar laminated muds, with interbedded coarse beds. LU1 was only recovered in cores 01UW-A and 01UW-C, multicores that captured an undisturbed sediment-water interface; core 01UW-B was sacrificially sampled for pore waters in the field. The millimeter-scale sorted silt and clay laminae are a key characteristic of this unit and exhibit normal as well as reverse grading (light and dark transition in CT scans; Figures 2.3C and 2.6) and are stacked rhythmically at ~1 cm frequency and totaling 8 "cycles" (Figure 2.3C). The matrix contains sand-sized grains (< 17.4 vol. %) in addition to the large silt and clay fraction (45.5 and 37.2 vol. %, respectively) (Figures 2.4 & 2.5A). There are distinctive coarse laminae within the unit, the most prominent at 9.3 cm and 10.8 cm (Figure 2.6). These contain numerous granules and very coarse sand grains (Figures 2.2 and 2.3A – B). Additional laminae are observed at depths of 5.7 and 6.7 cm but with fewer, very coarse sand grains (1-2 mm diameter) (Figure 2.6). Layers of very coarse sand to granules were also evident at depths of 2.5 and 4 cm; however, this portion of the sequence showed disturbance due to coring and handling; hence, further analysis of these laminae was not carried out. A ~1 cm diameter clast is associated with the coarse laminae at 9.3 cm, which deforms the underlying sediments (Figures 2.3C and 2.6). LU1 is soft, unconsolidated, and water saturated. The MSCL porosity values (88 ± 7%) account for the low bulk density (1.24 ± 0.03 g cm^{-3}), which highlights the transition between this unit and the

underlying diamict of LU2 (Figures 2.2D-E, 2.3B). The XRF Ca/Fe also shows the LU1-LU2 contact as this unit has a lower average value of 0.02 ± 0.003 relative to LU2 (Figures 2.2F and S1).

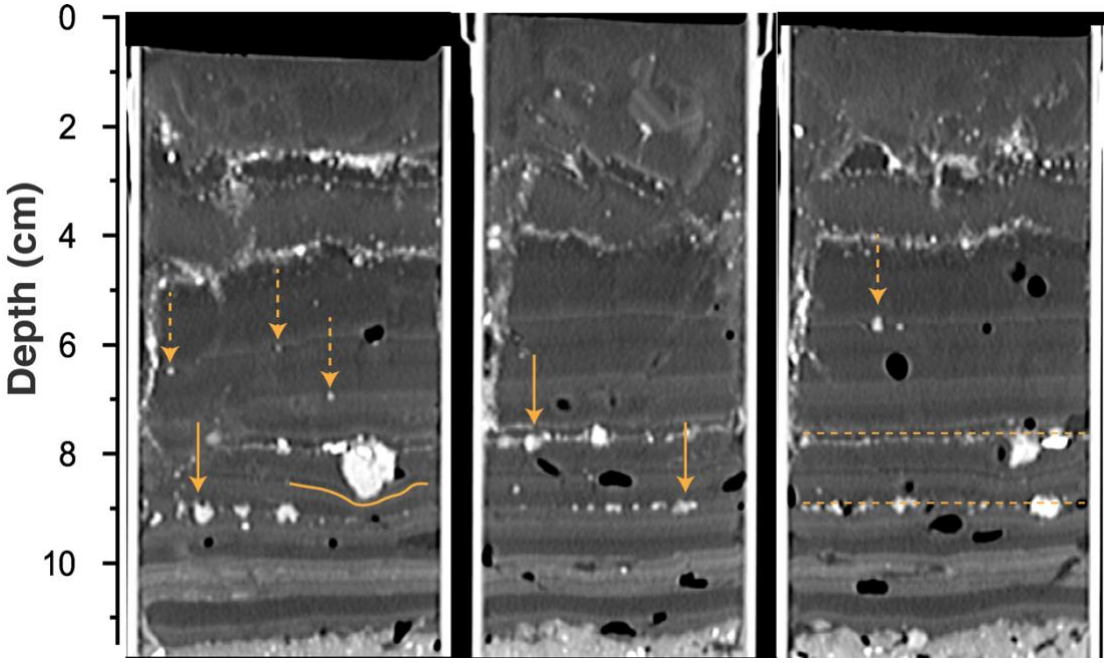

Figure 2.5 Sedimentary features in laminated sediments (facies 1) from SLM highlighted in X-ray computed tomography (CT) images. The features are highlighted in slices from 3-D surface rendering of CT images from 3 different planes of view spaced at 50o. Note the dropstone at 8-9 cm that depresses the underlying laminae, (orange line) as well as the extensive (n = > 10 coarse sand and granule-rich laminae at 8 cm and 9 cm (solid orange arrows and dashed orange lines). Laminae with dispersed (2-3) coarse grains are observed at 6 and 7 cm (dashed orange arrows). Dark circles are voids in the core created by degassing. Images are from core 01UW-C.

Lithostratigraphic Statistical Comparison

Kruskal-Wallis tests were used to assess statistical differences in the bulk density, porosity, and XRF data between the lithostratigraphic units (McKnight and Najab, 2010) (Figures 2.5D – E, Supplemental Figure 1.1). P-values from Kruskal-Wallis multiple pairwise-comparison tests show that all units are statistically different for all properties (p-values < 0.05),

and provide an independent measure to support the boundaries designated between the lithostratigraphic units. Similarities in clast abundances, grain size distributions, and bulk densities between LU2 and LU4 support grouping these lithologies into a common facies association (Facies 3). While LU3 and LU1 share similar grain size distributions, the difference in structure (Figure 2.3) supports differentiating these two lithostratigraphic units into separate facies (Table 2.1).

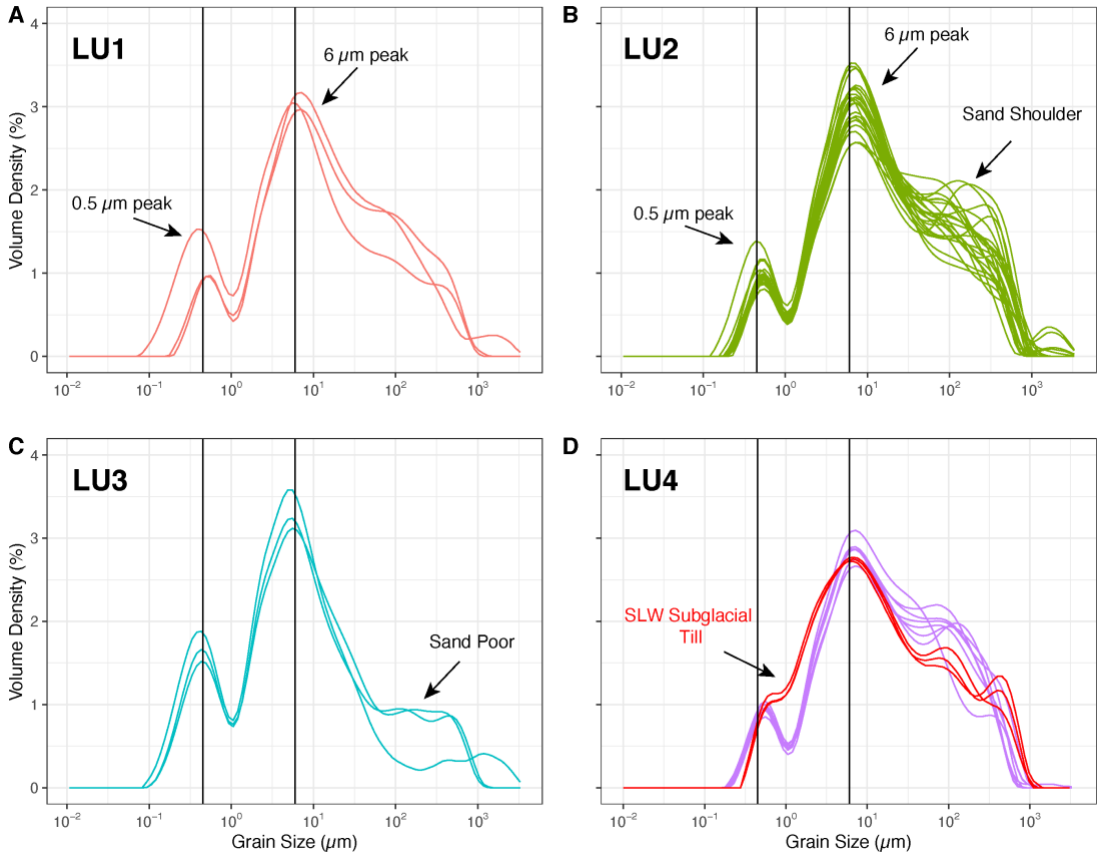

Figure 2.6 Grain size distributions of SLM sediment matrix (< 2 mm) by lithostratigraphic unit (LU 1-4). A) LU1 exhibits a bimodal distribution with dominant 0.5 µm and 8 µm modes. B) LU2 contains the fine-grain modes of LU1 but includes a sand shoulder. C) LU3 exhibits textural similarity to the sand-poor meltwater deposits from the Ross Sea (Prothro et al., 2018). C) LU4 (purple lines) displays textural similarity to LU2 and subglacial till from Subglacial Lake Whillans (SLW) (red lines) (data from Hodson et al., 2016).

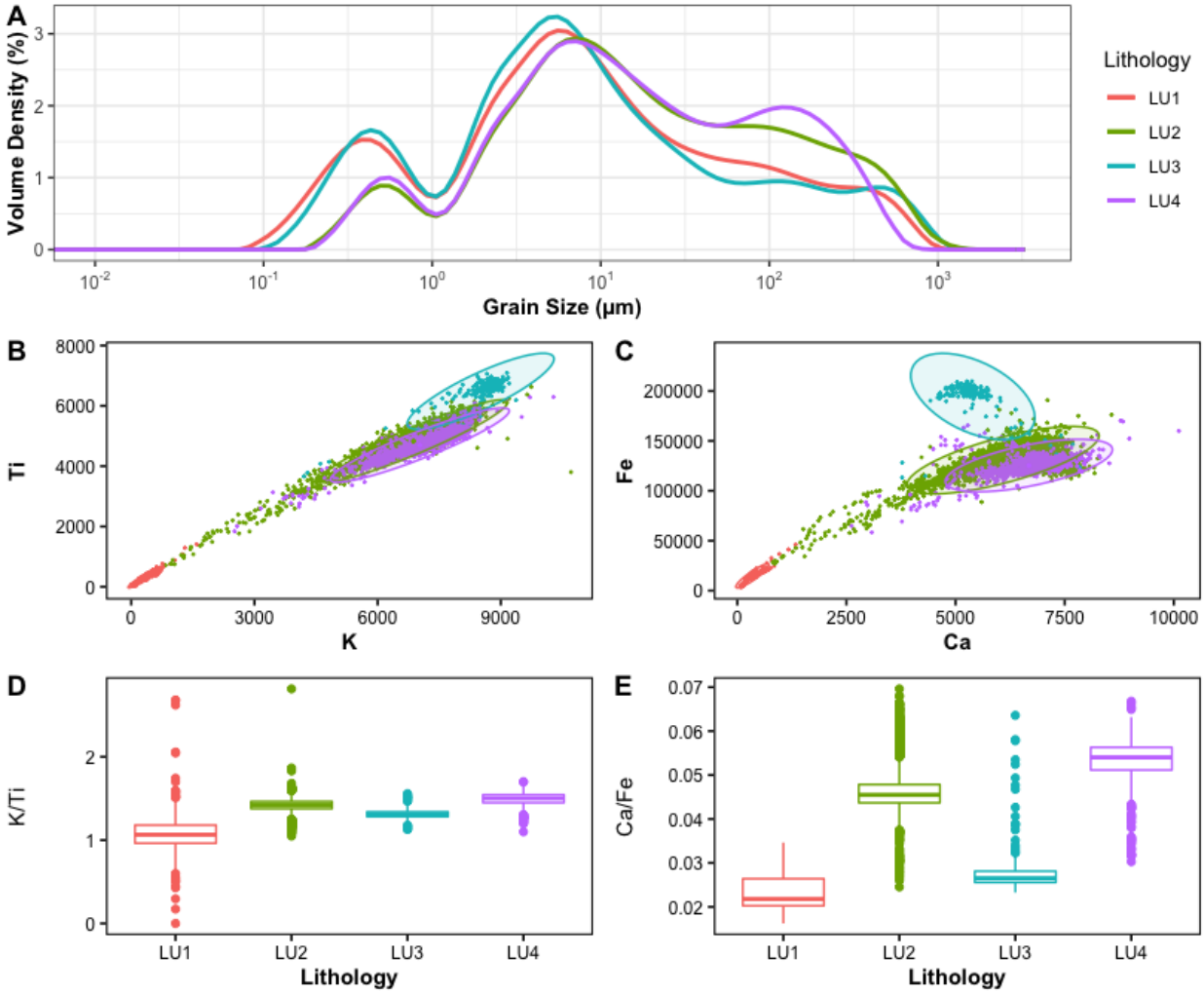

Figure 2.7 Physical and geochemical characterization of SLM sediments by lithostratigraphic unit. (A) Grain size distribution of sediment matrix (< 2 mm). XRF elemental counts of: (B) Ti vs K and (C) Fe vs Ca. Ellipses are drawn using a 95% confidence level for a multivariate t-distribution for each unit. Box plots showing the following summary statistics of (D) K/Ti and (E) Ca/Fe data: minimum (bottom whisker), lower quartile (box bottom), median (bold line), upper quartile (box top), maximum (top of whisker) and outliers (points).

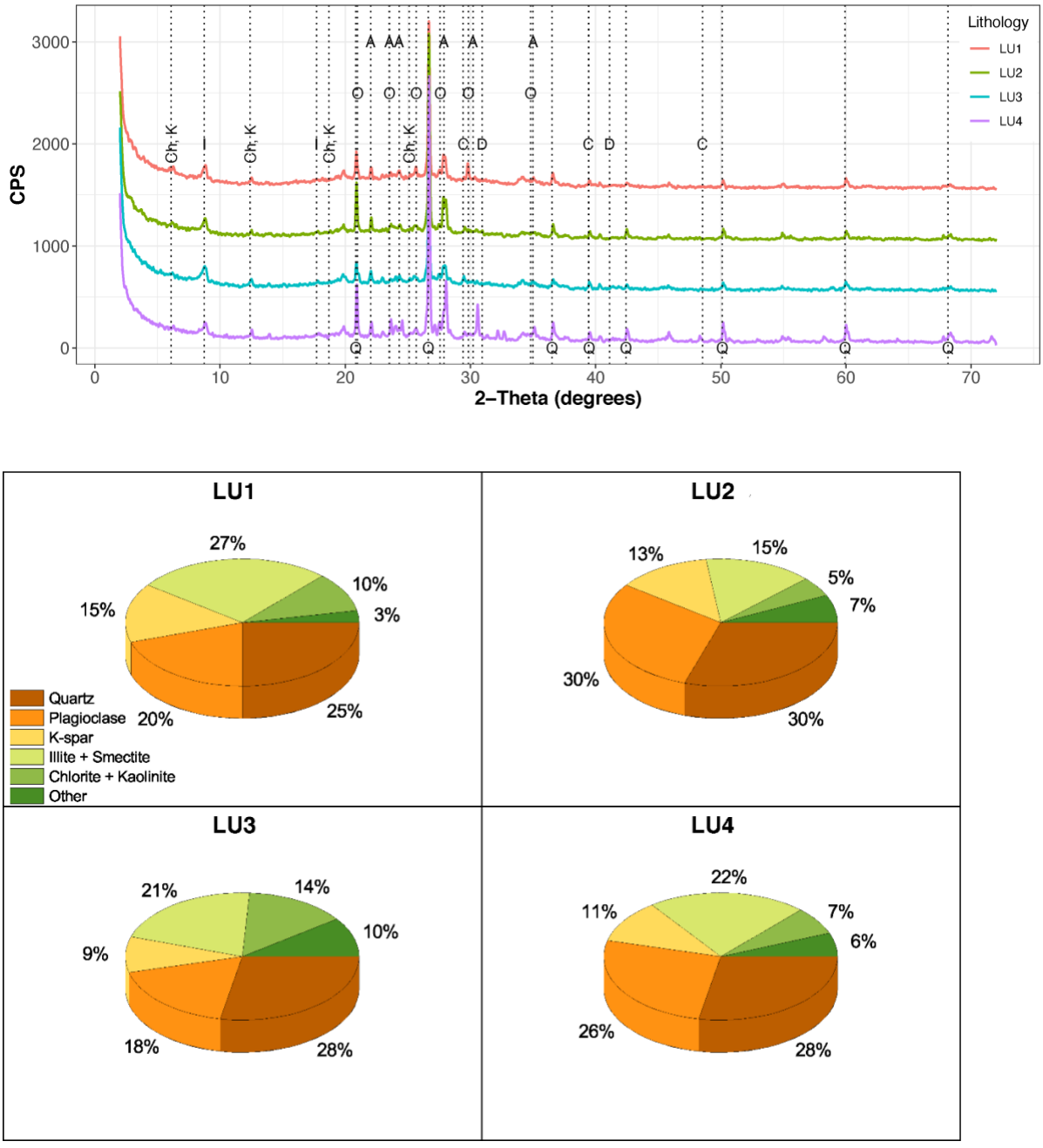

Figure 2. 8 Mineralogy of the mud fraction (<63 µm) in SLM sediments by lithostratigraphic unit. X-ray diffraction (XRD) spectra of the four lithostratigraphic units(LU1 – LU4) (top). Spectra are sequentially offset by 500 cps to reduce overlap. Ch: Chlorite, K: Kaolinite, I: Illite, Ab: Albite, Q: Quartz, O: Orthoclase, D: Dolomite, D: Calcite. Pie diagrams showing percentages of the major mineral components for the four lithostratigraphic units (1-4) determined by XRD (bottom). Full details are presented in Supplementary Table 1.3. The legend lists the phases as they appear clockwise in the diagram, starting with quartz in lower right.

Table 21 Summary of the facies (1 – 3) in SLM sediments based on common lithologic properties and the interpretation of the depositional processes and environments. LU = lithostratigraphic units.

Facies	LU	Description	Facies	Process[es]	Environmental Setting
1	1	Laminated silt and clay with occasional granule. Soft, water saturated. Relatively low values in bulk density, magnetic susceptibility, and Ca/Fe. Minor deformation structures underlying drop stones	Rhythmically interlaminated muds with coarse thin granule beds and dispersed clasts (Lsc)	Changes in sedimentation rate and sorting due to variable sediment content and pulsed/punctuated delivery from: i) fall-out from basal ice melting and, ii) upstream meltwater input into the lake	Subglacial lake
2	3	Fine-grained and massive muds, pebbles and gravel absent. Low bulk density, magnetic susceptibility, and Ca/Fe	Mud laminae/bed interbedded with diamict (stratified diamict) (SDi)	Suspension settling of fine-grained sediments from slowly flowing or ponded meltwater	Grounded ice punctuated with periods of ice bed separation due to subglacial meltwater
3	2 and 4	Very poorly sorted (clays – gravel), lacks sedimentary structure, high bulk density, magnetic susceptibility, Ca/Fe.	Massive, clast-rich matrix supported diamict (MDi)	Lodgement and deformation	Grounded ice

Mineralogy and Carbon Content

The fine-grained SLM sediments (<63 μm) were primarily composed of common silicate minerals such as quartz, feldspars (albite and orthoclase), and clay minerals (smectite, chlorite, illite, kaolinite) (Figure 2.8 and Supplementary Table 1.3). The major mineral species were common to the four units but did show some differences in relative abundances between units. Notably, LU1 and LU3 are comprised of higher amounts of clay minerals relative to quartz and feldspars (Figure 2.7). This variability is likely due to an increase in the clay size fraction (< 4 μm) observed in units LU1 and LU3 compared to LU2 and LU4 (Figures 2.4 & 2.7A). Similar to bulk mineralogy, total organic and inorganic carbon showed limited variability down core (Figure 2.2H).

Porewater Chemistry

To complement the sedimentological analysis, we analyzed chloride ion concentration and specific conductance as proxies for the salinity of the sediment pore waters. Chloride concentrations in the sediment pore water increased down the core from 1.2 mM at the sediment-water interface (core top) to 41.2 mM at the bottom (200 cm) (Figure 2.2I). Specific conductivity also increased with depth, with values of the water column, sediment-water interface, and bottom of core record of 224, 281, and 3,975 μS cm^{-1}, respectively. We used a two-component mixing model of Cl^- concentration to determine the percentage of glacial meltwater and seawater in the SLM lake and pore water (Michaud et al., 2016; Phillips and Gregg, 2001), with Cl^- concentration of 547 mM as the seawater endmember and 0.010 mM as the freshwater endmember, based on the highest snowpack Cl^- concentrations for interior West Antarctica

(Kreutz and Mayewski, 1999). The maximum likely seawater component of the porewaters increased from 0.2% at the sediment-water interface to 7.3% at the bottom of the record.

Discussion

Environmental Interpretation

Chloride (Cl^-) is a conservative tracer, with seawater as the primary Cl^- source for the sediment porewaters (e.g., Michaud et al 2016; Gustafson et al., 2022). The low Cl^- concentrations in the porewaters are consistent with the interpretation that the majority of the sediment porewater is from glacial ice melt (Michaud et al., 2016). The low Cl^- concentrations demonstrate that the reworked glaciomarine sediments were under freshwater conditions (Kuhn et al., 2017). The porewaters show a modest increase in chloride over the cored interval, consistent with the upward diffusion of ions from a deeper marine water source based on the modeling analysis of Gustafson et al. (2022).

Facies 3 is a massive clast-rich muddy diamict, LU2 and LU4 (Figures 2.2 and 2.3, Table 1.1). The lack of sorting and overall homogeneity of these diamicts are consistent with a subglacial till deposited beneath a grounded ice sheet due to a combination of lodgement and deformation (Evans et al., 2006; Smith et al., 2019). Such sediments have been previously described from beneath the Siple Coast ice streams (Hodson et al., 2016; Kamb, 2001; Tulaczyk et al., 1998) as well as on the deglaciated continental shelf (Domack et al., 1999; Licht et al., 1999; McKay et al., 2008; 2016). The range in shear strength values shows that both lodgement and deformation are likely key sedimentary processes, since deformation tills are characterized by low values (<20-40 kPa) and lodgement tills have higher shear strengths (>20-40 kPa) (Figure 2.2G) (Evans et al., 2005). The upper part of LU2 has physical properties (low density, increased

porosity, low shear strength) consistent with a volume increase or till dilation that arises as grains scoured over one another during shear (Smalley and Unwin, 1968; Alley, 1991, Benn and Evans, 2010). We interpret the top 15 cm as the dilated active zone, following Evans et al. (2006).

Facies 2 is a stratified diamict consisting of thin laminae and interbeds (thicknesses vary from <1 cm up to 5 cm; n = 6) of massive mud drapes that form sharp contacts with the surrounding diamict (Figures 2.2, 2.3, & 2.5). Notably, a 5 cm thick mud bed at 171 – 175 cm below surface lacks clasts (> 2mm) and sedimentary structures, such as laminae or coarse lags. The matrix of this mud bed is dominated by silts and clays with prominent modes at 8 μm and 0.8 μm in the grain size distribution (Figures 2.4 & 2.7A). These fine grained, sorted sediments indicate deposition via suspension settling from ponded or slowly flowing meltwater at the ice sheet bed (Lepp et al., 2022; Prothro et al., 2018; O Cofaigh et al., 2007; Buechi et al., 2017) and possibly a paleo-subglacial lake (Kuhn et al, 2017). The lack of sorted sand or gravel beds suggests that if there was flowing water, the water velocity must have remained below 20 cm s^{-1} or else coarser-grained beds and/or erosion surfaces would be present (Hjulstrom, 1939). The muds also lack sedimentary structures, such as the planar laminae, including granule layers and dropstones as seen in facies 1 (the subglacial lake sediments) suggesting that deposition in a lake-type setting is less likely. However, it is possible that conditions in a paleo subglacial lake were different from those of the current SLM, i.e., that roof melting of debris-rich basal ice, the source of the coarse sand and larger size fractions in facies 1, was not a significant sediment source. Further, the higher density and lower porosity of the muds in Facies 2, relative to facies 1, indicate sediment compaction and deformation, which is consistent with the overlying subglacial till facies 3, which would have been deposited by grounded ice. Thus, it is possible

that shearing of sediments, via loading from the overlying flowing ice resulted in the destruction of sedimentary laminae from the time of deposition (e.g., Clerc et al., 2012; Smith et al., 2018). The subglacial muds in LU3 (facies 2), have not previously been observed in sediment cores from other contemporary settings beneath the Siple Coast ice streams. Similar mm to cm thick sand dominated features within tills have been reported in terrestrial glacial sedimentary sequences from the Weichselian glaciation in northwest Germany and interpreted to reflect basal meltwater flows during phases of ice bed separation (Piotrowski and Tulaczyk, 1999). The sequence in facies 2 may be the result of similar processes as for the Weichselian sequence but with lower water flow velocities, resulting a smaller median grain size. Terrigenous silts with a similar ~6 μm grain size modes (Figure 2.4A) have been observed within glaciomarine sediments recovered from the deglaciated continental ice shelf in the Ross Sea as well as from offshore Thwaites Glacier and interpreted as sediments transported via meltwater plumes sourced from subglacial environments (Lepp et al., 2022; Prothro et al., 2018; Prothro et al., 2020; Simkins et al., 2017). We cannot discount subglacial lakes/ponds as the depositional environment for the muds, but on the balance of evidence we interpret the repeated placement of fine-grained sorted interbeds within subglacial till (Facies 2) to indicate intermittent meltwater discharge and decoupling of the ice-bed interface within a distributed system at the ice sheet bed at the SLM location. The ice bed coupling-decoupling has occurred on at least 6 occasions prior to modern lake formation given the number of mud beds. The thickness of these units are variable, suggesting varying flow magnitudes and/or rates of deposition. The thinner (< 1cm) mud layers could reflect punctuated and/or low-magnitude meltwater discharge events, while the thicker (5

cm) mud potentially reflects a longer and/or higher magnitude discharge phase with a higher suspended sediment load, following Lepp et al. (2022).

Facies 1 comprises laminated silts and clays, described as rhythmites (Siegfried et al., 2023), with thin granule-pebble beds, and caps the SLM sedimentary sequence (Figures 2.3B – C). This sediment facies archives deposition in the contemporary SLM (Siegfried et al., 2023) and rather than from sediment fall-out released by drilling operations (Priscu et al., 2021). The water-saturated and unconsolidated nature of the sediments and lack of deformation indicates an absence of ice grounding during this period of deposition. Notably, this facies was not present in the sediments recovered from Whillans Subglacial Lake (SLW), where evidence for ice grounding in the surface sediments was reported (Hodson et al., 2016). Expanding upon the depositional model that Siegfried et al. (2023) proposed, we identify two sediment depositional pathways for the accumulation of the SLM lake sediment facies: 1) sediment transported in suspension by subglacial meltwater into the lake and 2) sediment fall-out from basal ice melting (Table 2.1).

The diagnostic features of Facies 1 are the rhythmically laminated silts and clays, which were the focus of Siegfried et al. (2023). High-resolution images from CT-scan grayscale measurements, used as a grain size indicator (e.g., Reilly et al., 2017; 2019), demonstrate both normal and reverse grading of the fine-grained laminae (light overlain by dark laminae and vice versa) (Figure 2.6). These sediments reflect transport and suspension settling through the lake water column under oscillating energy environments (Table 2.1). The appearance of both normal and reverse grading suggests that changes in water velocities are gradational and that a single rhythmite sequence includes both a fining- and coarsening upwards pattern. Siegfried et al.

(2023) proposed three processes contributing to SLM rhythmite deposition: 1) sediments pre-sorted in SLC and eroded and transported to SLM; 2) channels are eroded between SLC and SLM; and 3) SLM water velocity changes are caused by water column thickness changes, which prevents fine-grained deposition during low-stand conditions.

Since rhythmites were not observed at SLW, which is more hydrologically isolated than SLM, Siegfried et al. (2023) argued that a combination of mechanisms 1 and 2 must be required for their deposition. Mechanism 1 requires transport, deposition, and then increased flow velocities to induce erosion of presorted silty sediments in an upstream basin such as SLC (must exceed 10^{-1} m s^{-1} to cause erosion following Schroeder et al., 2019). Similar velocities would be required to erode channels down into the underlying till of meltwater draining from SLC (Carter et al., 2017). Once eroded, the tilt and clay would be transported in suspension unless the flow velocity fell below the grain-dependent settling velocity in an environment such as SLM (Fredsoe and Deigaard, 1992). Facies 1 shares textural and compositional similarities to facies 3. Both facies 1 and 3 share a 0.5 μm and 8 μm grain modes (Figure 2.4) and are composed of similar silicate minerals (Figure 2.8), suggesting that facies 1 is derived from a similar upstream subglacial till source.

The sediment record may reflect internal lake dynamics in additional to external processes. Satellite ice-surface observations show that SLM completes a fill-drain cycle every 4 – 6 years and experiences a ~15 m change in water column thickness between low and high stands. Siegfried et al. (2023) proposed that flow velocities through the lake are altered following changes in water-column thickness. Neglecting cohesion, clay-sized particles (< 4 μm) will remain in suspension as long as the water velocity remains equal to or greater than the Stoke's

settling velocity. Following this scenario, high stand conditions would have minimal flow (negligible water velocity during coring at <1 cm s^{-1}, allowing clay deposition. As draining commences, mixing within the water column and flow velocities would increase, carrying clays in suspension with particles greater than 4 μm being deposited. As drainage continues and water velocity increases, deposition would be restricted to fine sands. As the lake begins to fill, flow velocities would likely decrease but mixing may restrict deposition to silts and sands, or until the energy is sufficiently lowered to allow clays to settle out.

In contrast to the fine-grained sediments (< 150 μm), the coarse pebble to granule planar laminae represent event-based deposition from rainout processes from the lake ceiling in contrast to the background sedimentation from suspension settling (Clerc et al., 2012; Livingstone et al., 2012; Siegfried et al., 2023). The event-based deposition is highlighted in the coarse laminae which contain a large (1 cm) diameter clast, the top of which is aligned with the pebble to granule layer, but that deforms the underlying sediments. This indicates the large clast and the granule layer were deposited simultaneously. The ~1 cm diameter clast is interpreted as a dropstone given the contortion and displacement of the underlying laminae (Thomas and Connell, 1985) (Figures 2.3B – C, 2.6). The most plausible source for the granule to pebble material is suspension settling of material melting out of basal debris-rich ice from the lake ceiling which contains clasts of that size (Priscu et al., 2021) and is analogous to ice-rafted debris in sub-ice shelf proximal settings (Livingstone et al., 2012). Water velocities of 50 cm s^{-1} and >100 cm s^{-1}, respectively, would be required for fluvial transport of granule to pebble sized material (Hjulstrom, 1939). These high flow rates are not consistent with the preservation of the fine-grained sediments and depressed laminae associated with the dropstones, nor with the low

current velocities (~1 cm s^{-1} or less) observed when sampling the lake during a drain cycle (Priscu et al., 2021). Because the coarse material (> 1 mm) is confined to discrete laminae and beds, sediment rainout from this source must have been an episodic event-based deposition. The prominent coarse sand-dominated laminae reflect sediment release into the lake from basal ice melt and are marker beds for this process. The SLM water temperature was -0.74°C during field operations, consistent with the pressure melting point of ice with a thickness of 1,087 m, so basal ice and lake water were at approximate thermal equilibrium (Priscu et al., 2021). Water flowing into or out of SLM (Siegfried et al 2016; Siegfried and Fricker, 2018) could generate an increase in frictional heat at the ice-water interface (Siegfried et al., 2023) causing basal melt, and releasing sediment. A parsimonious explanation for the finer grained sediments (fine sands, silts and clays) that overly the coarse layers is that they are also sourced from the basal ice, settling at lower velocities through the water column, based on grain size, and from meltwaters flowing into the lake from upstream.

Sediment Chronology

Recent work has shown that at least some portions of the WAIS grounding line along the Siple Coast retreated inland during the Holocene before readvancing to its modern position (Kingslake et al., 2018; Venturelli et al., 2020, Neuhaus et al., 2021, Venturelli et al., 2023). The sedimentary sequence at SLM ^{14}C-bearing organic matter, which allowed us to establish the timing (6.3 ± 1.0 ka) of the most recent marine incursion into and upstream of the SLM environment (Venturelli et al., 2023). This conclusion assumes that as the grounding line re-advances, the ^{14}C-bearing (marine) organic matter from the latest incursion is sequestered in the

subglacial sedimentary record together with previously deposited ancient (^{14}C-free) sediments (Venturelli et al., 2023; Venturelli et al., 2020).

The Cl^- and specific conductance of SLM sediment porewaters indicates the reworked glaciomarine sediments were deposited under freshwater conditions following a marine incursion, but the timing of the readvance at the SLM location and deposition of the lowest till recovered (LU4) remains unknown. The model of Neuhaus et al. (2021) indicates that the readvance of the WAIS grounding line at sites proximal to SLM beneath the Whillans Ice Stream (WIS) could have occurred as recently as 1100 years ago at SLW. These timing constraints from Neuhaus et al., (2021) for readvance are consistent with previously published ice stream reorganization events (Catania et al., 2012) as well as higher than present accumulation rates during the late Holocene (Bodart et al., 2022). Catania et al. (2012) proposed changes in meltwater discharge and/or basal freeze on as two mechanisms for driving the reconfiguration events during these periods. Changes in hydraulic gradient due to ice thickness changes or grounding line position may also have been responsible for the reorganization of subglacial meltwater (Lowe and Anderson, 2002). It is possible that the aqueous muds of facies 2 that reflect an active subglacial hydrologic system are related to hydrological changes associated with ice stream scale reorganization processes in the late-Holocene associated possibly with high mid-Holocene accumulation rates, or they could indicate local scale hydrological changes. In contrast to the lower aqueous muds, the laminated sediments of the contemporary SLM have the best constrained age of the four lithostratigraphic units reflecting deposition over a period ranging from 53 – 260 years (Siegfried et al., 2023) when laminations can be related to subglacial lake fill-drain cycles, as we have shown.

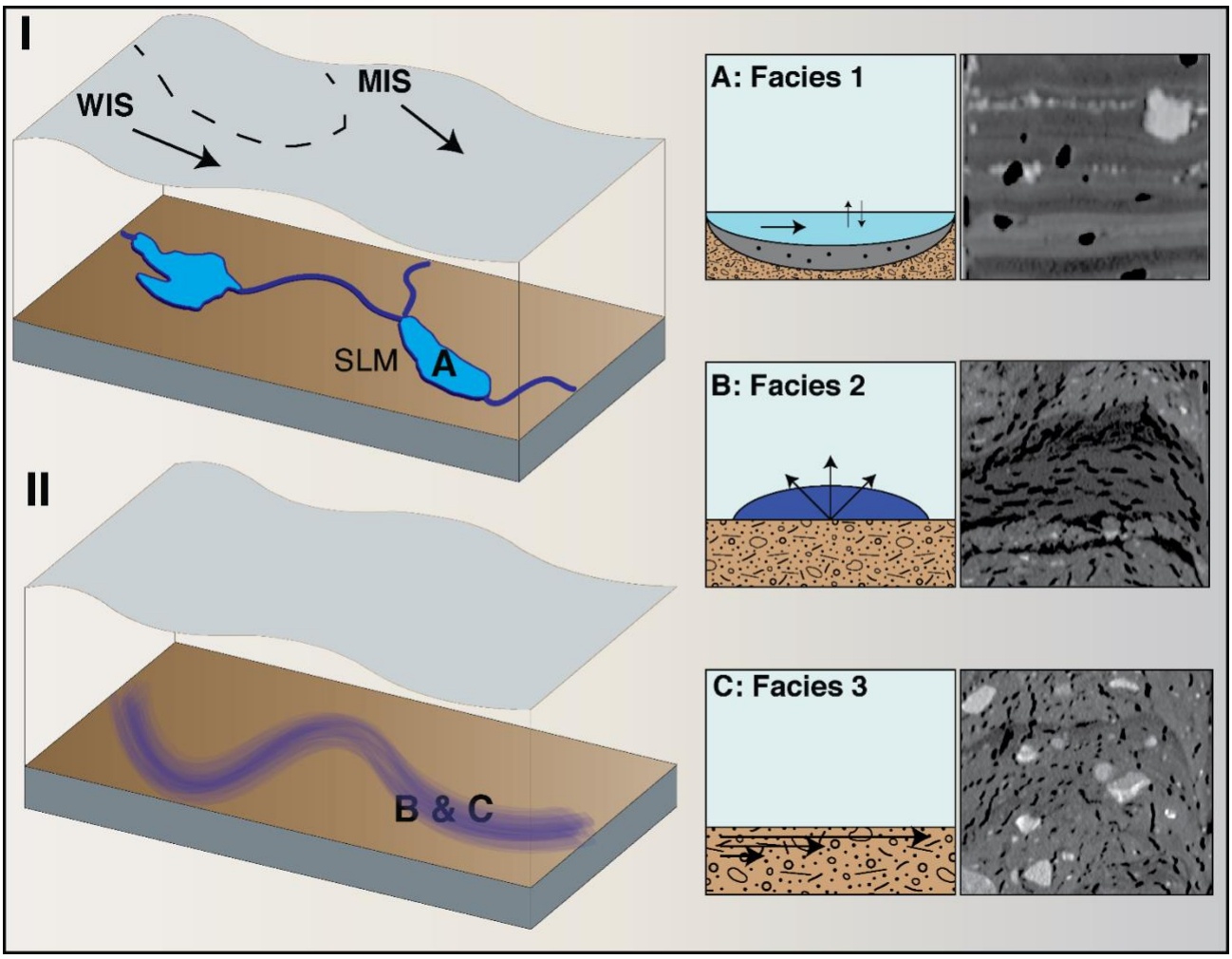

Figure 2. 9 Conceptual model of the development of the subglacial drainage system at the SLM location based on the sedimentary record. Left side panels show present day conditions and configuration after SLM formation (I) and conditions prior to the development of SLM. Right side panels (A-C) show conceptually the three facies, with slices from 3-D CT scanned images from the cores for comparison. The locations of A, B, and C are shown in panels I and II. (A) Rhythmically laminated lake sediments collect in the SLM basin and reflect periodic changes in subglacial hydrologic conditions flowing into the lake, water column height changes, and basal melt rates (Facies 1). Water filled cavities or broad and low channels contain slowly flowing or ponded meltwater allowing for suspension settling of fine-grained sediments, illustrated in (B) (Facies 2). Tills underly the areas adjacent to the channel margins and in regions upstream where the ice is grounded (C) (Facies 3).

Dynamic Basal Conditions and Hydrologic Regimes

Collectively, the sediments described in our study archive numerous lines of evidence of paleo-subglacial conditions that have varied temporally and likely spatially, corroborating previous hypotheses suggesting subglacial lake sediments as potential repositories of subglacial environmental change (Bentley et al., 2011: Siegfried et al., 2023). The SLM sedimentary record of subglacial processes includes: 1) emplacement of subglacial tills during ice-bed coupling, which record periods of grounded ice (facies 3); 2) deposition of sorted, meltwater deposits indicative of punctuated subglacial meltwater drainage events; 3) rhythmic sedimentation within a subglacial lake caused by alternating flow conditions and upstream dynamics (Figure 2.9). The sedimentary sequence in the SLM cored interval first records a period of grounded ice, (LU4, facies 3) that is interspersed with periods of ice-bed separation associated with meltwater flowing through a distributed subglacial hydrologic system (LU3, facies 2) (Figures 2.2 and 2.9). There is then a return to grounded ice conditions (LU2, facies 3) before the transition into the contemporary subglacial lake (LU1, facies 1). Notably, the upper portion of LU2 shows evidence for till dilation, likely reflecting increased subglacial water pressures immediately before the development of the contemporary subglacial lake.

The stiffest and most compact sediments, according to shear strength and bulk density/porosity data, are found at the bottom of the cored interval (Figures 2.2D, E, G) . The presence of this over consolidated stiff till prevented the collection of deeper sediments (Rosenheim, Michaud et al., 2023) and likely formed through a combination of lodgement and deformation, with sediment properties suggesting lodgement-favored formation (Halberstadt et al., 2018; O´Cofaigh et al., 2007). The stiff till requires a period of strong ice-bed coupling, low sediment porewater pressure, and high basal effective stresses. The stiff till grades into a softer

till, implying a shift towards deformation and shearing as the dominant sedimentary processes and lodgement as a secondary mechanism. The simplest explanation for this transition is an increase in sediment porewater pressure, facilitating the reworking of the underlying stiff till through deformation and shearing (O´Cofaigh et al., 2007). We interpret this transition to reflect a local increase in ice flow velocity due to the reduction in basal effective stress caused by an increase in porewater pressure, which reduced the resistive stresses at the ice-bed interface.

Following a period of streaming ice flow, the fine-grained interbeds (facies 2) indicate that the ice-bed interface alternated between coupled and decoupled states during a minimum of 6 events (Figures 2.2, 2.3, and 2.9A & D). Ice-bed separation was induced by pressurized meltwater that exceeded the ice stream overburden pressure. Fine-grained sediments were carried in suspension and then settled out in ponded or slowing flowing water (e.g., Greenwood et al., 2016). Based on our results, we propose two plausible endmember sources for the meltwater and associated sediment. One potential source would be the outburst floods from subglacial lakes located upstream or some other channel forms. Livingstone et al. (2016) argued that subglacial lakes drain via Nye-channels, which are channels that cut into the bed and erode the underlying substrate, and then develop into R-channels, which are conduits incised up into the ice. These observations are consistent with results proposed by Carter et al. (2017) that subglacial lakes drain via subglacial channels eroded into the underlying substrate. The transition from Nye to R channels reflects a switch in environments from erosional to depositional. The lack of erosional surfaces (e.g., sand or gravel lags) suggests that the SLM muds accumulated well downstream of the erosional zone (Nye channels). A second possible scenario is that the massive muds reflect relict subglacial lacustrine deposits following complete lake drainage, separated by grounding

events. A continuum of drainage environments likely exists between these two endmembers where water is temporarily stored before being transferred downstream.

The shear strength in the lower part of the till of LU2 is characteristic of deformation till, which transitions into dilated till evident in the upper 15 cm of LU2 indicating the presence of water at the ice bed interface, described by Evans et al. (2006) as a 'hydrogeological jack' that causes lifting of the overlying ice sheet and reduces friction at the ice-bed interface. This active layer represents the area of maximum downstream displacement in the sediments and increased movement of the ice stream across its bed. The absence of sorted, thinly bedded meltwater deposits of facies 2 indicates that porewater pressures were not high enough to cause extensive or complete basal decoupling (O´Cofaigh et al., 2007; Piotrowski and Tulaczyk, 1999). Although the availability of meltwater was limited to the sediment porewaters, the hydrogeologic jacking may have been a precursor to subglacial lake formation, which is estimated to have occurred between 53 and 260 years before core recovery (average 180 ± 20 years) (Siegfried et al., 2023).

The presence of rhythmically laminated silts and clays reflect deposition in a suspension load dominated environment in a subglacial lake with alternating rates of drainage (Figure 2.9). The observed sedimentary structures require relatively low flow velocities repetitively changing through time (Ojala et al., 2022; Siegfried et al 2023). The coarser silts indicate low-energy underflow currents, whereas the finer clays are evident of suspension settling in stagnant waters (Clerc et al., 2012). Changes in sedimentation and sorting could be due to water velocity changes within the lake while sediment delivery remains constant. Water column height changes associated with internal fill-drain processes or broader catchment-scale variability could modulate water velocities (Siegfried et al., 2023). Alternatively, the laminated sequence could be

the product of punctuated or pulsed sediment delivery in which sedimentation rates may vary dramatically between low and high through time. This continuum between processes influencing sorting and meltout most likely has persisted because of the changing subglacial hydrology and lake level changes (Siegfried and Fricker, 2021; Siegfried et al., 2023).

Conclusion

The temporally dynamic hydrologic basal conditions recorded in the SLM sediments provide the first example of multiple ice-bed separation events due to flowing water beneath an active ice stream. These findings have important implications for our understanding of the dynamics of Antarctic ice streams (e.g., Flowers, 2015) and for the biogeochemistry of the subglacial water cavity (e.g., Vick-Majors et al., 2020; Michaud and Priscu, 2023). The presence of meltwater at the ice stream bed interspersed with ice grounding events may be associated with regional ice stream reorganization events that were caused by ice thickness changes. The lake sediments and their structure also provide a record of dynamic subglacial hydrologic conditions on more recent time scales, of decades to centuries (Siegfried et al., 2023). Contemporary drainage of subglacial lakes (e.g. SLM and SLW) can fertilize the marine coastal ecosystem (Hawkings et al., 2020, Vick-Majors et al 2020; Davis et al 2023). The active and punctuated hydrologic regime evident from the sediment record indicates that a different drainage configuration may have existed at the SLM location earlier in the Holocene. The dynamic subglacial drainage situation would have produced important temporal pulses in nutrient supply to the adjacent oligotrophic marine cavity.

Acknowledgments

The Subglacial Antarctic Lakes Scientific Access (SALSA) project was funded by the National Science Foundation (NSF-OPP, grants 1543537, 1543396, 1543405, 1543441). We thank the United States Antarctic Program and Raytheon Polar Services for logistical support that enabled our field season, the New York Air National Guard and Kenn Borek Air for providing air support, V. Stanley and the Oregon State University Marine and Geology Repository, C. Dean as SALSA Project Manager, R. Ricards as SALSA Project Coordinator at McMurdo Station, B. Reilly for the development of SedCT and sharing script for automated clast counts, D. Mogk for XRD assistance. We thank B. Reilly for his useful conversations and sharing of scripts for data analysis related to CT scan images. We are grateful to the University of Nebraska-Lincoln hot water drill team for subglacial lake access. Partial support was provided to TC by the Geologic Society of America and by the Clay Minerals Society.

References Cited

Alley, R.B., 1991, Deforming-bed origin for southern Laurentide till sheets? Journal of Glaciology, v. 37, p. 67–76, doi:10.3189/S0022143000042817.

Alley, R.B., 1989, Water-pressure Coupling of Sliding and Bed Deformation: II. Velocity-Depth Profiles: Journal of Glaciology, v. 35, p. 119–129, doi:10.3189/002214389793701518.

Alley, R.B., Blankenship, D.D., Bentley, C.R., and Rooney, S., 1986, Deformation of till beneath ice stream B, West Antarctica: Nature, v. 322, p. 57–59.

Alley, R.B., Blankenship, D.D., Bentley, C.R., and Rooney, S.T., 1987, Till beneath ice stream B: 3. Till deformation: Evidence and implications: Journal of Geophysical Research: Solid Earth, v. 92, p. 8921–8929, doi:10.1029/JB092iB09p08921.

Anandakrishnan, S., and Alley, R.B., 1997, Stagnation of Ice Stream C, West Antarctica by water piracy: Geophysical Research Letters, v. 24, p. 265–268, doi:10.1029/96GL04016.

Beem, L.H., Tulaczyk, S.M., King, M.A., Bougamont, M., Fricker, H.A., and Christoffersen, P., 2014, Variable deceleration of Whillans Ice Stream, West Antarctica: Journal of Geophysical Research: Earth Surface, v. 119, p. 212–224, doi:https://doi.org/10.1002/2013JF002958.

Bell, R.E., 2008, The role of subglacial water in ice-sheet mass balance: Nature Geoscience, v. 1, p. 297–304, doi:10.1038/ngeo186.

Benn, D., and Evans, D.J., 2014, Glaciers and glaciation: Routledge.

Bentley, M.J., Christoffersen, P., Hodgson, D.A., Smith, A.M., Tulaczyk, S., and Le Brocq, A.M., 2011, Subglacial Lake Sediments and Sedimentary Processes: Potential Archives of Ice Sheet Evolution, Past Environmental Change, and the Presence Of Life, *in* Antarctic Subglacial Aquatic Environments, Geophysical Monograph Series, p. 83–110, doi:10.1002/9781118670354.ch6.

Bodart, J.A., Bingham, R.G., Young, D.A., MacGregor, J.A., Ashmore, D.W., Quartini, E., Hein, A.S., Vaughan, D.G., and Blankenship, D.D., 2023, High mid-Holocene accumulation rates over West Antarctica inferred from a pervasive ice-penetrating radar reflector: The Cryosphere, v. 17, p. 1497–1512, doi:10.5194/tc-17-1497-2023.

Bougamont, M., Christoffersen, P., Price, S.F., Fricker, H.A., Tulaczyk, S., and Carter, S.P., 2015, Reactivation of Kamb Ice Stream tributaries triggers century-scale reorganization of Siple Coast ice flow in West Antarctica: Geophysical Research Letters, v. 42, p. 8471–8480, doi:10.1002/2015GL065782.

Buechi, M.W., Frank, S.M., Graf, H.R., Menzies, J., and Anselmetti, F.S., 2017, Subglacial emplacement of tills and meltwater deposits at the base of overdeepened bedrock troughs: Sedimentology, v. 64, p. 658–685, doi:10.1111/sed.12319.

Carter, S.P., Fricker, H.A., and Siegfried, M.R., 2017, Antarctic subglacial lakes drain through sediment-floored canals: theory and model testing on real and idealized domains: The Cryosphere, v. 11, p. 381–405, doi:10.5194/tc-11-381-2017.

Carter, S.P., Fricker, H.A., and Siegfried, M.R., 2013, Evidence of rapid subglacial water piracy under Whillans Ice Stream, West Antarctica: Journal of Glaciology, v. 59, p. 1147–1162, doi:10.3189/2013JoG13J085.

Catania, G., Hulbe, C., Conway, H., Scambos, T.A., and Raymond, C.F., 2012, Variability in the mass flux of the Ross ice streams, West Antarctica, over the last millennium: Journal of Glaciology, v. 58, p. 741–752, doi:10.3189/2012JoG11J219.

Catania, G.A., Scambos, T.A., Conway, H., and Raymond, C.F., 2006, Sequential stagnation of Kamb Ice Stream, West Antarctica: Geophysical Research Letters, v. 33, doi:10.1029/2006GL026430.

Christoffersen, P., Tulaczyk, S., and Behar, A., 2010, Basal ice sequences in Antarctic ice stream: Exposure of past hydrologic conditions and a principal mode of sediment transfer: Journal of Geophysical Research: Earth Surface, v. 115, doi:https://doi.org/10.1029/2009JF001430.

Clerc, S., Buoncristiani, J.-F., Guiraud, M., Desaubliaux, G., and Portier, E., 2012, Depositional model in subglacial cavities, Killiney Bay, Ireland. Interactions between sedimentation, deformation and glacial dynamics: Quaternary Science Reviews, v. 33, p. 142–164, doi:10.1016/j.quascirev.2011.12.004.

Conway, H., Catania, G., Raymond, C.F., Gades, A.M., Scambos, T.A., and Engelhardt, H., 2002, Switch of flow direction in an Antarctic ice stream: Nature, v. 419, p. 465–467, doi:10.1038/nature01081.

Davis, C.L. et al., 2023, Biogeochemical and historical drivers of microbial community composition and structure in sediments from Mercer Subglacial Lake, West Antarctica: ISME Communications, v. 3, p. 8, doi:10.1038/s43705-023-00216-w.

Domack, E.W., Jacobson, E.A., Shipp, S., and Anderson, J.B., 1999, Late Pleistocene–Holocene retreat of the West Antarctic Ice-Sheet system in the Ross Sea: Part 2—Sedimentologic and stratigraphic signature: GSA Bulletin, v. 111, p. 1517–1536, doi:10.1130/0016-7606(1999)111<1517:LPHROT>2.3.CO;2.

Elsworth, C.W., and Suckale, J., 2016, Rapid ice flow rearrangement induced by subglacial drainage in West Antarctica: Geophysical Research Letters, v. 43, p. 11,697-11,707, doi:10.1002/2016GL070430.

Engelhardt, H., and Kamb, B., 1997, Basal hydraulic system of a West Antarctic ice stream: constraints from borehole observations: Journal of Glaciology, v. 43, p. 207–230, doi:10.3189/S0022143000003166.

Evans, D.J.A., Phillips, E.R., Hiemstra, J.F., and Auton, C.A., 2006, Subglacial till: Formation, sedimentary characteristics and classification: Earth-Science Reviews, v. 78, p. 115–176, doi:10.1016/j.earscirev.2006.04.001.

Evans, J., Pudsey, C.J., ÓCofaigh, C., Morris, P., and Domack, E., 2005, Late Quaternary glacial history, flow dynamics and sedimentation along the eastern margin of the Antarctic Peninsula Ice Sheet: Quaternary Science Reviews, v. 24, p. 741–774, doi:10.1016/j.quascirev.2004.10.007.

Flowers, G.E., 2015, Modelling water flow under glaciers and ice sheets: Proceedings of the Royal Society A: Mathematical, Physical and Engineering Sciences, v. 471, p. 20140907, doi:10.1098/rspa.2014.0907.

Folk, R.L., and Ward, W.C., 1957, Brazos River bar [Texas]; a study in the significance of grain size parameters: Journal of sedimentary research, v. 27, p. 3–26.

Fredsoe, J., and Deigaard, R., 1992, Mechanics of coastal sediment transport: World scientific publishing company, v. 3.

Fricker, H.A., Scambos, T., Bindschadler, R., and Padman, L., 2007, An Active Subglacial Water System in West Antarctica Mapped from Space: Science, v. 315, p. 1544–1548, doi:10.1126/science.1136897.

Greenwood, S.L., Clason, C.C., Helanow, C., and Margold, M., 2016, Theoretical, contemporary observational and palaeo-perspectives on ice sheet hydrology: Processes and products: Earth-Science Reviews, v. 155, p. 1–27, doi:10.1016/j.earscirev.2016.01.010.

Gustafson, C.D., Key, K., Siegfried, M.R., Winberry, J.P., Fricker, H.A., Venturelli, R.A., and Michaud, A.B., 2022, A dynamic saline groundwater system mapped beneath an Antarctic ice stream: Science, v. 376, p. 640–644, doi:10.1126/science.abm3301.

Hagelberg, T., Shackleton, N., Pisias, N., and Party, S.S., 1992, 5. DEVELOPMENT OF COMPOSITE DEPTH SECTIONS FOR SITES 844 THROUGH 8541, *in* Proceeding Ocean Drilling Program Initial Reports, 138 College Station, Texas, USA: Ocean Drilling Program, Texas A&M University.

Halberstadt, A.R.W., Simkins, L.M., Anderson, J.B., Prothro, L.O., and Bart, P.J., 2018, Characteristics of the deforming bed: till properties on the deglaciated Antarctic continental shelf: Journal of Glaciology, v. 64, p. 1014–1027, doi:10.1017/jog.2018.92.

Hawkings, J.R. et al., 2020, Enhanced trace element mobilization by Earth's ice sheets: Proceedings of the National Academy of Sciences, v. 117, p. 31648–31659, doi:10.1073/pnas.2014378117.

Hjulström, F., 1939, Transportation of detritus by moving water: Part 1. Transportation. Recent Marine Sediments, a Symposium:

Hodson, T.O., Powell, R.D., Brachfeld, S.A., Tulaczyk, S., and Scherer, R.P., 2016, Physical processes in Subglacial Lake Whillans, West Antarctica: Inferences from sediment cores: Earth and Planetary Science Letters, v. 444, p. 56–63, doi:10.1016/j.epsl.2016.03.036.

Hounsfield, G.N., 1973, Computerized transverse axial scanning (tomography): Part 1. Description of system: The British Journal of Radiology, v. 46, p. 1016–1022, doi:10.1259/0007-1285-46-552-1016.

Hulbe, C., and Fahnestock, M., 2007, Century-scale discharge stagnation and reactivation of the Ross ice streams, West Antarctica: Journal of Geophysical Research: Earth Surface, v. 112, doi:10.1029/2006JF000603.

Hulbe, C.L., Scambos, T.A., Klinger, M., and Fahnestock, M.A., 2016, Flow variability and ongoing margin shifts on Bindschadler and MacAyeal Ice Streams, West Antarctica: Journal of Geophysical Research: Earth Surface, v. 121, p. 283–293, doi:10.1002/2015JF003670.

Joughin, I., and Tulaczyk, S., 2002, Positive Mass Balance of the Ross Ice Streams, West Antarctica: Science, v. 295, p. 476–480, doi:10.1126/science.1066875.

Kamb, B., 2001, Basal Zone of the West Antarctic Ice Streams and its Role in Lubrication of Their Rapid Motion, *in* The West Antarctic Ice Sheet: Behavior and Environment, Antarctic Research Series, p. 157–199, doi:10.1029/AR077p0157.

Ketcham, R.A., and Carlson, W.D., 2001, Acquisition, optimization and interpretation of X-ray computed tomographic imagery: applications to the geosciences: 3D reconstruction, modelling & visualization of geological materials, v. 27, p. 381–400, doi:10.1016/S0098-3004(00)00116-3.

Kingslake, J., Scherer, R.P., Albrecht, T., Coenen, J., Powell, R.D., Reese, R., Stansell, N.D., Tulaczyk, S., Wearing, M.G., and Whitehouse, P.L., 2018, Extensive retreat and re-advance of the West Antarctic Ice Sheet during the Holocene: Nature, v. 558, p. 430–434, doi:10.1038/s41586-018-0208-x.

Kreutz, K.J., and Mayewski, P.A., 1999, Spatial variability of Antarctic surface snow glaciochemistry: implications for palaeoatmospheric circulation reconstructions: Antarctic Science, v. 11, p. 105–118, doi:10.1017/S0954102099000140.

Kuhn, G., Hillenbrand, C.-D., Kasten, S., Smith, J.A., Nitsche, F.O., Frederichs, T., Wiers, S., Ehrmann, W., Klages, J.P., and Mogollón, J.M., 2017, Evidence for a palaeo-subglacial lake on the Antarctic continental shelf: Nature Communications, v. 8, p. 15591, doi:10.1038/ncomms15591.

Lepp, A.P. et al., 2022, Sedimentary Signatures of Persistent Subglacial Meltwater Drainage From Thwaites Glacier, Antarctica: Frontiers in Earth Science, v. 10, https://www.frontiersin.org/articles/10.3389/feart.2022.863200.

Licht, K.J., Dunbar, N.W., Andrews, J.T., and Jennings, A.E., 1999, Distinguishing subglacial till and glacial marine diamictons in the western Ross Sea, Antarctica: Implications for a last glacial maximum grounding line: GSA Bulletin, v. 111, p. 91–103, doi:10.1130/0016-7606(1999)111<0091:DSTAGM>2.3.CO;2.

Lisiecki, L.E., and Herbert, T.D., 2007, Automated composite depth scale construction and estimates of sediment core extension: Paleoceanography, v. 22, doi:10.1029/2006PA001401.

Livingstone, S.J. et al., 2022, Subglacial lakes and their changing role in a warming climate: Nature Reviews Earth & Environment, v. 3, p. 106–124, doi:10.1038/s43017-021-00246-9.

Livingstone, S.J., Clark, C.D., Piotrowski, J.A., Tranter, M., Bentley, M.J., Hodson, A., Swift, D.A., and Woodward, J., 2012, Theoretical framework and diagnostic criteria for the identification of palaeo-subglacial lakes: Quaternary Science Reviews, v. 53, p. 88–110, doi:10.1016/j.quascirev.2012.08.010.

Livingstone, S.J., Utting, D.J., Ruffell, A., Clark, C.D., Pawley, S., Atkinson, N., and Fowler, A.C., 2016, Discovery of relict subglacial lakes and their geometry and mechanism of drainage: Nature Communications, v. 7, p. ncomms11767, doi:10.1038/ncomms11767.

Lowe, A.L., and Anderson, J.B., 2002, Reconstruction of the West Antarctic ice sheet in Pine Island Bay during the Last Glacial Maximum and its subsequent retreat history: Quaternary Science Reviews, v. 21, p. 1879–1897, doi:10.1016/S0277-3791(02)00006-9.

McKay, R.M., Dunbar, G.B., Naish, T.R., Barrett, P.J., Carter, L., and Harper, M., 2008, Retreat history of the Ross Ice Sheet (Shelf) since the Last Glacial Maximum from deep-basin sediment cores around Ross Island: Antarctic cryosphere and Southern Ocean climate evolution (Cenozoic-Holocene), v. 260, p. 245–261, doi:10.1016/j.palaeo.2007.08.015.

McKay, R., Golledge, N.R., Maas, S., Naish, T., Levy, R., Dunbar, G., and Kuhn, G., 2016, Antarctic marine ice-sheet retreat in the Ross Sea during the early Holocene: Geology, v. 44, p. 7–10, doi:10.1130/G37315.1.

McKight, P., and Najab, J., 2010, Kruskal-Wallis Test. The Corsini Encyclopedia of Psychology, 1, 1-10:

Meyers, P., and Teranes, J., 2001, Sediment Organic Matter in Tracking Environmental Change Using Lake Sediments Volume 2: Physical and Geochemical Methods:

Michaud, A.B., and Priscu, J.C., 2023, Sediment oxygen consumption in Antarctic subglacial environments: Limnology and Oceanography, v. 68, p. 1557–1566, doi:10.1002/lno.12366.

Michaud, A.B., Skidmore, M.L., Mitchell, A.C., Vick-Majors, T.J., Barbante, C., Turetta, C., vanGelder, W., and Priscu, J.C., 2016, Solute sources and geochemical processes in Subglacial Lake Whillans, West Antarctica: Geology, v. 44, p. 347–350, doi:10.1130/G37639.1.

Michaud, A.B., Vick-Majors, T.J., Achberger, A.M., Skidmore, M.L., Christner, B.C., Tranter, M., and Priscu, J.C., 2020, Environmentally clean access to Antarctic subglacial aquatic environments: Antarctic Science, v. 32, p. 329–340, doi:10.1017/S0954102020000231.

Moncrieff, A.C.M., 1989, Classification of poorly-sorted sedimentary rocks: Sedimentary Geology, v. 65, p. 191–194, doi:10.1016/0037-0738(89)90015-8.

Moore, D.M., and Reynolds Jr, R.C., 1989, X-ray Diffraction and the Identification and Analysis of Clay Minerals.: Oxford University Press (OUP).

Morlighem, M. et al., 2020, Deep glacial troughs and stabilizing ridges unveiled beneath the margins of the Antarctic ice sheet: Nature Geoscience, v. 13, p. 132–137, doi:10.1038/s41561-019-0510-8.

Mouginot, J., Rignot, E., and Scheuchl, B., 2019, Continent-Wide, Interferometric SAR Phase, Mapping of Antarctic Ice Velocity: Geophysical Research Letters, v. 46, p. 9710–9718, doi:10.1029/2019GL083826.

Neuhaus, S.U., Tulaczyk, S.M., Stansell, N.D., Coenen, J.J., Scherer, R.P., Mikucki, J.A., and Powell, R.D., 2021, Did Holocene climate changes drive West Antarctic grounding line retreat and readvance? The Cryosphere, v. 15, p. 4655–4673, doi:10.5194/tc-15-4655-2021.

Ó Cofaigh, C., Evans, J., Dowdeswell, J.A., and Larter, R.D., 2007, Till characteristics, genesis and transport beneath Antarctic paleo-ice streams: Journal of Geophysical Research: Earth Surface, v. 112, doi:10.1029/2006JF000606.

Ojala, A.E.K., Mäkinen, J., Kajuutti, K., Ahokangas, E., and Palmu, J.-P., 2022, Subglacial evolution from distributed to channelized drainage: Evidence from the Lake Murtoo area in SW Finland: Earth Surface Processes and Landforms, v. 47, p. 2877–2896, doi:10.1002/esp.5430.

Phillips, D.L., and Gregg, J.W., 2001, Uncertainty in source partitioning using stable isotopes: Oecologia, v. 127, p. 171–179, doi:10.1007/s004420000578.

Piotrowski, J.A., and Tulaczyk, S., 1999, Subglacial conditions under the last ice sheet in northwest Germany: ice-bed separation and enhanced basal sliding? Quaternary Science Reviews, v. 18, p. 737–751, doi:10.1016/S0277-3791(98)00042-0.

Price, S.F., Bindschadler, R.A., Hulbe, C.L., and Joughin, I.R., 2001, Post-stagnation behavior in the upstream regions of Ice Stream C, West Antarctica: Journal of Glaciology, v. 47, p. 283–294, doi:10.3189/172756501781832232.

Priscu, J.C. et al., 2013, A microbiologically clean strategy for access to the Whillans Ice Stream subglacial environment: Antarctic Science, v. 25, p. 637–647, doi:10.1017/S0954102013000035.

Priscu, J.C. et al., 2021, Scientific access into Mercer Subglacial Lake: scientific objectives, drilling operations and initial observations: Annals of Glaciology, v. 62, p. 340–352, doi:10.1017/aog.2021.10.

Pritchard, H.D., Arthern, R.J., Vaughan, D.G., and Edwards, L.A., 2009, Extensive dynamic thinning on the margins of the Greenland and Antarctic ice sheets: Nature, v. 461, p. 971–975, doi:10.1038/nature08471.

Prothro, L.O., Majewski, W., Yokoyama, Y., Simkins, L.M., Anderson, J.B., Yamane, M., Miyairi, Y., and Ohkouchi, N., 2020, Timing and pathways of East Antarctic Ice Sheet retreat: Quaternary Science Reviews, v. 230, p. 106166, doi:10.1016/j.quascirev.2020.106166.

Prothro, L.O., Simkins, L.M., Majewski, W., and Anderson, J.B., 2018, Glacial retreat patterns and processes determined from integrated sedimentology and geomorphology records: Marine Geology, v. 395, p. 104–119, doi:10.1016/j.margeo.2017.09.012.

Reilly, B.T. et al., 2019, Holocene break-up and reestablishment of the Petermann Ice Tongue, Northwest Greenland: Quaternary Science Reviews, v. 218, p. 322–342, doi:10.1016/j.quascirev.2019.06.023.

Reilly, B.T., Stoner, J.S., and Wiest, J., 2017, SedCT: MATLAB™ tools for standardized and quantitative processing of sediment core computed tomography (CT) data collected using a medical CT scanner: Geochemistry, Geophysics, Geosystems, v. 18, p. 3231–3240, doi:10.1002/2017GC006884.

Retzlaff, R., and Bentley, C.R., 1993, Timing of stagnation of Ice Stream C, West Antarctica, from short-pulse radar studies of buried surface crevasses: Journal of Glaciology, v. 39, p. 553–561, doi:10.3189/S0022143000016440.

Rignot, E., Mouginot, J., Scheuchl, B., van den Broeke, M., van Wessem, M.J., and Morlighem, M., 2019, Four decades of Antarctic Ice Sheet mass balance from 1979–2017: Proceedings of the National Academy of Sciences, v. 116, p. 1095–1103, doi:10.1073/pnas.1812883116.

Rosenheim, B.E. et al., 2023, A method for successful collection of multicores and gravity cores from Antarctic subglacial lakes: Limnology and Oceanography: Methods, v. 21, p. 279–294, doi:10.1002/lom3.10545.

Rothwell R. Guy, Hoogakker Babette, Thomson John, Croudace Ian W., and Frenz Michael, 2006, Turbidite emplacement on the southern Balearic Abyssal Plain (western Mediterranean Sea) during Marine Isotope Stages 1–3: an application of ITRAX XRF scanning of sediment cores to lithostratigraphic analysis: Geological Society, London, Special Publications, v. 267, p. 79–98, doi:10.1144/GSL.SP.2006.267.01.06.

Scambos, T.A., Haran, T.M., Fahnestock, M.A., Painter, T.H., and Bohlander, J., 2007, MODIS-based Mosaic of Antarctica (MOA) data sets: Continent-wide surface morphology and snow grain size: Remote Sensing of the Cryosphere Special Issue, v. 111, p. 242–257, doi:10.1016/j.rse.2006.12.020.

Schroeder, D.M., MacKie, E.J., Creyts, T.T., and Anderson, J.B., 2019, A subglacial hydrologic drainage hypothesis for silt sorting and deposition during retreat in Pine Island Bay: Annals of Glaciology, v. 60, p. 14–20, doi:10.1017/aog.2019.44.

Siegfried, M.R. et al., 2023, The life and death of a subglacial lake in West Antarctica: Geology, v. 51, p. 434–438, doi:10.1130/G50995.1.

Siegfried, M.R., and Fricker, H.A., 2021, Illuminating Active Subglacial Lake Processes With ICESat-2 Laser Altimetry: Geophysical Research Letters, v. 48, p. e2020GL091089, doi:10.1029/2020GL091089.

Siegfried, M.R., and Fricker, H.A., 2018, Thirteen years of subglacial lake activity in Antarctica from multi-mission satellite altimetry: Annals of Glaciology, v. 59, p. 42–55, doi:10.1017/aog.2017.36.

Siegfried, M.R., Fricker, H.A., Carter, S.P., and Tulaczyk, S., 2016, Episodic ice velocity fluctuations triggered by a subglacial flood in West Antarctica: Geophysical Research Letters, v. 43, p. 2640–2648, doi:10.1002/2016GL067758.

Simkins, L.M., Anderson, J.B., Greenwood, S.L., Gonnermann, H.M., Prothro, L.O., Halberstadt, A.R.W., Stearns, L.A., Pollard, D., and DeConto, R.M., 2017, Anatomy of a meltwater drainage system beneath the ancestral East Antarctic ice sheet: Nature Geoscience, v. 10, p. 691–697, doi:10.1038/ngeo3012.

Smalley, I.J., and Unwin, D.J., 1968, The Formation and Shape of Drumlins and their Distribution and Orientation in Drumlin Fields: Journal of Glaciology, v. 7, p. 377–390, doi:10.3189/S0022143000020591.

Smith, J.A., Graham, A.G.C., Post, A.L., Hillenbrand, C.-D., Bart, P.J., and Powell, R.D., 2019, The marine geological imprint of Antarctic ice shelves: Nature Communications, v. 10, p. 5635, doi:10.1038/s41467-019-13496-5.

Smith, A.M., Woodward, J., Ross, N., Bentley, M.J., Hodgson, D.A., Siegert, M.J., and King, E.C., 2018, Evidence for the long-term sedimentary environment in an Antarctic subglacial lake: Earth and Planetary Science Letters, v. 504, p. 139–151, doi:10.1016/j.epsl.2018.10.011.

Sperazza, M., Moore, J.N., and Hendrix, M.S., 2004, High-Resolution Particle Size Analysis of Naturally Occurring Very Fine-Grained Sediment Through Laser Diffractometry: Journal of Sedimentary Research, v. 74, p. 736–743, doi:10.1306/031104740736.

Thomas, G.S.P., and Connell, R.J., 1985, Iceberg drop, dump, and grounding structures from Pleistocene glacio-lacustrine sediments, Scotland: Journal of Sedimentary Research, v. 55, p. 243–249, doi:10.1306/212F8689-2B24-11D7-8648000102C1865D.

Tulaczyk, S., Kamb, B., Scherer, R.P., and Engelhardt, H.F., 1998, Sedimentary processes at the base of a West Antarctic ice stream; constraints from textural and compositional properties of subglacial debris: Journal of Sedimentary Research, v. 68, p. 487–496, doi:10.2110/jsr.68.487.

Venturelli, R.A. et al., 2023, Constraints on the Timing and Extent of Deglacial Grounding Line Retreat in West Antarctica: AGU Advances, v. 4, p. e2022AV000846, doi:10.1029/2022AV000846.

Venturelli, R.A., Siegfried, M.R., Roush, K.A., Li, W., Burnett, J., Zook, R., Fricker, H.A., Priscu, J.C., Leventer, A., and Rosenheim, B.E., 2020, Mid-Holocene Grounding Line Retreat and Readvance at Whillans Ice Stream, West Antarctica: Geophysical Research Letters, v. 47, p. e2020GL088476, doi:10.1029/2020GL088476.

Vick-Majors, T.J. et al., 2020, Biogeochemical Connectivity Between Freshwater Ecosystems beneath the West Antarctic Ice Sheet and the Sub-Ice Marine Environment: Global Biogeochemical Cycles, v. 34, p. e2019GB006446, doi:10.1029/2019GB006446.

Witus, A.E., Branecky, C.M., Anderson, J.B., Szczuciński, W., Schroeder, D.M., Blankenship, D.D., and Jakobsson, M., 2014, Meltwater intensive glacial retreat in polar environments and investigation of associated sediments: example from Pine Island Bay, West Antarctica: Quaternary Science Reviews, v. 85, p. 99–118, doi:10.1016/j.quascirev.2013.11.021.

Yan, S. et al., 2022, A newly discovered subglacial lake in East Antarctica likely hosts a valuable sedimentary record of ice and climate change: Geology, v. 50, p. 949–953, doi:10.1130/G50009.1.

CHAPTER THREE

IMPLICATIONS FOR SUB-ICE STREAM ACCRETIONARY PROCESSES AND CONDITIONS FROM THE BASAL ICE LAYER OF THE MERCER ICE STREAM, WEST ANTARCTICA

Contribution of Authors and Co-Authors

Manuscript in Chapter 3

Author: Timothy D. Campbell

Contributions: Project conception, image analysis, manuscript preparation.

Co-Author: Mark L. Skidmore

Contributions: Project conception, manuscript editing

Co-Author: John Winans

Contributions: Designed Deep SCINI camera system.

Co-Author: Justin Burnett

Contributions: Designed Deep SCINI camera system.

Co-Author: Robert Zook

Contributions: Designed Deep SCINI camera system.

John C. Priscu

Contributions: Chief scientist, project conception, manuscript editing.

Manuscript Information

Status of Manuscript:
X Prepared for submission to a peer-reviewed journal
☐ Officially submitted to a peer-reviewed journal
☐ Accepted by a peer-reviewed journal
☐ Published in a peer-reviewed journal

Abstract

The basal conditions of the Siple Coast ice streams, which are critical to understanding the potential for rapid deglaciation, remain poorly understood due to limited direct observations and measurements. In the 2018-2019 austral summer, a hot-water drill was used to access Mercer Subglacial Lake located 1087 m beneath the Mercer Ice Stream, West Antarctica. A ~5 m thick basal ice sequence was observed directly above the ice-water interface of Mercer Subglacial Lake, from which we developed new constraints on ice stream subglacial conditions and processes. Based on image analysis of the borehole walls, the basal ice sequence was composed of two main sequences that were differentiated by debris content. The stratified lower sequence, consisting of clear, massive, and solid ice facies, contained up to 25 times more sediment than the upper basal clear facies with dispersed suspended sediment. Variations in basal ice stratigraphy reflect changes in accretionary basal conditions, specifically two contrasting periods based on meltwater availability. We describe potential basal ice formation processes using models developed for Kamb Ice Stream, a nearby Siple Coast ice stream as well as recent models developed for frozen fringes and then discuss the implications for upstream basal conditions and meltwater activity beneath the Mercer Ice Stream. Collectively, our data show that basal ice facies variations reflect changes in accretionary basal conditions, the availability of subglacial meltwater, and the basal freezing rate.

Introduction

Much of the West Antarctic Ice Sheet (WAIS) is grounded below modern-day sea level, susceptible to rapid retreat due to the retrograde bed topography and contains enough ice to raise sea level by 5 – 6 m if fully melted (DeConto and Pollard, 2016). A challenge to predicting future mass balance changes and contribution to eustatic sea level rise is the dynamic uncertain behavior of WAIS ice streams, which transport large volumes of ice from the continental interior at high velocities (100s of m yr^{-1})and ultimately draining into the ocean after crossing the grounding line (e.g., Bamber et al., 2000; Kamb, 2001; Bennett, 2003; Rignot et al., 2011; Mouginot et al., 2019; Rignot et al., 2019).

The dynamic behavior of the West Antarctic ice streams spans decadal to centennial timescales (Hulbe and Fagnestock, 2007; Catantia et al., 2012). Examples of ice steam variability include large-scale velocity changes (Conway et al., 2002; Beem et al., 2014; Siegfried et al., 2016; Rignot et al., 2019), shutdown (Retzlaff and Bentley, 1993; Jacobel et al., 1996; Ng and Conway, 2004), and switching of flow direction (Fahnestock et al., 2000; Hulbe and Fahnestock, 2007; Catania et al., 2012; Hulbe et al., 2016; Elsworth and Suckale, 2016). Observations of similar dynamic ice stream behavior, but over millennial timescales, are given by the North Atlantic Heinrich events in which iceberg armadas were discharged from the Northern Hemisphere ice sheets and deposited coarse-grained sediment layers onto the marine floor with a 5 – 10 kyr periodicity (Heinrich, 1988; Hemming, 2004). Iceberg discharge events were due to snow accumulation, basal warming from the heat flux (frictional and geothermal), and increased lubrication from basal meltwater decreasing sliding friction. Ellsworth and Suckale (2016) concluded that rapid ice stream reorganization is largely modulated by basal conditions with

respect to the availability and distribution of subglacial meltwater highlighting the importance of ice stream basal conditions and interaction between the bed and overlying ice in modulating ice flow and ice sheet behavior. To date, studying the conditions at the base of ice streams remains difficult due to direct observation or direct measurements, and the lack of geologic archives that extend beyond the modern instrumental record.

The basal ice, which is a layer of ice found at the base of many ice sheets and glaciers at the interface between the underlying sediments and/or bedrock, is a potential tool in guiding the analysis of past and present sub-ice processes (e.g. Christoffersen et al., 2006, Bougamont and Christoffersen, 2012). Because basal accreted ice forms from the freezing of subglacial meltwater onto the sole of the ice sheet, basal ice layers (BIL) provide rare archives of spatial and temporal dynamics of subglacial hydrology and basal thermal conditions (Tulaczyk and Hossainzadeh, 2011). Debris-rich basal ice layers are produced by a range of processes operating at the bed, modulated by the abundance of meltwater and freezing conditions, that include regelation, glaciohydraulic supercooling, and net adfreezing/conductive cooling. Since the BIL forms at the bed, it exhibits a suite of physical and/or chemical characteristics such as debris content, crystal structure, bubble/gas composition, and solute concentration, that differentiates it from the overlying meteoric ice (Hubbard et al., 2009; Knight, 1997; Goossens et al., 2016). Basal ice sequences are a useful tool in constraining past sub-ice stream processes because the concentration and configuration of debris infers the availability of subglacial meltwater and basal thermal properties (Christoffersen et al., 2006). Our limited data on basal ice sequences has been derived primarily from the Kamb Ice Stream, (e.g. Vogel et al., 2005; Christoffersen et al., 2010). Other basal ice data are from deep ice cores drilled for paleoclimate analysis, e.g. Byrd

Station (Gow et al., 1968), Siple Dome (Gow and Meese 2007) where the glaciological setting is not dynamic.

We describe the basal ice stratigraphy observed in images from the hot water-drilled borehole wall of the Mercer Ice Stream above Mercer Subglacial Lake (SLM) (Figure 3.1). Details from these images were used to address sub-ice stream accretionary processes, meltwater availability, basal thermal state, and potential for past ice stream flow oscillations.

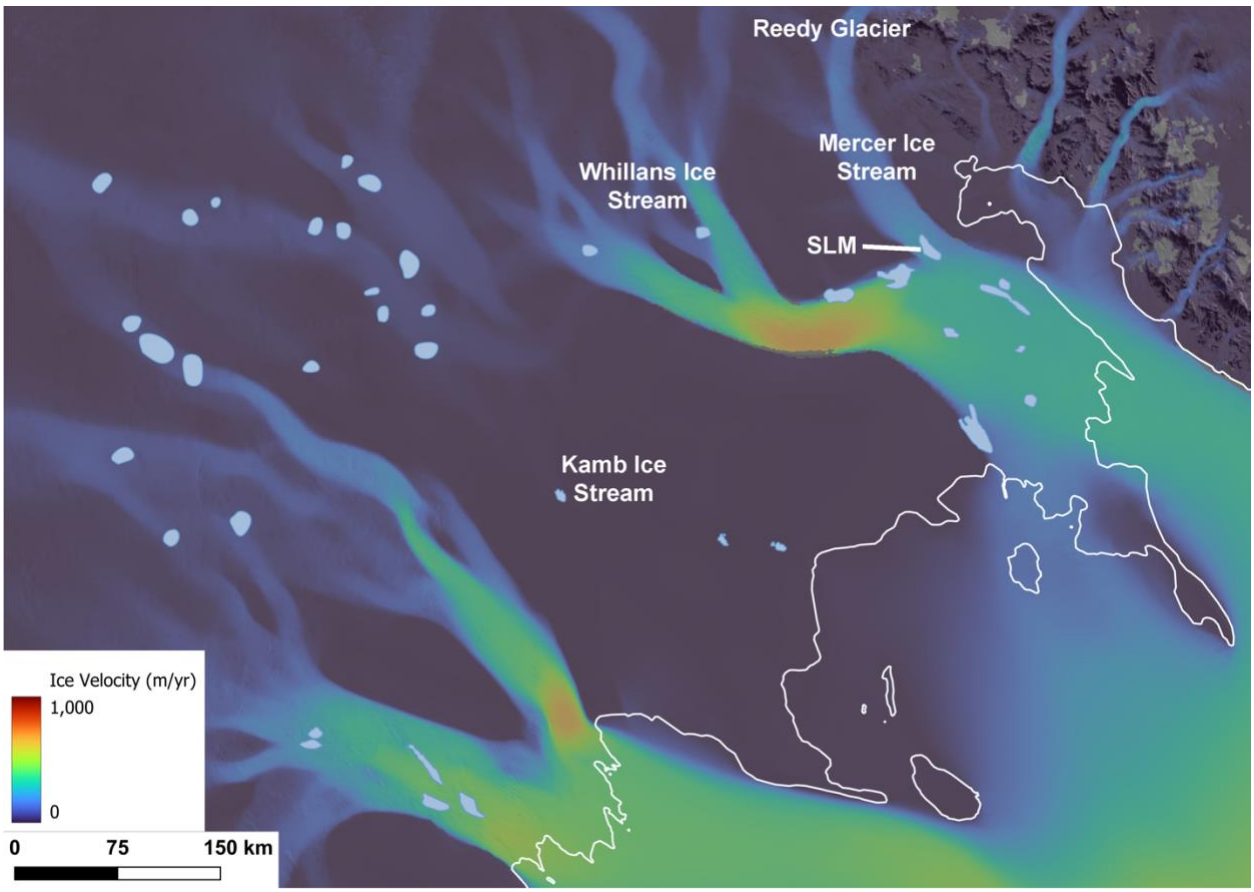

Figure 3.1 Map of Mercer Subglacial Lake located at the confluence of the Mercer and Whillans Ice Streams in West Antarctica. Surface ice velocity (Mouginot et al., 2019), subglacial lake outlines (Siegfried and Fricker, 2021), and modern grounding line position (Mouginot et al., 2017) are shown superimposed on a satellite image mosaic (Scambos et al., 2007).

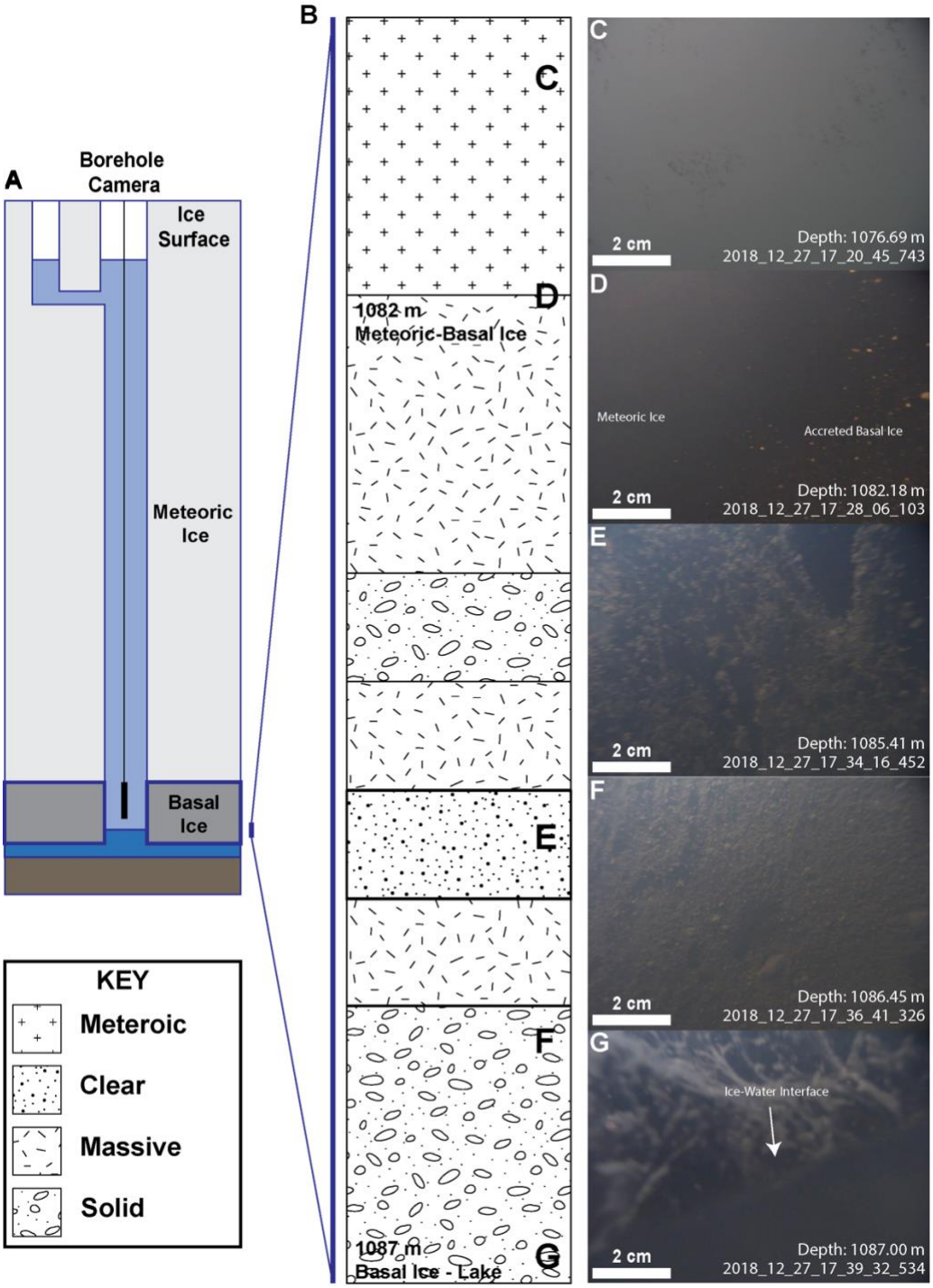

Figure 3.2 The SLM basal ice layer. (A) schematic vertical profile of Mercer Ice Stream (MIS) at SLM); (B) schematic drawing of the lower 6 m of the ice stream containing 5 m of basal ice from the SLM borehole; Side-looking borehole camera images showing the transition from (C) opaque. bubbly meteoric glacial ice to, (D) clear basal ice with suspended sediment, (E) massive ice with sediment, (F) solid sediment with pore ice, (G) ice-water interface. Modified from Priscu et al. (2021).

Borehole Observations and Image Analysis

In December 2018, a ~0.4 m diameter borehole was melted through 1087 m of ice using a clean access hot water drill over Mercer Subglacial Lake (SLM) (Figure 3.2A) (Priscu et al., (2021), which is located at the confluence of the Mercer (MIS) and Whillans (WIS) ice streams (Figure 3.1). Reedy Glacier is the primary tributary of the MIS and is a large outlet glacier of the East Antarctic Ice Sheet, while WIS receives ice from the interior of West Antarctica. Side facings cameras were mounted on the clump weight of the Deep SCINI ROV (Burnett et al., 2015) and deployed through the borehole. The clump weight was stopped at several time points during deployment (Supplementary Figure 2.1) to make observations at depths of 1083.25, 1083.5, and 1086.5 m below surface. The borehole camera system captured 11,581 images of the basal ice with 1296×960 pixel resolution. The camera was not always directly centered in the borehole, making it difficult to determine the exact field of view size, but, assuming the field of view was 30°, we estimate it to be approximately 8 cm x 6 cm. The 5 m thick basal ice layer began at 1082 m below ice surface and extended to the ice-water interface of SLM. The basal ice layer was bounded by the upper debris-bearing ice and was used as the indicator of the top of the accreted ice layer (Figure 3.2B – D) to the ice-lake water interface (Figure 3.2G).

The basal ice layer was characterized using the brightness distribution of the side-facing borehole camera imagery. Images are 3-D arrays with red, green, and blue values (ranging from 0 to 255 intensity levels) stored for each pixel (Supplementary Figure 2.2). The borehole camera images were converted to grayscale (2D array, intensity ranging from 0 to 255 intensity levels) (Supplementary Figure 2.2G – I) to highlight intensity differences within the images. The optical

properties of the images changed as a function of debris content. The mean brightness for a solid sediment particle was ~120 and ~50 for clear transparent ice with no visible debris (Figure 3.3).

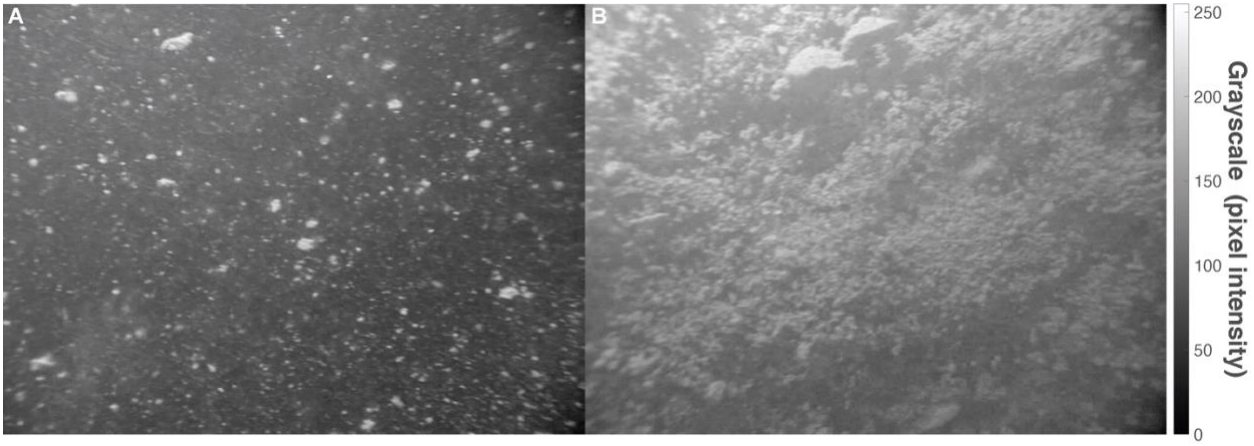

Figure 3.3 Grayscale images of basal ice facies following Hubbard et al. (2009). (A) clear ice with suspended sediment and (B) solid basal sediment with pore ice. Sediment particles in the clear ice have higher-brighter grayscale pixel values than the surrounding ice. The range of grayscale pixel values in the solid ice is narrower, thus justifying a different brightness threshold value in the image analysis.

Sediment content was estimated using an automated image analysis code in MATLAB that utilized the brightness distribution of sequential grayscale images to produce black-and-white, binary imagery based on thresholds (black pixels = clear accretion ice; white pixels = sediment debris) following Christofferson et al. (2010). The summation of white and black pixels was used to quantify sediment volume contained in accreted basal ice (Figure 3.4). Conservative thresholds were used to avoid overestimating sediment content (3-D structure) in a 2-D analysis. Owing to color intensity differences between the foreground and background of the different ice facies, different threshold values were used for the different ice types.

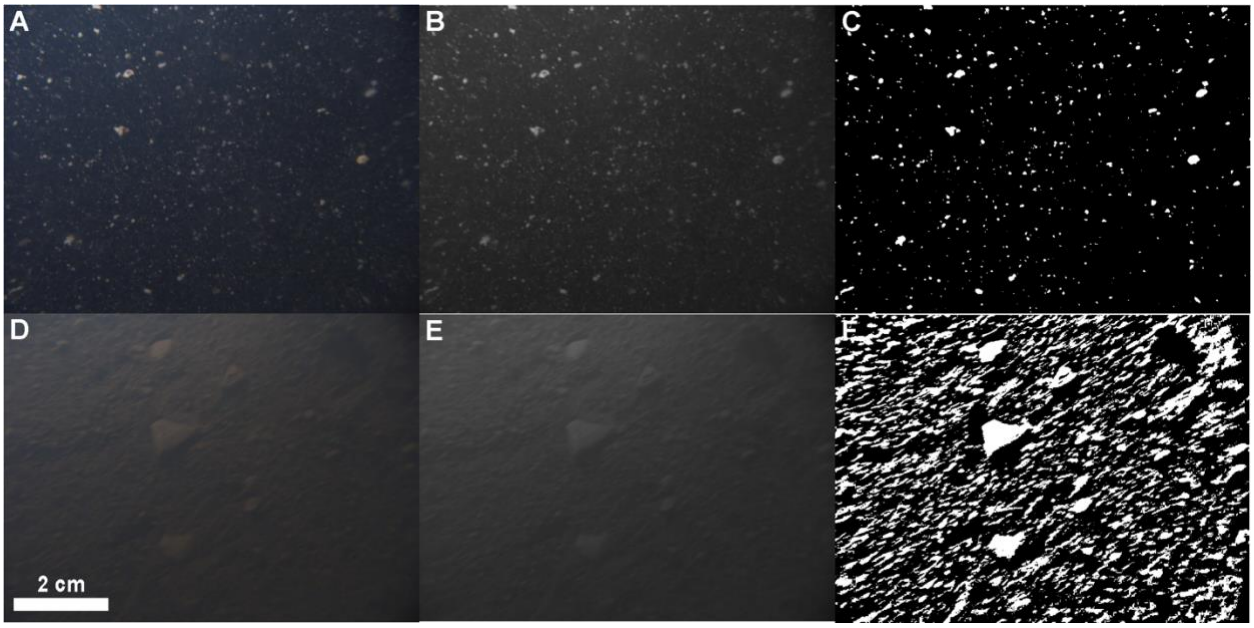

Figure 3.4 Demonstration of how debris content was estimated from image analysis of color, grayscale, and binary images for clear (A – C) and solid (D – F) ice types. White denotes debris, and black illustrates clear ice in C and F. The sediment content for the clear and solid ice examples were 1.9 and 26.6 vol. %, respectively

Basal Ice Layer Sequence

The borehole wall imagery of the basal ice showed large variations in the abundance of sediment, with a 5.0 m thick cumulative sequence identified above SLM (Figure 3.5; Supplementary Figure 2.3). Three main types of basal ice were identified, each showing different amounts of frozen debris: (1) clear basal ice with little or no suspended debris (**clear**) (Figure 3.4a), (2) debris and mud clots frozen in clear, transparent ice (**massive**); (Figure 3.2E), and (3) basal ice consisting of frozen sediment with pore ice (**solid**) (4d). The SLM basal ice sequence notably lacks laminated or banded ice (Hubbard et al., 2009). We estimate the debris content in the clear ice layer (1) to contain ~1% of the sediment, whereas the massive (2) and solid (3) ice layers contained ~15% and >20 %, respectively, (Figure 3.5). The upper 3.2 m contains fine-grained material and grains with diameters exceeding 1 cm are absent (Figure 3.3a). Fine and

medium sands (63 μm – 500 μm) are observed but these are likely soft sediment clasts of clotted silts and clays (Figures 3.3 & 3.4A – C). The lower 1.8 m consists of alternating layers (n = 3) of clear, dispersed, and sediment-rich ice facies (solid and massive ice facies) (Figure 3.5). Unlike the upper sequence, which only contains a single ice facies (clear ice), the lower sequence is composed of a) clear, b) massive, and c) solid ice facies types (Figure 3.5). The sequence is capped by a solid sediment unit, which is underlain by debris-poor clear ice. A unit of massive ice is observed below 1086 m below the surface before transitioning into a second unit of clear ice with minimal sediment content (< 1%). The bottom of this sequence contains a 1 m thick unit of solid sediment, with sediment concentrations exceeding 20%. The solid ice is a matrix-supported diamict that contains material exceeding 2 cm in diameter (Figures 3.3 & 3.4D – F). This two-sequence structure has been observed in basal ice from the Kamb Ice Stream (Christofferson et al., 2010) and Greenland Ice Sheet (Sugden et al., 1987; Knight, 1994). Sediment contained in the SLM BIL equates to a ~0.3 m thick sediment package if fully melted (Figure 3.5).

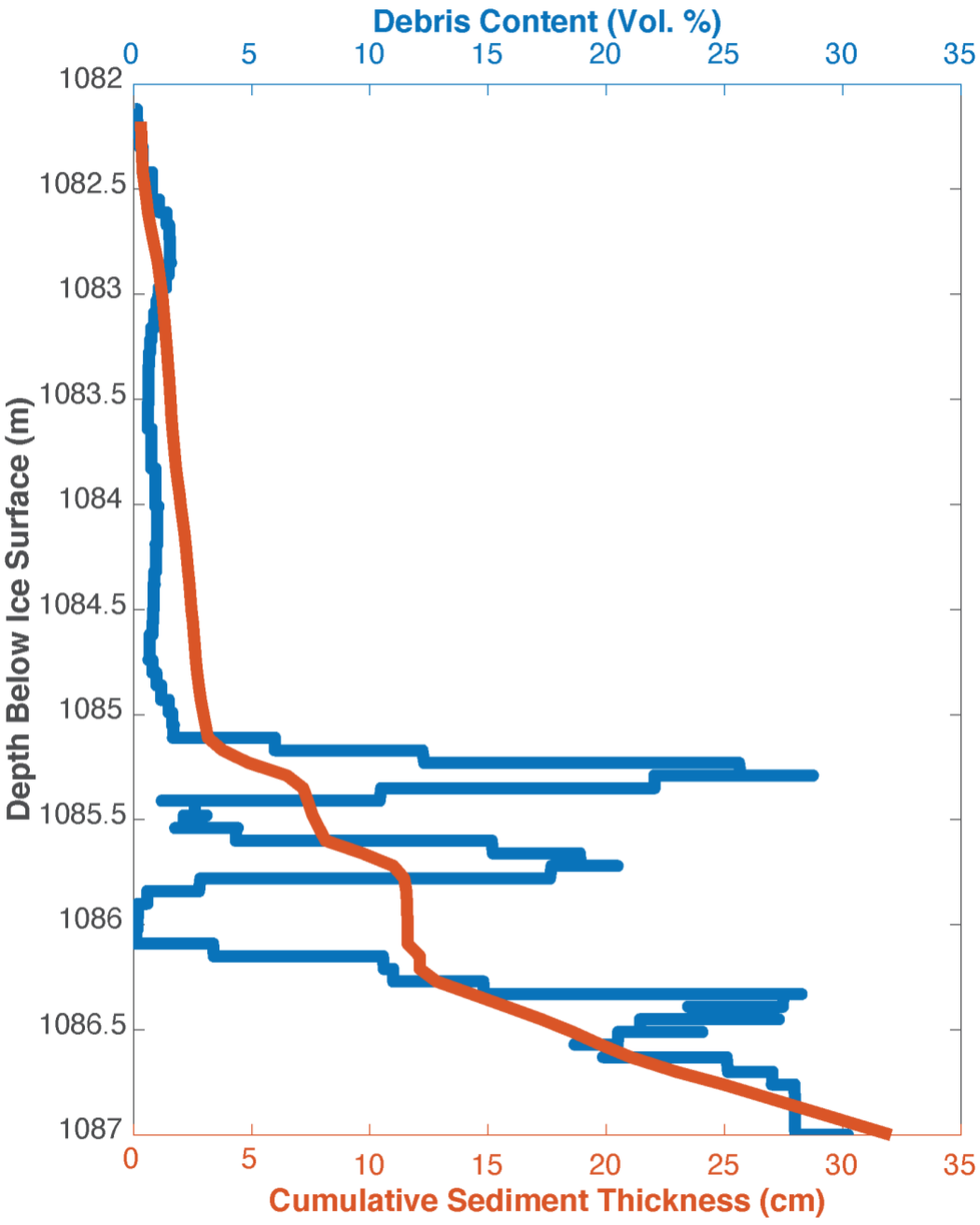

Figure 3.5 Stratigraphic log showing the debris content results using a moving average filter of the sequential down borehole image brightness analysis in the SLM basal ice layer (blue) (see Supplementary Figure 2.3) as well as cumulative sediment thickness of the debris entrained in the ice (red).

Basal Ice Facies

Accreted basal ice layers provide an archive of subglacial hydrologic and basal conditions over a range of spatial and temporal scales. The basal ice observed above SLM contains three layers where the estimated debris content is >10%, with all three layers observed in the bottom sequence, and separated by clear ice (Figure 3.5). In contrast, the upper 3.2 m of the SLM basal ice layer comprises massive, clear ice with minimal dispersed sediment (~1%). The three distinct basal layer present in SLM basal ice represent supply of subglacial meltwater and rate of basal freezing. Christoffersen et al. (2006) predicted the formation of four different basal ice facies controlled by the availability of meltwater and freeze-on conditions. These authors concluded that clear facies (<1% sediment) were produced from the congelation or accretion when supercooled meltwater separates the ice base from the sediment substrate or when groundwater is supplied to the base at a rate equal to the freezing rate and laminated facies, which were not observed in the SLM BIL, were produced by alternating regelation (debris-rich) and congelation (clear) events. The numerical model of Christoffersen et al. (2006) predicts that regelation events will be short (several hours) and separated by longer periods (months) of congelation. A stacking of the debris-rich laminae produced by regelation will cause the development of a massive, debris-rich facies. The stacking requires a meltwater-deprived environment. Solid facies are predicted to form if meltwater is depleted, and freezing rates are high (5 mm yr^{-1}).

Following the results from Christoffersen et al. (2006) model, we predict that the clear dispersed facies of the upper sequence formed during a period when the ice base was freezing while the subglacial hydrologic system supplied sufficient meltwater in an area upstream of our

current location in the interior of the ice sheet such as a water filled cavity or upstream subglacial lake. The presence of a thick clear ice package demonstrates that there was an abundant supply of subglacial water separating the ice from the sediment beneath the ice stream. The abundant meltwater indicates that basal water pressures were sufficient to separate the ice from its bed and may indicate high ice stream flow velocities during this time.

In contrast to our contention that the clear and dispersed facies that formed under conditions with abundant meltwater, our data also indicates that the solid facies formed under conditions with high freezing rates with highly restricted water flow causing three ice-bed contact events and the entrainment of higher volumes of sediment (> 20%). The rationale being that higher debris contents (solid) represent periods of very limited meltwater, which may be representative of past stagnant phases of the ice stream. An additional explanation for the alternation of debris-rich poor layers in the bottom sequence is given by Rempel et al. (2023), who used ring-shear experiments and observed sediment entrainment after sliding temperate ice over different types of unconsolidated substrates. Rempel et al. (2023) showed that when the ice slid over a bed of saturated loess, a ~0.5 – 1 cm thick layer of frozen debris (referred to as a "frozen fringe") accreted to the base of the ice. Additionally, they showed that dispersed sediment was observed above the upper boundary of the frozen fringe and thin sections and was concentrated along grain boundaries, whereas a clear boundary between debris-free ice and the frozen fringe was maintained while sliding over a coarser Horicon till. SLM till sediments are fine-grained and contain abundant material with diameters < 63 μm (Campbell et al., in prep). Modeling by Rempel et al. (2023) confirmed that vein liquid flow can entrain and transport silt-sized particles up into the lowermost basal ice. The observed solid sediment layers of the SLM

basal ice layer are thicker than the frozen fringes observed by Rempel et al. (2023), thus we interpret the oscillations to reflect significant changes in the basal conditions and availability of subglacial meltwater.

Our data, in concert with those of Rempel et al (2023), indicate that the entrainment of solid sediment into the BIL supports the interpretation of past stagnation of the Mercer ice stream as freezing of porewater within the subglacial sediment during a meltwater-restricted period would have increased the shear strength of the underlying sediments by decreasing basal till void ratio (volume of voids divided by the volume of solids). Strengthening of the sediment would increase the restive stresses acting at the ice stream bed, possibly decreasing ice flow velocity. SLM lake water temperature was measured to be within 0.05°C and 0.02°C of the freezing point (-0.74°C) (Priscu et al., 2021), demonstrating that a small perturbation or energy deficit to the system would induce freezing. Rempel et al. (2006) proposed that temperatures 1°C below the pressure melting point would be required to account for the freezing of till saturated with 20-40% porewater. Our interpretation of the basal ice sequences obtained from above SLM is further supported by recent modeling work by Meyer et al. (2018) showing that sediment deposited in the North Atlantic during Heinrich events must have been incorporated into the base of the Northern Hemisphere ice sheets through freeze-on during the inter-Heinrich period, rather than during rapid streaming flow and ice discharge. Meyer et al. concluded that the differential incorporation is the result of unfavorable conditions of fast ice stream flow to induce sediment freeze-on due to melt generated by frictional and geothermal heating. Meyer et al. (2018) further showed that the thickness of the frozen sediment layer is sensitive to the heat flux at the ice-bed interface and the water pressure, both of which control basal friction. As the basal water pressure

increases, both the frozen sediment thickness and the basal friction decrease, leading us to conclude that basal water pressures must have been low during solid sediment entrainment in the SLM BIL, favoring a cold and stagnant ice stream.

We used a range of average present-day freeze rates (1 – 5 mm yr^{-1} from Christoffersen et al. (2010)) to estimate the time required to accrete the entire SLM basal ice layer. At these freeze rates, it would take 1,000 – 5,000 years to form the 5 m thick layer of basal ice. Assuming a freezing rate of 3 mm per year, 1 – 2 thousand years of basal freezing history is likely recorded in this sequence, which constrains the bottom 2 m sequence to the last ~500 – 1000 years. Although, to our knowledge, there have been no reports of Mercer Ice Stream stagnation, there are several regional events of ice stream variability previously published, specifically, the grounding of Crary Ice Rise, MIS/WIS flow redirection, and WIS stagnation/reactivation (Table 3.1). Although there is no direct evidence for MIS stagnation, basal freeze-on of debris-rich ice could plausibly have occurred during one of these events or during a period that predates, thus demonstrating the utility of basal ice layers in recording past ice stream basal history.

Table 3.1 Previously published Ross Sea ice stream variability events. Timing of events is given by year Before Present (BP).

Event	Time (years BP)	Source
Grounding line retreat	4000[1] – 6000[2]	[1]Neuhaus et al. (2021) [2]Venturelli et al., (2023)
South Crary Ice Rise grounds	1120	Bindschadler et al. (1990)
Grounding line readvance	1000	Neuhaus et al. (2021)
WIS stagnates	850	Fahnestock et al. (2000)
WIS and MIS flow north of Crary	550	Bindschadler et al. (1990)
WIS reactivates	450	Hulbe and Fahnestock (2007)
SLM forms	180	Siegfried et al. (2023)
KIS stagnates	180	Catania et al. (2012)
WIS decelerates	60	Beem et al. (2014) Joughin et al. (2005)
Whillans Water Piracy	15	Carter et al. (2013)

Conclusion

We observed a 5 m thick basal ice sequence above the ice-water interface at SLM containing a sequence of sediment layers. The sediment sequence was composed of two main ice facies types, that were differentiated by debris content and that showed an alternating distribution vertically. The upper clear ice containing <1 % sediment is interrupted to represent an active subglacial hydrologic system and fast ice streaming. The lower sequence contains solid sediment (> 20%) and reflects low basal water pressures, high rates of basal freeze-on, which represent the strengthening of the bed and the past stagnation of the ice stream. Collectively, our results demonstrate the potential for basal ice layers to transport sediments to the Ross Ice Shelf and the subsequent melt-out of carbon and nutrients to the coastal marine (sub-ice) environment (Venturelli et al., 2023; Hawkings et al., 2020; Vick-Majors et al., 2020).

References Cited

Beem, L.H., Tulaczyk, S.M., King, M.A., Bougamont, M., Fricker, H.A., and Christoffersen, P., 2014, Variable deceleration of Whillans Ice Stream, West Antarctica: Journal of Geophysical Research: Earth Surface, v. 119, p. 212–224, doi:https://doi.org/10.1002/2013JF002958.

Bougamont, M., and Christoffersen, P., 2012, Hydrologic forcing of ice stream flow promotes rapid transport of sediment in basal ice: Geology, v. 40, p. 735–738, doi:10.1130/G33036.1.

Burnett, J., Rack, F., Zook, B., and Schmidt, B., 2015, Development of a borehole deployable remotely operated vehicle for investigation of sub-ice aquatic environments, *in* IEEE, p. 1–7.

Catania, G., Hulbe, C., Conway, H., Scambos, T.A., and Raymond, C.F., 2012, Variability in the mass flux of the Ross ice streams, West Antarctica, over the last millennium: Journal of Glaciology, v. 58, p. 741–752, doi:10.3189/2012JoG11J219.

Christoffersen, P., Tulaczyk, S., and Behar, A., 2010, Basal ice sequences in Antarctic ice stream: Exposure of past hydrologic conditions and a principal mode of sediment transfer: Journal of Geophysical Research: Earth Surface, v. 115, doi:https://doi.org/10.1029/2009JF001430.

Christoffersen, P., Tulaczyk, S., Carsey, F.D., and Behar, A.E., 2006, A quantitative framework for interpretation of basal ice facies formed by ice accretion over subglacial sediment: Journal of Geophysical Research: Earth Surface, v. 111, doi:10.1029/2005JF000363.

Conway, H., Catania, G., Raymond, C.F., Gades, A.M., Scambos, T.A., and Engelhardt, H., 2002, Switch of flow direction in an Antarctic ice stream: Nature, v. 419, p. 465–467, doi:10.1038/nature01081.

DeConto, R.M., and Pollard, D., 2016, Contribution of Antarctica to past and future sea-level rise: Nature, v. 531, p. 591–597, doi:10.1038/nature17145.

Fahnestock, M.A., Scambos, T.A., Bindschadler, R.A., and Kvaran, G., 2000, A millennium of variable ice flow recorded by the Ross Ice Shelf, Antarctica: Journal of Glaciology, v. 46, p. 652–664, doi:10.3189/172756500781832693.

Goossens, T., Sapart, C.J., Dahl-Jensen, D., Popp, T., El Amri, S., and Tison, J.-L., 2016, A comprehensive interpretation of the NEEM basal ice build-up using a multi-parametric approach: The Cryosphere, v. 10, p. 553–567, doi:10.5194/tc-10-553-2016.

Gow, A.J., and Meese, D., 2007, Physical properties, crystalline textures and c-axis fabrics of the Siple Dome (Antarctica) ice core: Journal of Glaciology, v. 53, p. 573–584, doi:10.3189/002214307784409252.

Heinrich, H., 1988, Origin and Consequences of Cyclic Ice Rafting in the Northeast Atlantic Ocean During the Past 130,000 Years: Quaternary Research, v. 29, p. 142–152, doi:10.1016/0033-5894(88)90057-9.

Hemming, S.R., 2004, Heinrich events: Massive late Pleistocene detritus layers of the North Atlantic and their global climate imprint: Reviews of Geophysics, v. 42, doi:10.1029/2003RG000128.

Hubbard, B., Cook, S., and Coulson, H., 2009, Basal ice facies: a review and unifying approach: Quaternary Science Reviews, v. 28, p. 1956–1969, doi:10.1016/j.quascirev.2009.03.005.

Hulbe, C., and Fahnestock, M., 2007, Century-scale discharge stagnation and reactivation of the Ross ice streams, West Antarctica: Journal of Geophysical Research: Earth Surface, v. 112, doi:10.1029/2006JF000603.

Hulbe, C.L., Scambos, T.A., Klinger, M., and Fahnestock, M.A., 2016, Flow variability and ongoing margin shifts on Bindschadler and MacAyeal Ice Streams, West Antarctica: Journal of Geophysical Research: Earth Surface, v. 121, p. 283–293, doi:10.1002/2015JF003670.

Jacobel, R.W., Scambos, T.A., Raymond, C.F., and Gades, A.M., 1996, Changes in the configuration of ice stream flow from the West Antarctic Ice Sheet: Journal of Geophysical Research: Solid Earth, v. 101, p. 5499–5504, doi:10.1029/95JB03735.

Knight, P.G., 1997, The basal ice layer of glaciers and ice sheets: Quaternary Science Reviews, v. 16, p. 975–993, doi:10.1016/S0277-3791(97)00033-4.

Meyer, C.R., Robel, A.A., and Rempel, A.W., 2019, Frozen fringe explains sediment freeze-on during Heinrich events: Earth and Planetary Science Letters, v. 524, p. 115725, doi:10.1016/j.epsl.2019.115725.

Mouginot, J., Rignot, E., and Scheuchl, B., 2019, Continent-Wide, Interferometric SAR Phase, Mapping of Antarctic Ice Velocity: Geophysical Research Letters, v. 46, p. 9710–9718, doi:10.1029/2019GL083826.

Ng, F., and Conway, H., 2004, Fast-flow signature in the stagnated Kamb Ice Stream, West Antarctica: Geology, v. 32, p. 481–484, doi:10.1130/G20317.1.

Rempel, A.W., 2008, A theory for ice-till interactions and sediment entrainment beneath glaciers: Journal of Geophysical Research: Earth Surface, v. 113, doi:10.1029/2007JF000870.

Rempel, A.W., Hansen, D.D., Zoet, L.K., and Meyer, C.R., 2023, Diffuse debris entrainment in glacier, lab and model environments: Annals of Glaciology, p. 1–13, doi:10.1017/aog.2023.31.

Retzlaff, R., and Bentley, C.R., 1993, Timing of stagnation of Ice Stream C, West Antarctica, from short-pulse radar studies of buried surface crevasses: Journal of Glaciology, v. 39, p. 553–561, doi:10.3189/S0022143000016440.

Scambos, T.A., Haran, T.M., Fahnestock, M.A., Painter, T.H., and Bohlander, J., 2007, MODIS-based Mosaic of Antarctica (MOA) data sets: Continent-wide surface morphology and snow grain size: Remote Sensing of the Cryosphere Special Issue, v. 111, p. 242–257, doi:10.1016/j.rse.2006.12.020.

Siegfried, M.R., Fricker, H.A., Carter, S.P., and Tulaczyk, S., 2016, Episodic ice velocity fluctuations triggered by a subglacial flood in West Antarctica: Geophysical Research Letters, v. 43, p. 2640–2648, doi:10.1002/2016GL067758.

Tulaczyk, S., and Hossainzadeh, S., 2011, Antarctica's Deep Frozen "Lakes": Science, v. 331, p. 1524–1525, doi:10.1126/science.1202888.

Vogel, S.W., Tulaczyk, S., Kamb, B., Engelhardt, H., Carsey, F.D., Behar, A.E., Lane, A.L., and Joughin, I., 2005, Subglacial conditions during and after stoppage of an Antarctic Ice Stream: Is reactivation imminent? Geophysical Research Letters, v. 32, doi:10.1029/2005GL022563.

CHAPTER FOUR

CONCLUSION

Concluding Remarks

Antarctica's subglacial environment is one of the most unexplored and least understood systems on the planet but is the key contributor to future sea level rise. As the rate of ice loss increases driven by a warming atmosphere and ocean, improved knowledge of the basal boundary conditions beneath the Antarctic ice sheets and their spatiotemporal variability will be critical for accurate ice sheet model development related to sea level rise predictions which will benefit society. Over the past 50 years, much has been learned about subglacial Antarctic environments. The presence of water and deformable soft sediments paved the way for explaining the high flow velocities of West Antarctica's ice streams. The discovery of interconnected subglacial lakes that harbor microbial ecosystems, modulate ice stream velocity changes, and record paleoenvironmental conditions inspired a new generation of research and transformed the way we view the continent. The reorganization of ice streams has been linked to alterations in the routing of subglacial meltwater and ice thickness variations, driving regional mass balance changes. Improved sediment dating techniques have resolved questions concerning the rapid migration and readvancement of the marine grounding line. Although there have been significant scientific discoveries, tackling the central questions of how much will the West Antarctic Ice Sheet melt and how soon will it happen demands more extensive temporal records of ice sheet change and over larger spatial scales. The overarching goal of this dissertation research has been to contribute two additional records of West Antarctic subglacial history to

offer insight into meltwater drainage, basal thermal history, and physical processes beneath the Mercer Ice Stream, West Antarctica. I used sediment cores collected from Mercer Subglacial Lake as well as ice properties and sediment debris observed in basal ice imagery to better understand past basal boundary conditions. My primary research objectives were:

- Characterize the properties of sediments collected from SLM and those observed in the basal ice layer above the lake.
- Develop an understanding of the processes and conditions responsible for the stratigraphic variability observed in the SLM sediment core record and basal ice sequence.
- Reconstruct the paleoenvironment of MIS, with specific attention to the hydrologic and basal thermal histories, thereby extending the observational record of these processes.

Objective 1:

To address Objective 1, I employed a suite of non-destructive and destructive analyses to characterize the physical and geochemical properties of sediment cores collected from SLM (Chapter 2). A continuous 2.06 m composite record was constructed. High resolution computer tomography, particle size analysis, and elemental ratios differentiated sediment bodies into unique sedimentary facies, including massive-to-stratified diamicts, massive muds, and laminated mud with dropstones. Mineralogical differences were shown by x-ray powder diffraction. I analyzed borehole imagery that captured a 5 m thick sequence of accreted basal ice above the subglacial lake (Chapter 3). Color pixel and grayscale brightness intensities demonstrated differences in the concentration of sediment incorporated into the ice layer. The basal ice layer comprised two main sequences. The upper 3.2 m of basal ice was clear with

minimal sediment (1%) while the lower 1.8 m comprised clear, massive, and solid ice types which contained up to 25 times more sediment than the upper sequence.

Objective 2:

To address Objective 2, I used the property descriptions from Objective 1 to develop models for sediment entrainment and deposition. The sediment record comprised glacial tills interbedded with meltwater drainage deposits and capped by rhymically laminated lake sediments (Chapter 2). Geochemistry of the sediment porewater showed that glacier ice melt was the primary water source. The glacial tills were deposited beneath a grounded ice stream by a combination of deformation and lodgement. Meltwater deposits accumulated by suspension settling in a slowly flowing or ponded subglacial drainage system. The rhythmically laminated lake sediments reflect a continuum of processes associated with fall-out from basal ice melt, upstream meltwater input into the lake, and water column thickness changes associated with fill-drain cycles. These processes were associated with evolving depositional environments included grounded ice stream, subglacial meltwater drainage, and subglacial lacustrine (Chapter 2). The three distinct ice facies present in SLM basal ice represent variations in the supply of subglacial meltwater, rates of basal freezing, and basal boundary conditions (Chapter 3). The clear ice of the upper sequence formed under conditions with abundant meltwater below the pressure melting temperature, at pressures that exceeded the overburden pressure of the overlying ice stream to induce ice-bed decoupling. In contrast, the lower sequence containing 25x more sediment indicates basal conditions favoring high freezing rates with water restricted mainly to pore water flow causing a state of ice-bed coupling and the entrainment of high sediment contents. Solid sediment layers are separated by thin debris-poor layers suggesting punctuated periods of

elevated meltwater discharge. In summary, the concentration of sediment entrainment is dependent on the extent of basal freezing and the supply of subglacial meltwater.

Objective 3:

To address Objective 3, I reconstructed the subglacial history of the Mercer Ice Stream using the two paleoenvironmental records recovered from SLM. Evolving depositional environments included grounded ice stream, subglacial meltwater drainage, and subglacial lacustrine (Chapter 2) and are broadly reflected by the meltwater history archived by the basal ice sequence that records an upper, meltwater abundant regime and a lower, meltwater restrictive environment at times when the temperature of the water was below the pressure melting temperature to cause freeze-on (Chapter 3). Integrating previously published geophysical observations and spectral analysis of sediment laminae, carbon dating of subglacial sediments, and estimates of basal freeze-on rates, I constrained the timing of sediment deposition and basal ice accretion at SLM to have occurred within the late Holocene. The timing of changes in meltwater delivery and oscillating basal conditions during this time coincide with broader regional scale ice stream reorganizational events.

Future Outlook

Over the past two decades, advances in geophysical and sedimentological studies have driven our understanding of Antarctica's subglacial environment forward. We have learned that links exist between the routing of subglacial meltwater and ice stream behavior, and this has inspired new hypotheses concerning the spatiotemporal evolution of meltwater beneath the ice sheet. Dating of subglacial sediments and interpreting depositional ages remains challenging and may

continue to be a limitation of this environment into the future. Thus, improved integration of theory, numerical modeling, and direct observation is needed to reduce our knowledge gaps.

REFERENCES CITED

Alley, R.B., 1991, Deforming-bed origin for southern Laurentide till sheets? Journal of Glaciology, v. 37, p. 67–76, doi:10.3189/S0022143000042817.

Alley, R.B., 1989, Water-pressure Coupling of Sliding and Bed Deformation: II. Velocity-Depth Profiles: Journal of Glaciology, v. 35, p. 119–129, doi:10.3189/002214389793701518.

Alley, R., Anandakrishnan, S., Bentley, C., and Lord, N., 1994, A water-piracy hypothesis for the stagnation of Ice Stream C, Antarctica: Annals of Glaciology, v. 20, p. 187–194.

Alley, R.B., Blankenship, D.D., Bentley, C.R., and Rooney, S., 1986, Deformation of till beneath ice stream B, West Antarctica: Nature, v. 322, p. 57–59.

Alley, R.B., Blankenship, D.D., Bentley, C.R., and Rooney, S.T., 1987, Till beneath ice stream B: 3. Till deformation: Evidence and implications: Journal of Geophysical Research: Solid Earth, v. 92, p. 8921–8929, doi:10.1029/JB092iB09p08921.

Alley, R.B., Cuffey, K., Evenson, E., Strasser, J., Lawson, D., and Larson, G., 1997, How glaciers entrain and transport basal sediment: physical constraints: Quaternary Science Reviews, v. 16, p. 1017–1038.

Alley, R.B., Lawson, D.E., Evenson, E.B., Strasser, J.C., and Larson, G.J., 1998, Glaciohydraulic supercooling: a freeze-on mechanism to create stratified, debris-rich basal ice: II. Theory: Journal of Glaciology, v. 44, p. 563–569.

Amante, C., and Eakins, B.W., 2009, ETOPO1 arc-minute global relief model: procedures, data sources and analysis:

Anandakrishnan, S., and Alley, R.B., 1997, Stagnation of Ice Stream C, West Antarctica by water piracy: Geophysical Research Letters, v. 24, p. 265–268, doi:10.1029/96GL04016.

Anderson, J.B., Conway, H., Bart, P.J., Witus, A.E., Greenwood, S.L., McKay, R.M., Hall, B.L., Ackert, R.P., Licht, K., and Jakobsson, M., 2014, Ross Sea paleo-ice sheet drainage and deglacial history during and since the LGM: Quaternary Science Reviews, v. 100, p. 31–54.

Artemieva, I.M., 2022, Antarctica ice sheet basal melting enhanced by high mantle heat: Earth-science reviews, v. 226, p. 103954.

Beem, L.H., Tulaczyk, S.M., King, M.A., Bougamont, M., Fricker, H.A., and Christoffersen, P., 2014, Variable deceleration of Whillans Ice Stream, West Antarctica: Journal of Geophysical Research: Earth Surface, v. 119, p. 212–224, doi:https://doi.org/10.1002/2013JF002958.

Bell, R.E., 2008, The role of subglacial water in ice-sheet mass balance: Nature Geoscience, v. 1, p. 297–304, doi:10.1038/ngeo186.

Bell, R.E., Ferraccioli, F., Creyts, T.T., Braaten, D., Corr, H., Das, I., Damaske, D., Frearson, N., Jordan, T., and Rose, K., 2011, Widespread persistent thickening of the East Antarctic Ice Sheet by freezing from the base: Science, v. 331, p. 1592–1595.

Benn, D., and Evans, D.J., 2014, Glaciers and glaciation: Routledge.

Bennett, M.R., 2003, Ice streams as the arteries of an ice sheet: their mechanics, stability and significance: Earth-Science Reviews, v. 61, p. 309–339.

Bentley, M.J., Christoffersen, P., Hodgson, D.A., Smith, A.M., Tulaczyk, S., and Le Brocq, A.M., 2011, Subglacial Lake Sediments and Sedimentary Processes: Potential Archives of Ice Sheet Evolution, Past Environmental Change, and the Presence Of Life, *in* Antarctic Subglacial Aquatic Environments, Geophysical Monograph Series, p. 83–110, doi:10.1002/9781118670354.ch6.

Blankenship, D.D., Bentley, C.R., Rooney, S., and Alley, R.B., 1986, Seismic measurements reveal a saturated porous layer beneath an active Antarctic ice stream: Nature, v. 322, p. 54–57.

Blankenship, D.D., Bentley, C.R., Rooney, S.T., and Alley, R.B., 1987, Till beneath ice stream B: 1. Properties derived from seismic travel times: Journal of Geophysical Research: Solid Earth, v. 92, p. 8903–8911, doi:10.1029/JB092iB09p08903.

Bodart, J.A., Bingham, R.G., Young, D.A., MacGregor, J.A., Ashmore, D.W., Quartini, E., Hein, A.S., Vaughan, D.G., and Blankenship, D.D., 2023, High mid-Holocene accumulation rates over West Antarctica inferred from a pervasive ice-penetrating radar reflector: The Cryosphere, v. 17, p. 1497–1512, doi:10.5194/tc-17-1497-2023.

Bougamont, M., and Christoffersen, P., 2012, Hydrologic forcing of ice stream flow promotes rapid transport of sediment in basal ice: Geology, v. 40, p. 735–738, doi:10.1130/G33036.1.

Bougamont, M., Christoffersen, P., Price, S.F., Fricker, H.A., Tulaczyk, S., and Carter, S.P., 2015, Reactivation of Kamb Ice Stream tributaries triggers century-scale reorganization of Siple Coast ice flow in West Antarctica: Geophysical Research Letters, v. 42, p. 8471–8480, doi:10.1002/2015GL065782.

Buechi, M.W., Frank, S.M., Graf, H.R., Menzies, J., and Anselmetti, F.S., 2017, Subglacial emplacement of tills and meltwater deposits at the base of overdeepened bedrock troughs: Sedimentology, v. 64, p. 658–685, doi:10.1111/sed.12319.

Burnett, J., Rack, F., Zook, B., and Schmidt, B., 2015, Development of a borehole deployable remotely operated vehicle for investigation of sub-ice aquatic environments, *in* IEEE, p. 1–7.

Carter, S.P., Fricker, H.A., and Siegfried, M.R., 2017, Antarctic subglacial lakes drain through sediment-floored canals: theory and model testing on real and idealized domains: The Cryosphere, v. 11, p. 381–405, doi:10.5194/tc-11-381-2017.

Carter, S.P., Fricker, H.A., and Siegfried, M.R., 2013, Evidence of rapid subglacial water piracy under Whillans Ice Stream, West Antarctica: Journal of Glaciology, v. 59, p. 1147–1162, doi:10.3189/2013JoG13J085.

Catania, G., Hulbe, C., Conway, H., Scambos, T.A., and Raymond, C.F., 2012, Variability in the mass flux of the Ross ice streams, West Antarctica, over the last millennium: Journal of Glaciology, v. 58, p. 741–752, doi:10.3189/2012JoG11J219.

Catania, G.A., Scambos, T.A., Conway, H., and Raymond, C.F., 2006, Sequential stagnation of Kamb Ice Stream, West Antarctica: Geophysical Research Letters, v. 33, doi:10.1029/2006GL026430.

Center, N., 2009, ETOPO1 1 arc-minute global relief model: NOAA National Centers for Environmental Information.(date accessed: 2021-1-05) doi, v. 10, p. V5C8276M.

Christoffersen, P., Tulaczyk, S., and Behar, A., 2010, Basal ice sequences in Antarctic ice stream: Exposure of past hydrologic conditions and a principal mode of sediment transfer: Journal of Geophysical Research: Earth Surface, v. 115, doi:https://doi.org/10.1029/2009JF001430.

Christoffersen, P., Tulaczyk, S., Carsey, F.D., and Behar, A.E., 2006, A quantitative framework for interpretation of basal ice facies formed by ice accretion over subglacial sediment: Journal of Geophysical Research: Earth Surface, v. 111, doi:10.1029/2005JF000363.

Church, J.A., Clark, P.U., Cazenave, A., Gregory, J.M., Jevrejeva, S., Levermann, A., Merrifield, M.A., Milne, G.A., Nerem, R.S., and Nunn, P.D., 2013, Sea level change: PM Cambridge University Press.

Clarke, G.K., 2005, Subglacial processes: Annu. Rev. Earth Planet. Sci., v. 33, p. 247–276.

Clarke, G.K.C., 1987, Subglacial till: A physical framework for its properties and processes: Journal of Geophysical Research: Solid Earth, v. 92, p. 9023–9036, doi:https://doi.org/10.1029/JB092iB09p09023.

Clerc, S., Buoncristiani, J.-F., Guiraud, M., Desaubliaux, G., and Portier, E., 2012, Depositional model in subglacial cavities, Killiney Bay, Ireland. Interactions between sedimentation, deformation and glacial dynamics: Quaternary Science Reviews, v. 33, p. 142–164, doi:10.1016/j.quascirev.2011.12.004.

Conway, H., Catania, G., Raymond, C.F., Gades, A.M., Scambos, T.A., and Engelhardt, H., 2002, Switch of flow direction in an Antarctic ice stream: Nature, v. 419, p. 465–467, doi:10.1038/nature01081.

Cook, S.J., and Knight, P.G., 2009, Glaciohydraulic supercooling: Progress in Physical Geography: Earth and Environment, v. 33, p. 705–710, doi:10.1177/0309133309342653.

Cook, S.J., Knight, P.G., Waller, R.I., Robinson, Z.P., and Adam, W.G., 2007, The geography of basal ice and its relationship to glaciohydraulic supercooling: Svínafellsjökull, southeast Iceland: Quaternary Science Reviews, v. 26, p. 2309–2315, doi:10.1016/j.quascirev.2007.07.010.

Creyts, T.T., and Schoof, C.G., 2009, Drainage through subglacial water sheets: Journal of Geophysical Research: Earth Surface, v. 114, doi:10.1029/2008JF001215.

Cuffey, K.M., and Paterson, W.S.B., 2010, The physics of glaciers: Academic Press.

Davis, C.L. et al., 2023, Biogeochemical and historical drivers of microbial community composition and structure in sediments from Mercer Subglacial Lake, West Antarctica: ISME Communications, v. 3, p. 8, doi:10.1038/s43705-023-00216-w.

DeConto, R.M., and Pollard, D., 2016, Contribution of Antarctica to past and future sea-level rise: Nature, v. 531, p. 591–597, doi:10.1038/nature17145.

Depoorter, M.A., Bamber, J.L., Griggs, J.A., Lenaerts, J.T.M., Ligtenberg, S.R.M., van den Broeke, M.R., and Moholdt, G., 2013, Calving fluxes and basal melt rates of Antarctic ice shelves: Nature, v. 502, p. 89–92, doi:10.1038/nature12567.

Domack, E.W., Jacobson, E.A., Shipp, S., and Anderson, J.B., 1999, Late Pleistocene–Holocene retreat of the West Antarctic Ice-Sheet system in the Ross Sea: Part 2—Sedimentologic and stratigraphic signature: GSA Bulletin, v. 111, p. 1517–1536, doi:10.1130/0016-7606(1999)111<1517:LPHROT>2.3.CO;2.

Dow, C.F., Ross, N., Jeofry, H., Siu, K., and Siegert, M.J., 2022, Antarctic basal environment shaped by high-pressure flow through a subglacial river system: Nature Geoscience, v. 15, p. 892–898, doi:10.1038/s41561-022-01059-1.

Dow, C.F., Werder, M.A., Nowicki, S., and Walker, R.T., 2016, Modeling Antarctic subglacial lake filling and drainage cycles: The Cryosphere, v. 10, p. 1381–1393, doi:10.5194/tc-10-1381-2016.

Edwards, T.L., Nowicki, S., Marzeion, B., Hock, R., Goelzer, H., Seroussi, H., Jourdain, N.C., Slater, D.A., Turner, F.E., and Smith, C.J., 2021, Projected land ice contributions to twenty-first-century sea level rise: Nature, v. 593, p. 74–82.

Elsworth, C.W., and Suckale, J., 2016, Rapid ice flow rearrangement induced by subglacial drainage in West Antarctica: Geophysical Research Letters, v. 43, p. 11,697-11,707, doi:10.1002/2016GL070430.

Engelhardt, H., and Kamb, B., 1997, Basal hydraulic system of a West Antarctic ice stream: constraints from borehole observations: Journal of Glaciology, v. 43, p. 207–230, doi:10.3189/S0022143000003166.

Evans, D.J.A., Phillips, E.R., Hiemstra, J.F., and Auton, C.A., 2006, Subglacial till: Formation, sedimentary characteristics and classification: Earth-Science Reviews, v. 78, p. 115–176, doi:10.1016/j.earscirev.2006.04.001.

Evans, J., Pudsey, C.J., ÓCofaigh, C., Morris, P., and Domack, E., 2005, Late Quaternary glacial history, flow dynamics and sedimentation along the eastern margin of the Antarctic Peninsula Ice Sheet: Quaternary Science Reviews, v. 24, p. 741–774, doi:10.1016/j.quascirev.2004.10.007.

Fahnestock, M.A., Scambos, T.A., Bindschadler, R.A., and Kvaran, G., 2000, A millennium of variable ice flow recorded by the Ross Ice Shelf, Antarctica: Journal of Glaciology, v. 46, p. 652–664, doi:10.3189/172756500781832693.

Favier, L., Durand, G., Cornford, S.L., Gudmundsson, G.H., Gagliardini, O., Gillet-Chaulet, F., Zwinger, T., Payne, A., and Le Brocq, A.M., 2014, Retreat of Pine Island Glacier controlled by marine ice-sheet instability: Nature Climate Change, v. 4, p. 117–121.

Flowers, G.E., 2015, Modelling water flow under glaciers and ice sheets: Proceedings of the Royal Society A: Mathematical, Physical and Engineering Sciences, v. 471, p. 20140907, doi:10.1098/rspa.2014.0907.

Folk, R.L., and Ward, W.C., 1957, Brazos River bar [Texas]; a study in the significance of grain size parameters: Journal of sedimentary research, v. 27, p. 3–26.

Fredsoe, J., and Deigaard, R., 1992, Mechanics of coastal sediment transport: World scientific publishing company, v. 3.

Fretwell, P. et al., 2013, Bedmap2: improved ice bed, surface and thickness datasets for Antarctica: The Cryosphere, v. 7, p. 375–393, doi:10.5194/tc-7-375-2013.

Fricker, H.A., Scambos, T., Bindschadler, R., and Padman, L., 2007, An Active Subglacial Water System in West Antarctica Mapped from Space: Science, v. 315, p. 1544–1548, doi:10.1126/science.1136897.

Goossens, T., Sapart, C.J., Dahl-Jensen, D., Popp, T., El Amri, S., and Tison, J.-L., 2016, A comprehensive interpretation of the NEEM basal ice build-up using a multi-parametric approach: The Cryosphere, v. 10, p. 553–567, doi:10.5194/tc-10-553-2016.

Gow, A.J., Epstein, S., and Sheehy, W., 1979, On the Origin of Stratified Debris in Ice Cores from the Bottom of the Antarctic Ice Sheet: Journal of Glaciology, v. 23, p. 185–192, doi:10.3189/S0022143000029828.

Gow, A.J., and Meese, D., 2007, Physical properties, crystalline textures and c-axis fabrics of the Siple Dome (Antarctica) ice core: Journal of Glaciology, v. 53, p. 573–584, doi:10.3189/002214307784409252.

Greenwood, S.L., Clason, C.C., Helanow, C., and Margold, M., 2016, Theoretical, contemporary observational and palaeo-perspectives on ice sheet hydrology: Processes and products: Earth-Science Reviews, v. 155, p. 1–27, doi:10.1016/j.earscirev.2016.01.010.

Gulev, S.K., Thorne, P.W., Ahn, J., Dentener, F.J., Domingues, C.M., Gerland, S., Gong, D., Kaufman, D.S., Nnamchi, H.C., and Quaas, J., 2021, Changing state of the climate system:

Gustafson, C.D., Key, K., Siegfried, M.R., Winberry, J.P., Fricker, H.A., Venturelli, R.A., and Michaud, A.B., 2022, A dynamic saline groundwater system mapped beneath an Antarctic ice stream: Science, v. 376, p. 640–644, doi:10.1126/science.abm3301.

Hagelberg, T., Shackleton, N., Pisias, N., and Party, S.S., 1992, 5. DEVELOPMENT OF COMPOSITE DEPTH SECTIONS FOR SITES 844 THROUGH 8541, *in* Proceeding Ocean Drilling Program Initial Reports, 138 College Station, Texas, USA: Ocean Drilling Program, Texas A&M University.

Halberstadt, A.R.W., Simkins, L.M., Anderson, J.B., Prothro, L.O., and Bart, P.J., 2018, Characteristics of the deforming bed: till properties on the deglaciated Antarctic continental shelf: Journal of Glaciology, v. 64, p. 1014–1027, doi:10.1017/jog.2018.92.

Halberstadt, A.R.W., Simkins, L.M., Greenwood, S.L., and Anderson, J.B., 2016, Past ice-sheet behaviour: retreat scenarios and changing controls in the Ross Sea, Antarctica: The Cryosphere, v. 10, p. 1003–1020, doi:10.5194/tc-10-1003-2016.

Hallet, B., 1979, Subglacial Regelation Water Film: Journal of Glaciology, v. 23, p. 321–334, doi:10.3189/S0022143000029932.

Hawkings, J.R. et al., 2020, Enhanced trace element mobilization by Earth's ice sheets: Proceedings of the National Academy of Sciences, v. 117, p. 31648–31659, doi:10.1073/pnas.2014378117.

Heinrich, H., 1988, Origin and Consequences of Cyclic Ice Rafting in the Northeast Atlantic Ocean During the Past 130,000 Years: Quaternary Research, v. 29, p. 142–152, doi:10.1016/0033-5894(88)90057-9.

Hemming, S.R., 2004, Heinrich events: Massive late Pleistocene detritus layers of the North Atlantic and their global climate imprint: Reviews of Geophysics, v. 42, doi:10.1029/2003RG000128.

Hjulström, F., 1939, Transportation of detritus by moving water: Part 1. Transportation. Recent Marine Sediments, a Symposium:

Hodson, T.O., Powell, R.D., Brachfeld, S.A., Tulaczyk, S., and Scherer, R.P., 2016, Physical processes in Subglacial Lake Whillans, West Antarctica: Inferences from sediment cores: Earth and Planetary Science Letters, v. 444, p. 56–63, doi:10.1016/j.epsl.2016.03.036.

Hounsfield, G.N., 1973, Computerized transverse axial scanning (tomography): Part 1. Description of system: The British Journal of Radiology, v. 46, p. 1016–1022, doi:10.1259/0007-1285-46-552-1016.

Hubbard, B., 1991, Freezing-rate effects on the physical characteristics of basal ice formed by net adfreezing: Journal of Glaciology, v. 37, p. 339–347, doi:10.3189/S0022143000005773.

Hubbard, B., Cook, S., and Coulson, H., 2009, Basal ice facies: a review and unifying approach: Quaternary Science Reviews, v. 28, p. 1956–1969, doi:10.1016/j.quascirev.2009.03.005.

Hubbard, B., and Sharp, M., 1989, Basal ice formation and deformation: a review: Progress in Physical Geography: Earth and Environment, v. 13, p. 529–558, doi:10.1177/030913338901300403.

Hughes, T., 1973, Is the west Antarctic Ice Sheet disintegrating? Journal of Geophysical Research (1896-1977), v. 78, p. 7884–7910, doi:10.1029/JC078i033p07884.

Hulbe, C., and Fahnestock, M., 2007, Century-scale discharge stagnation and reactivation of the Ross ice streams, West Antarctica: Journal of Geophysical Research: Earth Surface, v. 112, doi:10.1029/2006JF000603.

Hulbe, C.L., Scambos, T.A., Klinger, M., and Fahnestock, M.A., 2016, Flow variability and ongoing margin shifts on Bindschadler and MacAyeal Ice Streams, West Antarctica: Journal of Geophysical Research: Earth Surface, v. 121, p. 283–293, doi:10.1002/2015JF003670.

Jacobel, R.W., Scambos, T.A., Raymond, C.F., and Gades, A.M., 1996, Changes in the configuration of ice stream flow from the West Antarctic Ice Sheet: Journal of Geophysical Research: Solid Earth, v. 101, p. 5499–5504, doi:10.1029/95JB03735.

Joughin, I., and Alley, R.B., 2011, Stability of the West Antarctic ice sheet in a warming world: Nature Geoscience, v. 4, p. 506–513, doi:10.1038/ngeo1194.

Joughin, I., and Tulaczyk, S., 2002, Positive Mass Balance of the Ross Ice Streams, West Antarctica: Science, v. 295, p. 476–480, doi:10.1126/science.1066875.

Jouzel, J., Petit, J.R., Souchez, R., Barkov, N.I., Lipenkov, V.Ya., Raynaud, D., Stievenard, M., Vassiliev, N.I., Verbeke, V., and Vimeux, F., 1999, More Than 200 Meters of Lake Ice Above Subglacial Lake Vostok, Antarctica: Science, v. 286, p. 2138–2141, doi:10.1126/science.286.5447.2138.

Kamb, B., 2001, Basal Zone of the West Antarctic Ice Streams and its Role in Lubrication of Their Rapid Motion, *in* The West Antarctic Ice Sheet: Behavior and Environment, Antarctic Research Series, p. 157–199, doi:10.1029/AR077p0157.

Kamb, B., 1987, Glacier surge mechanism based on linked cavity configuration of the basal water conduit system: Journal of Geophysical Research: Solid Earth, v. 92, p. 9083–9100, doi:10.1029/JB092iB09p09083.

Ketcham, R.A., and Carlson, W.D., 2001, Acquisition, optimization and interpretation of X-ray computed tomographic imagery: applications to the geosciences: 3D reconstruction, modelling & visualization of geological materials, v. 27, p. 381–400, doi:10.1016/S0098-3004(00)00116-3.

Kingslake, J., Scherer, R.P., Albrecht, T., Coenen, J., Powell, R.D., Reese, R., Stansell, N.D., Tulaczyk, S., Wearing, M.G., and Whitehouse, P.L., 2018, Extensive retreat and re-advance of the West Antarctic Ice Sheet during the Holocene: Nature, v. 558, p. 430–434, doi:10.1038/s41586-018-0208-x.

Knight, P.G., 1997, The basal ice layer of glaciers and ice sheets: Quaternary Science Reviews, v. 16, p. 975–993, doi:10.1016/S0277-3791(97)00033-4.

Kreutz, K.J., and Mayewski, P.A., 1999, Spatial variability of Antarctic surface snow glaciochemistry: implications for palaeoatmospheric circulation reconstructions: Antarctic Science, v. 11, p. 105–118, doi:10.1017/S0954102099000140.

Kuhn, G., Hillenbrand, C.-D., Kasten, S., Smith, J.A., Nitsche, F.O., Frederichs, T., Wiers, S., Ehrmann, W., Klages, J.P., and Mogollón, J.M., 2017, Evidence for a palaeo-subglacial lake on the Antarctic continental shelf: Nature Communications, v. 8, p. 15591, doi:10.1038/ncomms15591.

Lawson, D.E., Strasser, J.C., Evenson, E.B., Alley, R.B., Larson, G.J., and Arcone, S.A., 1998, Glaciohydraulic supercooling: a freeze-on mechanism to create stratified, debris-rich basal ice: I. Field evidence: Journal of Glaciology, v. 44, p. 547–562, doi:10.3189/S0022143000002069.

Lee, H., Calvin, K., Dasgupta, D., Krinner, G., Mukherji, A., Thorne, P., Trisos, C., Romero, J., Aldunce, P., and Barrett, K., 2023, Climate change 2023: synthesis report. Contribution of working groups I, II and III to the sixth assessment report of the intergovernmental panel on climate change:, doi:doi: 10.59327/IPCC/AR6-9789291691647.001.

Lepp, A.P. et al., 2022, Sedimentary Signatures of Persistent Subglacial Meltwater Drainage From Thwaites Glacier, Antarctica: Frontiers in Earth Science, v. 10, https://www.frontiersin.org/articles/10.3389/feart.2022.863200.

Licht, K.J., and Andrews, J.T., 2002, The 14C Record of Late Pleistocene Ice Advance and Retreat in the Central Ross Sea, Antarctica: Arctic, Antarctic, and Alpine Research, v. 34, p. 324–333, doi:10.1080/15230430.2002.12003501.

Licht, K.J., Dunbar, N.W., Andrews, J.T., and Jennings, A.E., 1999, Distinguishing subglacial till and glacial marine diamictons in the western Ross Sea, Antarctica: Implications for a last glacial maximum grounding line: GSA Bulletin, v. 111, p. 91–103, doi:10.1130/0016-7606(1999)111<0091:DSTAGM>2.3.CO;2.

Lisiecki, L.E., and Herbert, T.D., 2007, Automated composite depth scale construction and estimates of sediment core extension: Paleoceanography, v. 22, doi:10.1029/2006PA001401.

Livingstone, S.J. et al., 2022, Subglacial lakes and their changing role in a warming climate: Nature Reviews Earth & Environment, v. 3, p. 106–124, doi:10.1038/s43017-021-00246-9.

Livingstone, S.J., Clark, C.D., Piotrowski, J.A., Tranter, M., Bentley, M.J., Hodson, A., Swift, D.A., and Woodward, J., 2012, Theoretical framework and diagnostic criteria for the identification of palaeo-subglacial lakes: Quaternary Science Reviews, v. 53, p. 88–110, doi:10.1016/j.quascirev.2012.08.010.

Livingstone, S.J., Utting, D.J., Ruffell, A., Clark, C.D., Pawley, S., Atkinson, N., and Fowler, A.C., 2016, Discovery of relict subglacial lakes and their geometry and mechanism of drainage: Nature Communications, v. 7, p. ncomms11767, doi:10.1038/ncomms11767.

Lowe, A.L., and Anderson, J.B., 2002, Reconstruction of the West Antarctic ice sheet in Pine Island Bay during the Last Glacial Maximum and its subsequent retreat history: Quaternary Science Reviews, v. 21, p. 1879–1897, doi:10.1016/S0277-3791(02)00006-9.

McKay, R.M., Dunbar, G.B., Naish, T.R., Barrett, P.J., Carter, L., and Harper, M., 2008, Retreat history of the Ross Ice Sheet (Shelf) since the Last Glacial Maximum from deep-basin sediment cores around Ross Island: Antarctic cryosphere and Southern Ocean climate evolution (Cenozoic-Holocene), v. 260, p. 245–261, doi:10.1016/j.palaeo.2007.08.015.

McKay, R., Golledge, N.R., Maas, S., Naish, T., Levy, R., Dunbar, G., and Kuhn, G., 2016, Antarctic marine ice-sheet retreat in the Ross Sea during the early Holocene: Geology, v. 44, p. 7–10, doi:10.1130/G37315.1.

McKight, P., and Najab, J., 2010, Kruskal-Wallis Test. The Corsini Encyclopedia of Psychology, 1, 1-10:

Mercer, J.H., 1978, West Antarctic ice sheet and CO2 greenhouse effect: a threat of disaster: Nature, v. 271, p. 321–325, doi:10.1038/271321a0.

Meyer, C.R., Robel, A.A., and Rempel, A.W., 2019, Frozen fringe explains sediment freeze-on during Heinrich events: Earth and Planetary Science Letters, v. 524, p. 115725, doi:10.1016/j.epsl.2019.115725.

Meyers, P., and Teranes, J., 2001, Sediment Organic Matter in Tracking Environmental Change Using Lake Sediments Volume 2: Physical and Geochemical Methods:

Michaud, A.B., and Priscu, J.C., 2023, Sediment oxygen consumption in Antarctic subglacial environments: Limnology and Oceanography, v. 68, p. 1557–1566, doi:10.1002/lno.12366.

Michaud, A.B., Skidmore, M.L., Mitchell, A.C., Vick-Majors, T.J., Barbante, C., Turetta, C., vanGelder, W., and Priscu, J.C., 2016, Solute sources and geochemical processes in Subglacial Lake Whillans, West Antarctica: Geology, v. 44, p. 347–350, doi:10.1130/G37639.1.

Michaud, A.B., Vick-Majors, T.J., Achberger, A.M., Skidmore, M.L., Christner, B.C., Tranter, M., and Priscu, J.C., 2020, Environmentally clean access to Antarctic subglacial aquatic environments: Antarctic Science, v. 32, p. 329–340, doi:10.1017/S0954102020000231.

Moncrieff, A.C.M., 1989, Classification of poorly-sorted sedimentary rocks: Sedimentary Geology, v. 65, p. 191–194, doi:10.1016/0037-0738(89)90015-8.

Moore, D.M., and Reynolds Jr, R.C., 1989, X-ray Diffraction and the Identification and Analysis of Clay Minerals.: Oxford University Press (OUP).

Morlighem, M. et al., 2020, Deep glacial troughs and stabilizing ridges unveiled beneath the margins of the Antarctic ice sheet: Nature Geoscience, v. 13, p. 132–137, doi:10.1038/s41561-019-0510-8.

Mosola, A.B., and Anderson, J.B., 2006, Expansion and rapid retreat of the West Antarctic Ice Sheet in eastern Ross Sea: possible consequence of over-extended ice streams? Quaternary Science Reviews, v. 25, p. 2177–2196, doi:10.1016/j.quascirev.2005.12.013.

Mouginot, J., Rignot, E., and Scheuchl, B., 2019, Continent-Wide, Interferometric SAR Phase, Mapping of Antarctic Ice Velocity: Geophysical Research Letters, v. 46, p. 9710–9718, doi:10.1029/2019GL083826.

Neuhaus, S.U., Tulaczyk, S.M., Stansell, N.D., Coenen, J.J., Scherer, R.P., Mikucki, J.A., and Powell, R.D., 2021, Did Holocene climate changes drive West Antarctic grounding line retreat and readvance? The Cryosphere, v. 15, p. 4655–4673, doi:10.5194/tc-15-4655-2021.

Neumann, B., Vafeidis, A.T., Zimmermann, J., and Nicholls, R.J., 2015, Future Coastal Population Growth and Exposure to Sea-Level Rise and Coastal Flooding - A Global Assessment: PLOS ONE, v. 10, p. e0118571, doi:10.1371/journal.pone.0118571.

Ng, F.S.L., 2000, Canals under sediment-based ice sheets: Annals of Glaciology, v. 30, p. 146–152, doi:10.3189/172756400781820633.

Ng, F., and Conway, H., 2004, Fast-flow signature in the stagnated Kamb Ice Stream, West Antarctica: Geology, v. 32, p. 481–484, doi:10.1130/G20317.1.

Nicholls, R.J., Lincke, D., Hinkel, J., Brown, S., Vafeidis, A.T., Meyssignac, B., Hanson, S.E., Merkens, J.-L., and Fang, J., 2021, A global analysis of subsidence, relative sea-level change and coastal flood exposure: Nature Climate Change, v. 11, p. 338–342, doi:10.1038/s41558-021-00993-z.

Nye, J.F., 1976, Water Flow in Glaciers: Jökulhlaups, Tunnels and Veins: Journal of Glaciology, v. 17, p. 181–207, doi:10.3189/S002214300001354X.

Ó Cofaigh, C., Evans, J., Dowdeswell, J.A., and Larter, R.D., 2007, Till characteristics, genesis and transport beneath Antarctic paleo-ice streams: Journal of Geophysical Research: Earth Surface, v. 112, doi:10.1029/2006JF000606.

Ojala, A.E.K., Mäkinen, J., Kajuutti, K., Ahokangas, E., and Palmu, J.-P., 2022, Subglacial evolution from distributed to channelized drainage: Evidence from the Lake Murtoo area in SW Finland: Earth Surface Processes and Landforms, v. 47, p. 2877–2896, doi:10.1002/esp.5430.

Phillips, D.L., and Gregg, J.W., 2001, Uncertainty in source partitioning using stable isotopes: Oecologia, v. 127, p. 171–179, doi:10.1007/s004420000578.

Piotrowski, J.A., and Tulaczyk, S., 1999, Subglacial conditions under the last ice sheet in northwest Germany: ice-bed separation and enhanced basal sliding? Quaternary Science Reviews, v. 18, p. 737–751, doi:10.1016/S0277-3791(98)00042-0.

Price, S.F., Bindschadler, R.A., Hulbe, C.L., and Joughin, I.R., 2001, Post-stagnation behavior in the upstream regions of Ice Stream C, West Antarctica: Journal of Glaciology, v. 47, p. 283–294, doi:10.3189/172756501781832232.

Priscu, J.C. et al., 2013, A microbiologically clean strategy for access to the Whillans Ice Stream subglacial environment: Antarctic Science, v. 25, p. 637–647, doi:10.1017/S0954102013000035.

Priscu, J.C. et al., 1999, Geomicrobiology of Subglacial Ice Above Lake Vostok, Antarctica: Science, v. 286, p. 2141–2144, doi:10.1126/science.286.5447.2141.

Priscu, J.C. et al., 2021, Scientific access into Mercer Subglacial Lake: scientific objectives, drilling operations and initial observations: Annals of Glaciology, v. 62, p. 340–352, doi:10.1017/aog.2021.10.

Pritchard, H.D., Arthern, R.J., Vaughan, D.G., and Edwards, L.A., 2009, Extensive dynamic thinning on the margins of the Greenland and Antarctic ice sheets: Nature, v. 461, p. 971–975, doi:10.1038/nature08471.

Prothro, L.O., Majewski, W., Yokoyama, Y., Simkins, L.M., Anderson, J.B., Yamane, M., Miyairi, Y., and Ohkouchi, N., 2020, Timing and pathways of East Antarctic Ice Sheet retreat: Quaternary Science Reviews, v. 230, p. 106166, doi:10.1016/j.quascirev.2020.106166.

Prothro, L.O., Simkins, L.M., Majewski, W., and Anderson, J.B., 2018, Glacial retreat patterns and processes determined from integrated sedimentology and geomorphology records: Marine Geology, v. 395, p. 104–119, doi:10.1016/j.margeo.2017.09.012.

Reilly, B.T. et al., 2019, Holocene break-up and reestablishment of the Petermann Ice Tongue, Northwest Greenland: Quaternary Science Reviews, v. 218, p. 322–342, doi:10.1016/j.quascirev.2019.06.023.

Reilly, B.T., Stoner, J.S., and Wiest, J., 2017, SedCT: MATLAB™ tools for standardized and quantitative processing of sediment core computed tomography (CT) data collected using a medical CT scanner: Geochemistry, Geophysics, Geosystems, v. 18, p. 3231–3240, doi:10.1002/2017GC006884.

Rempel, A.W., 2008, A theory for ice-till interactions and sediment entrainment beneath glaciers: Journal of Geophysical Research: Earth Surface, v. 113, doi:10.1029/2007JF000870.

Rempel, A.W., Hansen, D.D., Zoet, L.K., and Meyer, C.R., 2023, Diffuse debris entrainment in glacier, lab and model environments: Annals of Glaciology, p. 1–13, doi:10.1017/aog.2023.31.

Retzlaff, R., and Bentley, C.R., 1993, Timing of stagnation of Ice Stream C, West Antarctica, from short-pulse radar studies of buried surface crevasses: Journal of Glaciology, v. 39, p. 553–561, doi:10.3189/S0022143000016440.

Rignot, E., Mouginot, J., Scheuchl, B., van den Broeke, M., van Wessem, M.J., and Morlighem, M., 2019, Four decades of Antarctic Ice Sheet mass balance from 1979–2017: Proceedings of the National Academy of Sciences, v. 116, p. 1095–1103, doi:10.1073/pnas.1812883116.

Roberts, M.J., Tweed, F.S., Russell, A.J., Knudsen, Ó., Lawson, D.E., Larson, G.J., Evenson, E.B., and Björnsson, H., 2002, Glaciohydraulic supercooling in Iceland: Geology, v. 30, p. 439–442, doi:10.1130/0091-7613(2002)030<0439:GSII>2.0.CO;2.

Robinson, D.E., Menzies, J., Wellner, J.S., and Clark, R.W., 2021, Subglacial sediment deformation in the Ross Sea, Antarctica: Quaternary Science Advances, v. 4, p. 100029, doi:10.1016/j.qsa.2021.100029.

Rooney, S.T., Blankenship, D.D., Alley, R.B., and Bentley, C.R., 1987, Till beneath ice stream B: 2. Structure and continuity: Journal of Geophysical Research: Solid Earth, v. 92, p. 8913–8920, doi:10.1029/JB092iB09p08913.

Rosenheim, B.E. et al., 2023, A method for successful collection of multicores and gravity cores from Antarctic subglacial lakes: Limnology and Oceanography: Methods, v. 21, p. 279–294, doi:10.1002/lom3.10545.

Röthlisberger, H., 1972, Water Pressure in Intra- and Subglacial Channels: Journal of Glaciology, v. 11, p. 177–203, doi:10.3189/S0022143000022188.

Rothwell R. Guy, Hoogakker Babette, Thomson John, Croudace Ian W., and Frenz Michael, 2006, Turbidite emplacement on the southern Balearic Abyssal Plain (western Mediterranean Sea) during Marine Isotope Stages 1–3: an application of ITRAX XRF scanning of sediment cores to lithostratigraphic analysis: Geological Society, London, Special Publications, v. 267, p. 79–98, doi:10.1144/GSL.SP.2006.267.01.06.

Scambos, T.A. et al., 2017, How much, how fast?: A science review and outlook for research on the instability of Antarctica's Thwaites Glacier in the 21st century: Global and Planetary Change, v. 153, p. 16–34, doi:10.1016/j.gloplacha.2017.04.008.

Scambos, T.A., Haran, T.M., Fahnestock, M.A., Painter, T.H., and Bohlander, J., 2007, MODIS-based Mosaic of Antarctica (MOA) data sets: Continent-wide surface morphology and snow grain size: Remote Sensing of the Cryosphere Special Issue, v. 111, p. 242–257, doi:10.1016/j.rse.2006.12.020.

Scherer, R.P., Aldahan, A., Tulaczyk, S., Possnert, G., Engelhardt, H., and Kamb, B., 1998, Pleistocene collapse of the West Antarctic ice sheet: Science, v. 281, p. 82–85.

Scherer, R.P., Sjunneskog, C.M., Iverson, N.R., and Hooyer, T.S., 2004, Assessing subglacial processes from diatom fragmentation patterns: Geology, v. 32, p. 557–560.

Schoof, C., 2007, Ice sheet grounding line dynamics: Steady states, stability, and hysteresis: Journal of Geophysical Research: Earth Surface, v. 112, doi:10.1029/2006JF000664.

Schoof, C., 2011, Marine ice sheet dynamics. Part 2. A Stokes flow contact problem: Journal of Fluid Mechanics, v. 679, p. 122–155.

Schroeder, D.M., MacKie, E.J., Creyts, T.T., and Anderson, J.B., 2019, A subglacial hydrologic drainage hypothesis for silt sorting and deposition during retreat in Pine Island Bay: Annals of Glaciology, v. 60, p. 14–20, doi:10.1017/aog.2019.44.

Seneviratne, S.I., Wartenburger, R., Guillod, B.P., Hirsch, A.L., Vogel, M.M., Brovkin, V., van Vuuren, D.P., Schaller, N., Boysen, L., and Calvin, K.V., 2018, Climate extremes, land–climate feedbacks and land-use forcing at 1.5 C: Philosophical Transactions of the Royal Society A: Mathematical, Physical and Engineering Sciences, v. 376, p. 20160450.

Shreve, R.L., 1972, Movement of Water in Glaciers: Journal of Glaciology, v. 11, p. 205–214, doi:10.3189/S002214300002219X.

Siegfried, M.R. et al., 2023, The life and death of a subglacial lake in West Antarctica: Geology, v. 51, p. 434–438, doi:10.1130/G50995.1.

Siegfried, M.R., and Fricker, H.A., 2021, Illuminating Active Subglacial Lake Processes With ICESat-2 Laser Altimetry: Geophysical Research Letters, v. 48, p. e2020GL091089, doi:10.1029/2020GL091089.

Siegfried, M.R., and Fricker, H.A., 2018, Thirteen years of subglacial lake activity in Antarctica from multi-mission satellite altimetry: Annals of Glaciology, v. 59, p. 42–55, doi:10.1017/aog.2017.36.

Siegfried, M.R., Fricker, H.A., Carter, S.P., and Tulaczyk, S., 2016, Episodic ice velocity fluctuations triggered by a subglacial flood in West Antarctica: Geophysical Research Letters, v. 43, p. 2640–2648, doi:10.1002/2016GL067758.

Simkins, L.M., Anderson, J.B., Greenwood, S.L., Gonnermann, H.M., Prothro, L.O., Halberstadt, A.R.W., Stearns, L.A., Pollard, D., and DeConto, R.M., 2017, Anatomy of a meltwater drainage system beneath the ancestral East Antarctic ice sheet: Nature Geoscience, v. 10, p. 691–697, doi:10.1038/ngeo3012.

Smalley, I.J., and Unwin, D.J., 1968, The Formation and Shape of Drumlins and their Distribution and Orientation in Drumlin Fields: Journal of Glaciology, v. 7, p. 377–390, doi:10.3189/S0022143000020591.

Smith, J.A., Graham, A.G.C., Post, A.L., Hillenbrand, C.-D., Bart, P.J., and Powell, R.D., 2019, The marine geological imprint of Antarctic ice shelves: Nature Communications, v. 10, p. 5635, doi:10.1038/s41467-019-13496-5.

Smith, A.M., Woodward, J., Ross, N., Bentley, M.J., Hodgson, D.A., Siegert, M.J., and King, E.C., 2018, Evidence for the long-term sedimentary environment in an Antarctic subglacial lake: Earth and Planetary Science Letters, v. 504, p. 139–151, doi:10.1016/j.epsl.2018.10.011.

Souchez, R., Petit, J.R., Tison, J.-L., Jouzel, J., and Verbeke, V., 2000, Ice formation in subglacial Lake Vostok, Central Antarctica: Earth and Planetary Science Letters, v. 181, p. 529–538, doi:10.1016/S0012-821X(00)00228-4.

Sperazza, M., Moore, J.N., and Hendrix, M.S., 2004, High-Resolution Particle Size Analysis of Naturally Occurring Very Fine-Grained Sediment Through Laser Diffractometry: Journal of Sedimentary Research, v. 74, p. 736–743, doi:10.1306/031104740736.

Sweet, W.V., Hamlington, B.D., Kopp, R.E., Weaver, C.P., Barnard, P.L., Bekaert, D., Brooks, W., Craghan, M., Dusek, G., and Frederikse, T., 2022, Global and regional sea level rise

scenarios for the United States: Updated mean projections and extreme water level probabilities along US coastlines: National Oceanic and Atmospheric Administration.

Thomas, G.S.P., and Connell, R.J., 1985, Iceberg drop, dump, and grounding structures from Pleistocene glacio-lacustrine sediments, Scotland: Journal of Sedimentary Research, v. 55, p. 243–249, doi:10.1306/212F8689-2B24-11D7-8648000102C1865D.

Tulaczyk, S., and Hossainzadeh, S., 2011, Antarctica's Deep Frozen "Lakes": Science, v. 331, p. 1524–1525, doi:10.1126/science.1202888.

Tulaczyk, S., Kamb, B., Scherer, R.P., and Engelhardt, H.F., 1998, Sedimentary processes at the base of a West Antarctic ice stream; constraints from textural and compositional properties of subglacial debris: Journal of Sedimentary Research, v. 68, p. 487–496, doi:10.2110/jsr.68.487.

Venturelli, R.A. et al., 2023, Constraints on the Timing and Extent of Deglacial Grounding Line Retreat in West Antarctica: AGU Advances, v. 4, p. e2022AV000846, doi:10.1029/2022AV000846.

Venturelli, R.A., Siegfried, M.R., Roush, K.A., Li, W., Burnett, J., Zook, R., Fricker, H.A., Priscu, J.C., Leventer, A., and Rosenheim, B.E., 2020, Mid-Holocene Grounding Line Retreat and Readvance at Whillans Ice Stream, West Antarctica: Geophysical Research Letters, v. 47, p. e2020GL088476, doi:10.1029/2020GL088476.

Vick-Majors, T.J. et al., 2020, Biogeochemical Connectivity Between Freshwater Ecosystems beneath the West Antarctic Ice Sheet and the Sub-Ice Marine Environment: Global Biogeochemical Cycles, v. 34, p. e2019GB006446, doi:10.1029/2019GB006446.

Vogel, S.W., Tulaczyk, S., Kamb, B., Engelhardt, H., Carsey, F.D., Behar, A.E., Lane, A.L., and Joughin, I., 2005, Subglacial conditions during and after stoppage of an Antarctic Ice Stream: Is reactivation imminent? Geophysical Research Letters, v. 32, doi:10.1029/2005GL022563.

Walder, J.S., 1986, Hydraulics of Subglacial Cavities: Journal of Glaciology, v. 32, p. 439–445, doi:10.3189/S0022143000012156.

Walder, J.S., and Fowler, A., 1994, Channelized subglacial drainage over a deformable bed: Journal of Glaciology, v. 40, p. 3–15, doi:10.3189/S0022143000003750.

Weertman, J., 1961, Mechanism for the Formation of Inner Moraines Found Near the Edge of Cold Ice Caps and Ice sheets: Journal of Glaciology, v. 3, p. 965–978, doi:10.3189/S0022143000017378.

Weertman, J., 1957, On the Sliding of Glaciers: Journal of Glaciology, v. 3, p. 33–38, doi:10.3189/S0022143000024709.

Weertman, J., 1974, Stability of the junction of an ice sheet and an ice shelf: Journal of Glaciology, v. 13, p. 3–11.

Weertman, J., 1964, The Theory of Glacier Sliding: Journal of Glaciology, v. 5, p. 287–303, doi:10.3189/S0022143000029038.

Witus, A.E., Branecky, C.M., Anderson, J.B., Szczuciński, W., Schroeder, D.M., Blankenship, D.D., and Jakobsson, M., 2014, Meltwater intensive glacial retreat in polar environments and investigation of associated sediments: example from Pine Island Bay, West Antarctica: Quaternary Science Reviews, v. 85, p. 99–118, doi:10.1016/j.quascirev.2013.11.021.

Yan, S. et al., 2022, A newly discovered subglacial lake in East Antarctica likely hosts a valuable sedimentary record of ice and climate change: Geology, v. 50, p. 949–953, doi:10.1130/G50009.1.

Zielinski, G.A., Mayewski, P.A., Meeker, L.D., Whitlow, S., Twickler, M.S., Morrison, M., Meese, D.A., Gow, A.J., and Alley, R.B., 1994, Record of Volcanism Since 7000 B.C. from the GISP2 Greenland Ice Core and Implications for the Volcano-Climate System: Science, v. 264, p. 948–952, doi:10.1126/science.264.5161.948.

Zwally, H.J., Abdalati, W., Herring, T., Larson, K., Saba, J., and Steffen, K., 2002, Surface Melt-Induced Acceleration of Greenland Ice-Sheet Flow: Science, v. 297, p. 218–222, doi:10.1126/science.1072708.

APPENDICES

APPENDIX A

CHAPTER TWO SUPPLEMENTARY MATERIALS

Mercer Ice Stream subglacial lake sediments reveal an archive of dynamic subglacial hydrologic conditions.

Timothy D. Campbell et al.

Supplementary Information

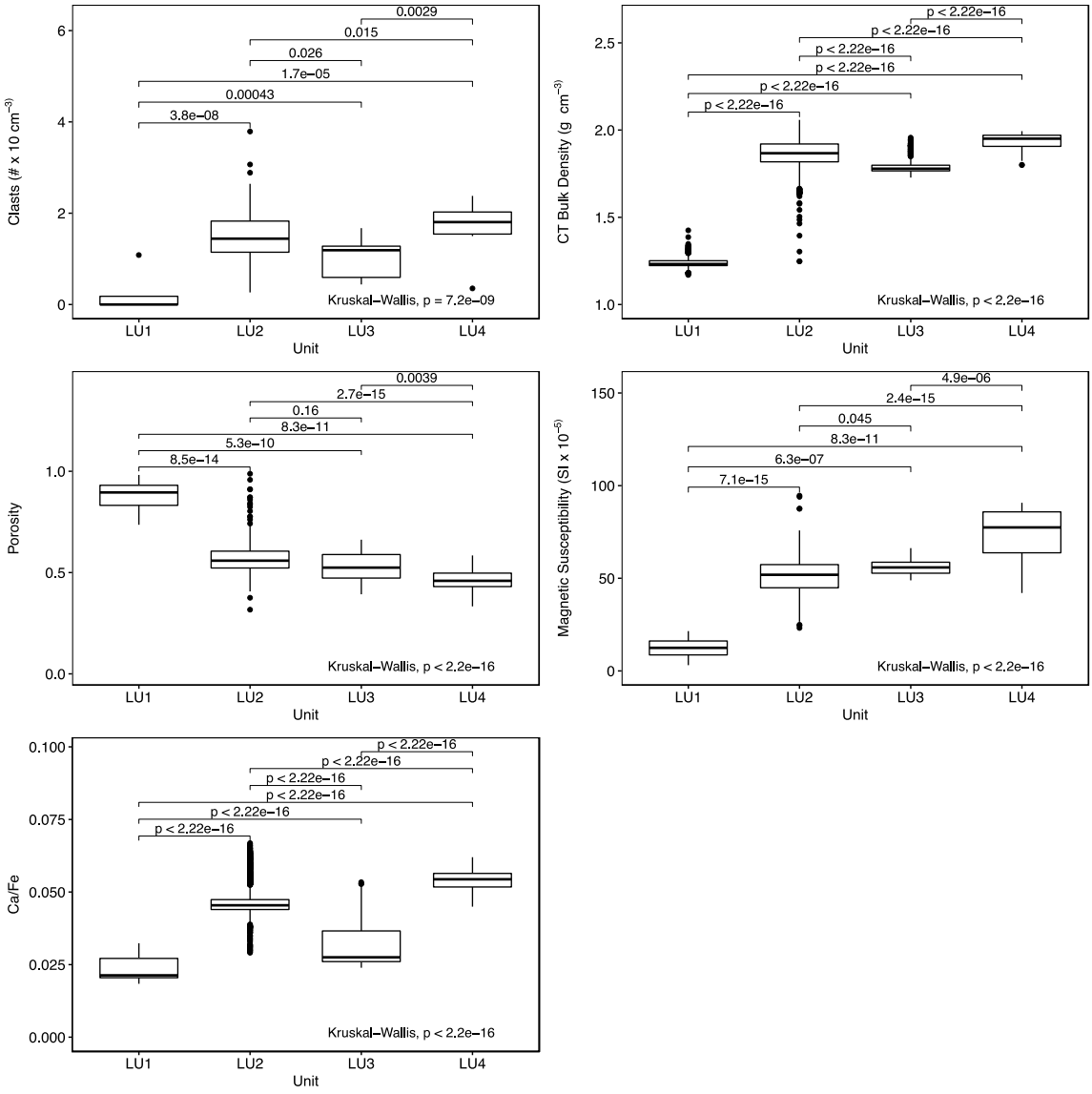

Supplementary Figure 1.1 Box plots of clasts (>2 mm) index (A), bulk density (B), porosity (C), Magnetic Susceptbility (D), and Ca/Fe (E) by lithostratigraphic unit. P-values from Kruskal-Wallis multiple pairwise-comparison tests are presented and show that all units are statistically different for all properties (p-values < 0.05). Statistically significant differences were used to justify lithostratigraphic designations.

Core Name	Core Type	Core Diameter (cm)	Parent Core Length (cm)	# of Parent Core Sections	Core Depth Top (cm)	Core Depth Bottom (cm)	Section Length (cm)
SLM1801-01UW-A	MC	6	42	1	0	42	42
SLM1801-01UW-B	MC	6	38	1	0	38	38
SLM1801-01UW-C	MC	6	40	1	0	40.5	40.5
SLM1801-01FF-1	FF	10	100	5	0	45	45
SLM1801-01FF-2	FF	10	100	5	45	50	5
SLM1801-01FF-3	FF	10	100	5	50	80	30
SLM1801-01FF-4	FF	10	100	5	80	85	5
SLM1801-01FF-5	FF	10	100	5	85	100	15
SLM1801-02FF-1	FF	10	172	2	0	100	100
SLM1801-02FF-2	FF	10	172	2	100	172	72

Supplementary Table 1.1 List of core names, core diameters, and core lengths. Cores SLM1801-01FF and SLM1801-02FF were split in the field into 5 and 2 sections, respectively. Sections SLM1801-01FF-2 and SLM1801-01FF-4 were sampled in the field as whole round samples for immediate analytical work, including measurement of porewater specific conductivity. Abbreviations used in text and table: MC = Multicore, FF = Free-Fall Gravity Core.

CT WBD ($g\ cm^{-3}$)	UNIT	Count	Mean	SD	Median	IQR	Min	Max
	LU1	920	1.24	0.03	1.23	0.03	1.17	1.43
	LU2	10317	1.87	0.07	1.87	0.10	1.25	2.06
	LU3	466	1.79	0.04	1.78	0.03	1.73	1.96
	LU4	1245	1.94	0.04	1.95	0.06	1.80	1.99
MSCL Porosity								
	LU1	22	0.88	0.07	0.90	0.10	0.74	0.98
	LU2	258	0.57	0.09	0.56	0.08	0.32	0.99
	LU3	14	0.53	0.08	0.52	0.12	0.39	0.66
	LU4	41	0.46	0.05	0.46	0.07	0.33	0.58
Mag. Susc.								
($SI \times 10^{-5}$)	LU1	22	12.54	5.21	12.42	7.52	3.11	21.48
	LU2	258	51.84	11.85	51.87	12.50	23.20	94.63
	LU3	14	56.12	5.26	55.82	5.97	48.88	66.26
	LU4	41	73.90	12.97	77.43	22.11	42.03	90.75
Ca/Fe								
	LU1	517	0.023	0.004	0.022	0.006	0.016	0.035
	LU2	4802	0.046	0.005	0.045	0.004	0.025	0.069
	LU3	189	0.028	0.006	0.025	0.002	0.023	0.063
	LU4	915	0.053	0.004	0.054	0.005	0.030	0.0667
K/Ti								
	LU1	517	1.083	0.241	1.065	0.218	0	2.681
	LU2	4802	1.420	0.075	1.422	0.087	1.049	2.816
	LU3	189	1.313	0.067	1.311	0.059	1.129	1.557
	LU4	915	1.494	0.077	1.502	0.096	1.101	1.700
Clast Index								
(# 10 cm^{-3})	LU1	12	0.15	0.31	0.00	0.18	0.00	1.08
	LU2	131	1.49	0.55	1.44	0.68	0.26	3.79
	LU3	8	1.04	0.45	1.19	0.68	0.44	1.67
	LU4	14	1.74	0.48	1.81	0.48	0.35	2.38

Supplementary Table 1.2 Summary statistics from the Kruskal-Wallis test for clast index, sediment density, porosity, magnetic susceptibility, and Ca/Fe ratio.

Core	Interval	Depth (cm)	Quartz	Albite	Illite	Microcline	Chlorite	Kaolinite	Dolomite	Calcite	Amphibole	Other
01UW-A	0 to 4	2	23.7	18.2	30.3	17	8.2	0	1.4	0	0	1.2
01UW-A	6 to 10	8	26.5	21.6	23.2	13.5	11.1	0	0	0	2.5	1.6
01UW-A	18 to 20	19	26.8	31.7	12.1	9.9	6.4	0.3	0	0	12.8	0
01UW-A	36 to 38	41	33.7	22.7	16.6	13.1	2.9	0	0	0	0	11
01FF	40 to 45	156.5	30.2	30.9	12.6	14.1	7	0.1	3.1	0.5	0	1.5
01FF	55 to 57	165	29.4	32.9	16.9	16	4.4	0.3	0	0	0	0.1
01FF	66 to 68	176	28.1	17.6	20.7	9.1	14.2	0	9	0.1	0	1.2
01FF	71 to 73	181	30.4	27.5	15.5	12.2	10.1	0	0	0	0	4.3
01FF	80 to 85	191.5	30.3	22.4	21.9	11	5.5	0	0	0	8.4	0.5
01FF	92 to 94	202	22.2	28.9	28.1	9.4	5.7	0.4	2.3	2.3	0.1	0.6

Supplementary Table 1.3 Percentage data of mineral phase identification made using x-ray diffraction of <63 μm sediment fraction.

APPENDIX B

CHAPTER THREE SUPPLEMENTARY MATERIALS

Implications for sub-ice stream accretionary processes and conditions from the Basal Ice Laker of the Mercer Ice Stream, West Antarctica

Timothy D. Campbell et al.

Supplementary Information

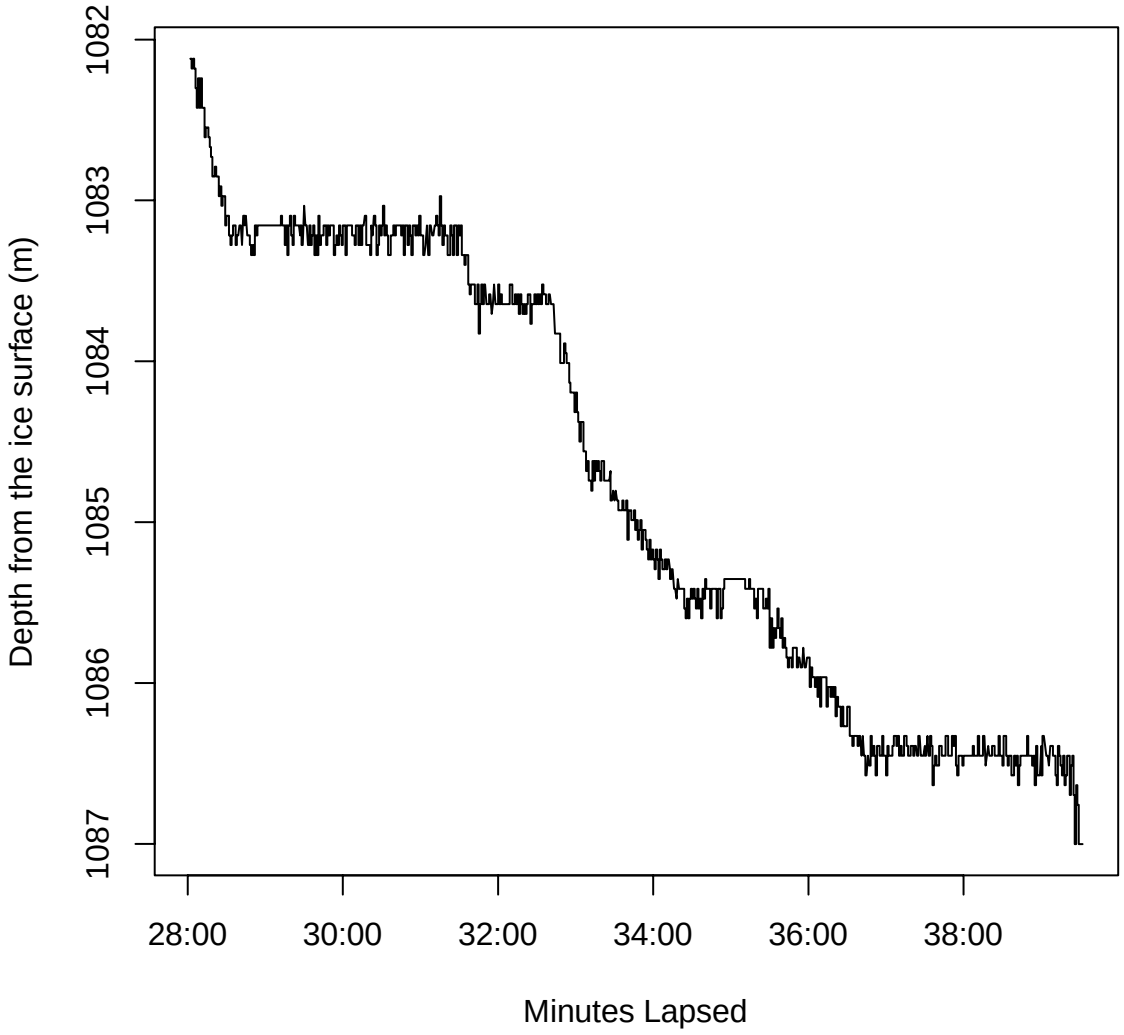

Supplementary Figure 2.1 Clump weight camera deployment through the SLM basal ice layer over time and depth.

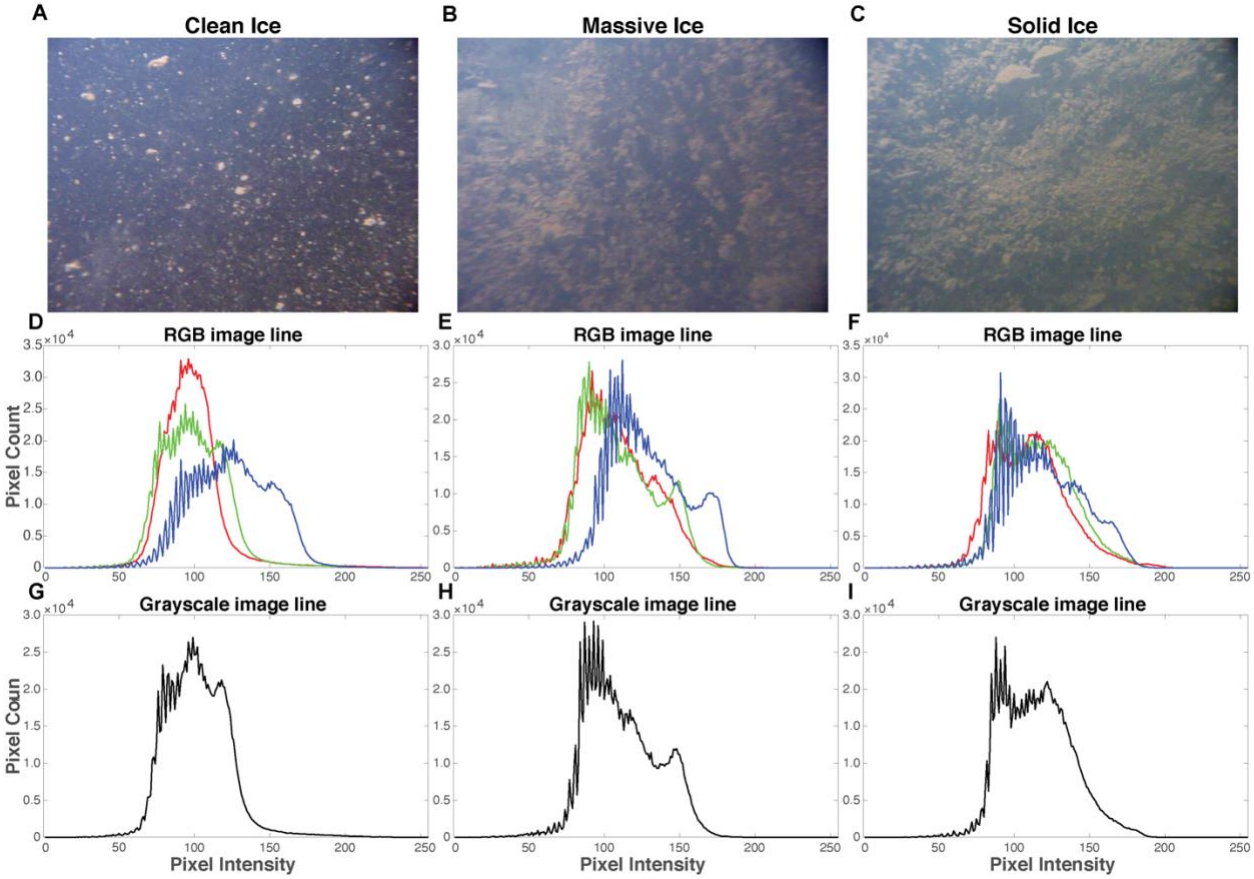

Supplementary Figure 2.2 Image color and brightness intensity distributions for clear ice (A), dispersed ice (B), and solid ice (C). D – F show red, green, and blue color frequency distributions of the original-colored image. G – I show brightness frequency distributions of the grayscale version of the colored image. Differences between the optical properties justified the use of brightness thresholds to differentiate sediment debris from ice.

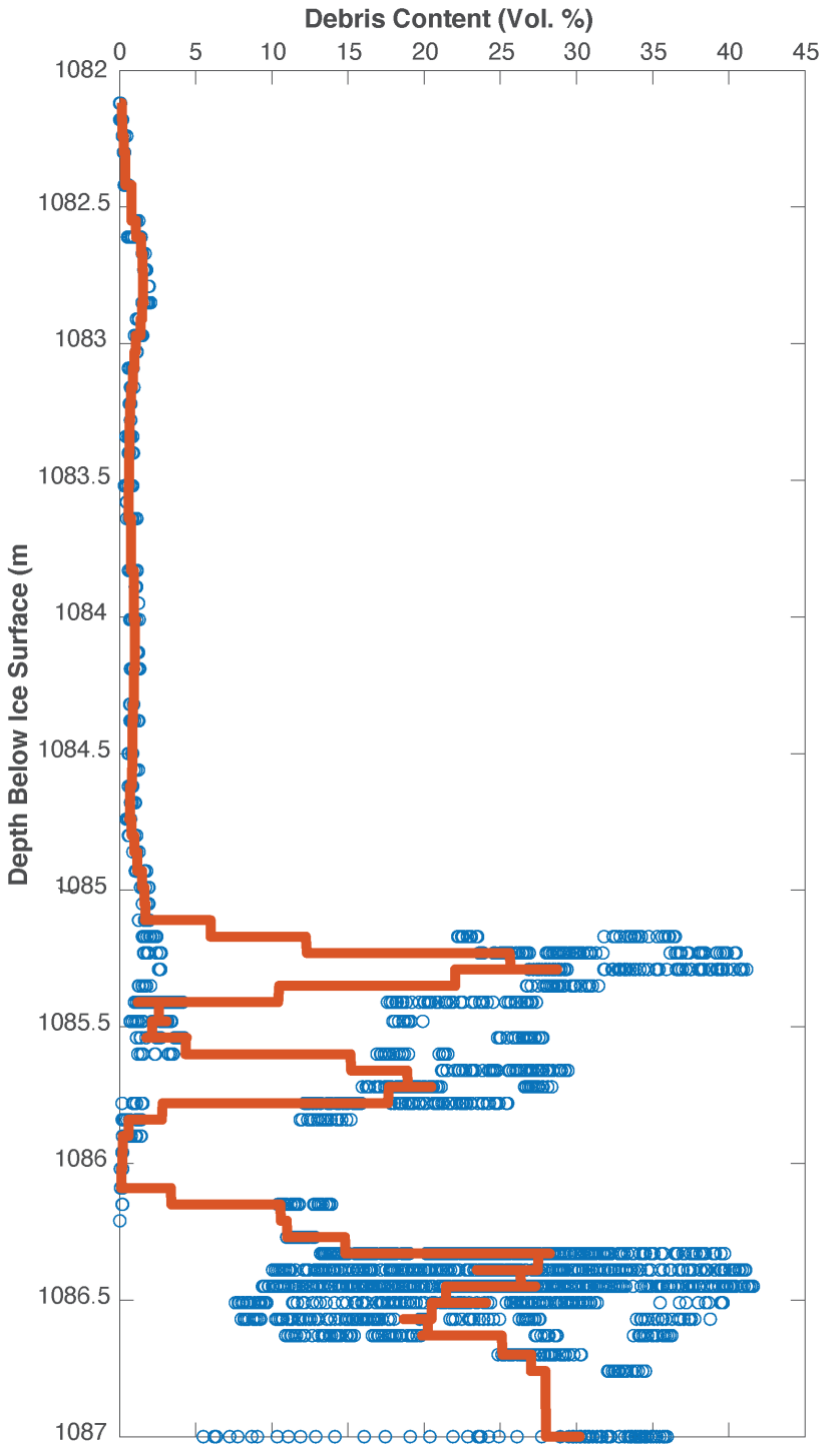

Supplementary Figure 2.3 Stratigraphic log showing the debris content results of the sequential down borehole image brightness analysis in the SLM basal ice layer (blue points) and smoothed using a moving average filter (red) (shown in Figure 3.5).